แหล่งที่มาของตะกอนที่ทับถมทางตอนใต้ของทะเลอันดามันตั้งแต่ยุคน้ำแข็งครั้งสุดท้าย

นางสาวสุรัตตา บุญสมบูรณ์สกุล

วิทยานิพนธ์นี้เป็นส่วนหนึ่งของการศึกษาตามหลักสูตรปริญญาวิทยาศาสตรดุษฎีบัณฑิต
สาขาวิชาวิทยาศาสตร์ทางทะเล ภาควิชาวิทยาศาสตร์ทางทะเล
คณะวิทยาศาสตร์ จุฬาลงกรณ์มหาวิทยาลัย
ปีการศึกษา 2559

PROVENANCE OF DETRITAL SEDIMENTS IN SOUTHERN ANDAMAN SEA SINCE THE LAST GLACIATION

Miss Suratta Bunsomboonsakul

A Dissertation Submitted in Partial Fulfillment of the Requirements
for the Degree of Doctor of Philosophy Program in Marine Science
Department of Marine Science
Faculty of Science
Chulalongkorn University
Academic Year 2016

Thesis Title	PROVENANCE OF DETRITAL SEDIMENTS IN SOUTHERN ANDAMAN SEA SINCE THE LAST GLACIATION
By	Miss Suratta Bunsomboonsakul
Field of Study	Marine Science
Thesis Advisor	Assistant Professor Dr. Penjai Sompongchaiyakul
Thesis Co-Advisor	Professor Dr. Zhifei Liu

Accepted by the Faculty of Science, Chulalongkorn University in Partial Fulfillment of the Requirements for the Doctoral Degree

.....Dean of the Faculty of Science
(Associate Professor Dr. Polkit Sangvanich)

THESIS COMMITTEE

.....Chairman
(Assistant Professor Dr. Sanit Piyapattanakorn)
.....Thesis Advisor
(Assistant Professor Dr. Penjai Sompongchaiyakul)
.....Thesis Co-Advisor
(Professor Dr. Zhifei Liu)
.....Examiner
(Assistant Professor Dr. Sirichai Dharmvanij)
.....Examiner
(Dr. Patama Singhruck)
.....External Examiner
(Dr. Somkiat Khokiattiwong)

สุรัตตา บุญสมบูรณ์สกุล : แหล่งที่มาของตะกอนที่ทับถมทางตอนใต้ของทะเลอันดามันตั้งแต่ยุคน้ำแข็งครั้งสุดท้าย (PROVENANCE OF DETRITAL SEDIMENTS IN SOUTHERN ANDAMAN SEA SINCE THE LAST GLACIATION) อ.ที่ปรึกษาวิทยานิพนธ์หลัก: ผศ. ดร. เพ็ญใจ สมพงษ์ชัยกุล, อ.ที่ปรึกษาวิทยานิพนธ์ร่วม: ดร. จือเฟย หลิว, 119 หน้า.

ทะเลอันดามันเป็นทะเลกึ่งปิดจึงเป็นพื้นที่ที่เหมาะสมสำหรับศึกษากระบวนการขนส่งตะกอนจากแหล่งกำเนิด งานวิจัยนี้มีจุดมุ่งหมาย 4 ประการคือ 1) เพื่อแสดงการสะสมตัวของแร่ดินเหนียวบนตะกอนผิวหน้าในทะเลอันดามัน สู่การเข้าใจกระบวนการขนส่งตะกอนในยุคปัจจุบัน; 2) เพื่อเข้าใจรูปแบบการเปลี่ยนแปลงของแร่ดินเหนียวตั้งแต่ยุคน้ำแข็งครั้งสุดท้าย; 3) เพื่ออธิบายวิวัฒนาการของระบบลมมรสุม; และ 4) เพื่ออธิบายกลไกการเปลี่ยนแปลงของสิ่งแวดล้อมทางทะเลอันเนื่องมาจากการเปลี่ยนแปลงสภาพภูมิอากาศตั้งแต่ยุคน้ำแข็งครั้งสุดท้าย เก็บตะกอนผิวหน้า 61 ตัวอย่าง วิเคราะห์แร่ดินเหนียวเพื่อบ่งชี้แหล่งที่มาตะกอนและกระบวนการขนส่งตะกอนในยุคปัจจุบันและแท่งตะกอนทะเล 4 แท่ง จากทะเลอันดามันตอนใต้ (ADM 2, ADM 6, MASS-III-07 และ MASS-III-10) วิเคราะห์แร่ดินเหนียวและธรณีเคมีของโลหะ เพื่ออธิบายวิวัฒนาการสิ่งแวดล้อมของทะเลอันดามันตั้งแต่ยุคน้ำแข็งในอดีต และการศึกษาอายุตะกอนด้วยคาร์บอน-14 และออกซิเจนไอโซโทป ($\delta^{18}O$) โดยการวิเคราะห์ฟอรามินิเฟอราเพื่อปรับเทียบอายุของตะกอน

จากข้อมูลแร่ดินเหนียวในตะกอนผิวหน้า บ่งชี้ว่าตะกอนที่สะสมในทะเลอันดามันมี 4 แหล่งกำเนิด ได้แก่ ประเทศพม่า คาบสมุทรมลายู สุมาตรา และประเทศไทย โดยแหล่งกำเนิดหลักของตะกอนในทะเลอันดามันมาจากประเทศพม่าซึ่งมาจากแม่น้ำอิรวดีและแม่น้ำสาละวิน โดยพบกลุ่มแร่สเมคไตต์ (~ 44%) เป็นแร่หลัก ขณะที่คาบสมุทรมลายู สุมาตรา และประเทศไทย มีกลุ่มแร่เคโอลิไนต์ เป็นแร่หลัก (47%, 80% และ 68% ตามลำดับ) จากข้อมูลพบว่ากระบวนการหินวิทยาเป็นกระบวนการหลักที่ควบคุมการเกิดของแร่ดินเหนียวจากประเทศพม่า (แหล่งกำเนิดหลัก) ขณะที่คาบสมุทรมลายู สุมาตรา และประเทศไทย ถูกควบคุมโดยสภาพภูมิอากาศ ส่วนการขนส่งตะกอนในทะเลอันดามันถูกควบคุมโดย 2 กระบวนการ คือ กระแสน้ำชั้นบนที่มีความสัมพันธ์โดยตรงกับมรสุม และความแตกต่างของการตกตะกอนของแร่ดินเหนียวกลุ่มแร่สเมคไตต์

จากข้อมูลแท่งตะกอนไม่พบการเปลี่ยนแปลงของแหล่งตะกอน บ่งชี้ว่าตั้งแต่ยุคน้ำแข็งครั้งสุดท้ายจนถึงปัจจุบัน ไม่มีการเปลี่ยนแปลงของแหล่งกำเนิดตะกอน อย่างไรก็ดีข้อมูลแร่ดินเหนียวในแท่งตะกอน ADM2 และ MASS-III-10 มีความสัมพันธ์กับการเปลี่ยนแปลงระดับน้ำทะเลและลมมรสุม ในขณะที่แท่งตะกอน ADM6 อิทธิพลของลมมรสุมจะเด่นในช่วงโฮโลซีน แต่แท่งตะกอน MASS-III-07 ไม่สามารถระบุปัจจัยควบคุมการเปลี่ยนแปลงได้ อัตราการตกตะกอนในแท่งตะกอน ADM6 สูงกว่า ADM2 น่าจะเกิดเนื่องจากสภาพอุทกพลศาสตร์ เพราะพบชั้นตะกอนที่ถูกรบกวนบริเวณส่วนล่างของแท่งตะกอน ADM6 แท่งตะกอนน้ำตื้น MASS-III-07 มีอัตราการตกตะกอน (12.3 ซม./พันปี) สูงกว่า MASS-III-10 (2.2-9.9 ซม./พันปี) แม้ว่าแท่งตะกอนทั้งสองแท่งเก็บมาจากบริเวณใกล้เคียงกัน แต่อัตราการตกตะกอนแตกต่างกัน บ่งชี้ว่าสภาพพื้นทะเลบริเวณดังกล่าวมีอิทธิพลรบกวนตะกอนซึ่งส่งผลต่อการสะสมตะกอน ส่วนหน้าของแท่งตะกอน MASS-III-07 หายไป ตะกอนที่เก็บได้มีอายุตั้งแต่ 15,000 ปีขึ้นไป ซึ่งเป็นไปได้ว่าตะกอนส่วนหน้านี้ถูกพัดพาออกไปโดยอิทธิพลจากกระแสน้ำจากช่องแคบมะละกาในช่วงมรสุมตะวันออกเฉียงเหนือ แม้ว่าจะพบว่าลมมรสุมจะมีอิทธิพลต่อการสะสมของตะกอนในทะเลอันดามัน แต่ข้อมูลที่ได้ก็ยังไม่เพียงพอต่อการอธิบายวิวัฒนาการของระบบลมมรสุม

ภาควิชา	วิทยาศาสตร์ทางทะเล	ลายมือชื่อนิสิต	.....
สาขาวิชา	วิทยาศาสตร์ทางทะเล	ลายมือชื่อ อ.ที่ปรึกษาหลัก	.....
ปีการศึกษา	2559	ลายมือชื่อ อ.ที่ปรึกษาร่วม	.....

5373928123 : MAJOR MARINE SCIENCE
KEYWORDS:

SURATTA BUNSOMBOONSAKUL: PROVENANCE OF DETRITAL SEDIMENTS IN SOUTHERN ANDAMAN SEA SINCE THE LAST GLACIATION. ADVISOR: ASST. PROF. DR. PENJAI SOMPONGCHAIYAKUL, CO-ADVISOR: PROF. DR. ZHIFEI LIU, 119 pp.

The Andaman Sea is a semi-enclosed system which offers such a good case for studying the source to sink transport process of sediment. This work has main objectives which are: 1) to reveal clay mineral assemblages in surface sediments, and understand present transport process; 2) to understand the clay mineral variation since the last glaciation; 3) to reconstruct the Indian monsoon evolution; 4) to explain the possible mechanism of marine environmental variation driven by climate change since the last glaciation. The materials used in this study include 61 surface sediment samples which were analyzed for clay minerals in order to characterize modern ocean transportation process, and 4 sediment cores (ADM 2, ADM 6, MASS-III-07, and MASS-III-10) in the southern Andaman Sea which were analyzed for clay minerals and element geochemistry, to reconstruct paleoenvironment over the last glaciation. The AMS-^{14}C and oxygen isotopes (δ^{18}O) dating from planktonic foraminifera were measured to establish a chronology of the cores.

The clay mineralogy of surface samples revealed four potential provenances, including Myanmar, Malay Peninsula, Sumatra, and Thailand. The major provenance is from Myanmar, which dominated by smectite (44%) from Irrawaddy and Salween river system. The Malay Peninsula, Sumatra, and Thailand are predominated with kaolinite (80%, 68%, and 47% respectively). From clay mineral assemblages, it can be identified that three provenances, Malay Peninsula, Sumatra, and Thailand, are controlled by climatological condition, while Myanmar (major provenance) is controlled by lithological setting. The modern transportation process of sediments in the Andaman Sea is controlled by two processes; surface circulations that are directly related to SW and NE monsoon, and differential setting of smectite.

Clay mineral variation in the sediment cores revealed no significant change in downcore variation. The clay mineral variations over the last glaciation of ADM2 and MASS-III-10 are related to the sea level and monsoon, ADM6 is under the monsoon influence during Holocene, while MASS-III-07 shows unclear controlling factor. As the results, it can indicate that the relative contributions of the sources did not vary through time since the last glaciation except MASS-III-10. It was found the different amount of sediment input between glacial and interglacial time, suggesting it may be due to another factor such as the river discharge. Core ADM2 is characterized by lower sedimentation rates in comparison to ADM6. The high sedimentation rate of ADM6 may occur due to high hydrodynamic condition because ADM6 was found the turbidity layer in the lower part of the core. The shallow water cores; MASS-III-07 shows high sedimentation rate (12.3 cm/ka) than MASS-III-10 (2.2 - 9.9 cm/ka). Although these two shallow water cores are located in the same area, their sedimentation rates were different. The high sedimentation rate of MASS-III-07 suggested that the core location may be existed in the disturbance zone, of which may be influenced by the current driven into the Andaman Sea from Malacca Strait by NE monsoon. The current may wash off some of the surface sediment that corresponded well with losing of the core top. Although it was found that the monsoon influence on the sediment deposition in the Andaman Sea, the results are not enough to explain the reconstruction of Indian monsoon evolution.

Department:	Marine Science	Student's Signature	.....
Field of Study:	Marine Science	Advisor's Signature	.....
Academic Year:	2016	Co-Advisor's Signature	.....

ACKNOWLEDGEMENTS

This thesis is for a joint doctoral degree co-supervising by Assistant Prof. Dr. Penjai Sompongchaiyakul, Chulalongkorn University and Prof. Dr. Zhifei Liu, Tongji University. The thesis content is on a scientific topic of marine geology of the Andaman Sea under collaboration between two research groups of Chulalongkorn University and Tongji University, focusing on sedimentology disciplines.

I would like to sincerely thank my supervisors Prof. Dr. Zhifei Liu and Assistant Prof. Dr. Penjai Sompongchaiyakul. Especially, I would like to express my deepest appreciation to Prof. Liu for all effort, guidance, consistent encouragement, including the financial support for study budgets and living in Shanghai.

Thank Dr. Shi Xuefa, Dr. Somkiat Khokiattiwong, Assistant Prof. Dr. Anond Snidvongs, Prof. Dr. Sebastian Krastel, Dr. Klaus Schwarzer, and Assistant Prof. Dr. Penjai Sompongchaiyakul for the sediment materials from their cooperative projects and their kindly advises. Furthermore, I would like to thank Assistant Prof. Dr. Sirichai Dharmvanij for the excellent comments. Thank to Assistant Prof. Dr. Patama Singhruck and Dr. Gerry Plumley for their reviewing.

I sincerely appreciated my friend at Tongji University for their efforts and assistances, especially in the laboratory. In addition, I would like to thank State Key Laboratory of Marine Geology for providing laboratory facilities, thank to Dr. Yanli Li, who advise me all about laboratory techniques. Thank also giving to Dr. Yulong Zhao, Dr. Shaohua Zhao, Thanakorn Jiwarungrueangkul, Dr. Xiajing Li, Dr. Annette Schröder, Dr. Ronan Joussain, Dr. Chen Quen and others at Tongji University. I also appreciate professors and staffs from both universities, without them this study would not have been possible.

Finally, I am grateful to thank my important and beloved family for all their loving support through all my study time. Regret to my grandparents who are main supporting but they passed away before all thing done.

CONTENTS

Page
THAI ABSTRACT iv
ENGLISH ABSTRACT v
ACKNOWLEDGEMENTS vi
CONTENTS vii
LIST OF FIGURES x
LIST OF TABLES xvi
CHAPTER 1 1
INTRODUCTION 1
1.1 Rationales 1
1.2 Review of previous study 5
1.3 Objectives and significance of this study 12
CHAPTER 2 14
GEOLOGICAL AND ENVIRONMENTAL BACKGROUNDS 14
2.1 Geological setting 15
2.2 Climate condition and Oceanography 18
2.2.1 Climate conditions 19
Monsoon variation 19
2.2.2 Oceanography 20
Surface Circulation 21
2.3 River discharge surrounding the Andaman Sea 26
CHAPTER 3 32
MATERIALS, METHODS, AND AGE MODELS 32
3.1 Sample materials 33
3.1.1 ADM 2 36
3.1.2 ADM 6 36
3.1.3 MASS-III-10 38
3.1.4 MASS-III-07 38
3.1.5 Myanmar surface sediments 40

Page

3.1.6 Thailand surface sediments 40
3.2 Analytical methods 41
3.2.1 Stable oxygen isotope 41
3.2.2 Carbon-14 dating 42
3.2.3 Bulk Carbonate content 42
3.2.4 Clay mineralogical analysis 43
3.2.5 X-ray fluorescence (XRF) element core scanning 45
3.2.6 X-ray fluorescence (XRF) elemental geochemistry 46
3.3 Age Models 47
3.3.1 Age model of Core ADM2 48
3.3.2 Age model of Core ADM6 50
3.3.3 Age model of core MASS-III-10 52
3.3.4 Age model of core MASS-III-07 54
3.3.5 Summary of chronological frameworks 55
CHAPTER 4 58
CLAY MINERAL IN SURFACE SEDIMENT OF THE ANDAMAN SEA 58
4.1 Composition of clay minerals in the provenance area 59
4.2 Clay minerals in surface sediments 64
4.3 Modern ocean transportation process 69
CHAPTER 5 71
CLAY MINERAL VARIATION SINCE THE LAST GLACIATION 71
5.1 Clay mineral assemblages 71
5.1.1 Characteristics of clay mineralogy records in sediment cores 71
Clay minerals of Core ADM 2 71
Clay minerals of Core ADM 6 72
Clay minerals of Core MASS-III-10 73
Clay minerals of Core MASS-III-07 74
5.2 Provenance Analysis 76
CHAPTER 6 82

Page

ENVIRONMENT RECONSTRUCTION OF THE ANDAMAN SEA 82
6.1 Element geochemistry variation 82
6.2 Paleoclimate reconstruction 84
6.2.1 Comparison of major elements to clay mineral variation 84
6.2.2 Sedimentation control factors 90
CHAPTER 7 92
Conclusions and Prospective 92
7.1 Conclusion 92
7.2 Perspectives 95
Appendix A 98
Appendix B 101
REFERENCES 107
VITA 119

LIST OF FIGURES

Figure 1 Schematic of a generalized sediment dispersal system showing the source to sink system. Sources are indicated by black text, sinks are yellow, processes are shown in white italics, and locations in white regular (National Science Foundation, 2004). 2

Figure 2 The sediment dispersal pathway from its originated source through the process to sink environments (the sediment routing system). 3

Figure 3 Bathymetric map of the Andaman Sea 16

Figure 4 Overview of the South Asian Monsoon (SAM), the monsoon is a giant sea breeze that is fundamentally driven by differences of heat capacities between land and ocean, and following temperature differences between warmer land and cooler ocean surfaces. a) Winds generated after Southwest (summer) monsoon b) Winds generated after Northeast (winter) monsoon (modified from Loschnigg and Webster, 2000; Gebregiorgis, 2017) 20

Figure 5 Surface currents in the Andaman Sea were driven by the northeast monsoon (December–May) and the southwest monsoon (June–November). Arrows represent the current strength (modified after Brown, 2007). 23

Figure 6 Sea surface temperature distribution in the Indian Ocean and eastern Arabian Sea. During winter influence present as left and summer as right. Contour lines represent annual sea surface salinities (SSS) (psu) from Levitus et al. (2010). Surface circulation pattern during winter and summer present by black arrows. Winter and summer SST (°C) ranges are shown in color gradient. (Modified after Gebregiorgis et al., 2016). 25

Figure 7 Fluvial drainage systems and their annual suspended sediment discharge to the Andaman Sea. White arrows with numbers indicate observed fluvial sediment discharge (in million metric tons, Mt, annually) from the Indochina Peninsula. See table 5 for detailed sediment discharge data of all major rivers. 28

Figure 8 Sitemap of sediment sample locations in the Andaman Sea. The star signs are sediment cores and triangle signs are surface sediments used in this study. Circle signs represent the reference cores studied in the Andaman Sea and diamond signs are river and surface sediments conducted in the surrounding area. 35

Figure 9 Lithographic descriptions of Cores ADM2 and ADM6 37

Figure 10 Lithographic descriptions of core MASS-III-10 and..... 39

Figure 11 Age model of Core ADM2 based on 14C dating, showing by depth (cm) vs age (ka). The tilted triangles presents age controlled points, which were obtained from the oxygen isotope stratigraphy. Color shade presents the Marine Isotopic Stage (MIS) 2. 49

Figure 12 Age model of core ADM6 based on 14C dating, showing by depth (cm) vs age (ka). The tilted triangles presents age controlled points, which were obtained from the oxygen isotope stratigraphy. Color shade presented Marine Isotopic Stage (MIS). 51

Figure 13 Age model of core MASS-III-10 based on 14C dating, showing by depth (cm) vs age (ka). The tilted triangles presents age controlled points, which were obtained from the oxygen isotope stratigraphy. Color shade presented Marine Isotopic Stage (MIS)..... 53

Figure 14 Age model of core MASS-III-07 based on 14C dating, showing by depth (cm) vs age (ka). The tilted triangles presents age controlled points, which were obtained from the oxygen isotope stratigraphy. Color shade presented Marine Isotopic Stage (MIS)..... 55

Figure 15 The time scale of ADM 2, ADM 6, MASS-III-10, and MASS-III07 are obtained by combining 14C AMS ages and correlation with core MD77-169 (Colin et al., 1998) as reference. The age model for these cores were established by correlating the δ18O obtained on G. ruber with core MD77-169 by using Analyseries software (Paillard et al., 1996). Depth (cm) versus

age (50 ka) diagram showing variations in the sedimentation rates (cm/ka). The tilted triangles presents age controlled points and color shade presented MIS stage. 57

Figure 16 Average clay mineral assemblages (%) of four main clay contents; smectite (blue), kaolinite (red), illite (green), and chlorite (orange) by various provinces in the Andaman Sea and surrounding drainage basins. The data calculated from various provinces are listed in Table 9. Data of river draining samples of Malay Peninsula from Wang et al. (2011); data of river samples of Sumatra from Liu et al. (2012). 62

Figure 17 a) Clay ternary diagram which represents the influence on the clay assemblage of the climate, the topography and the lithology of the source rock (from Velde, 1985) b) Interpretation of control factor influence on the clay assemblages in the different provenance area; four potential provenance are plotted in the diagram as Malay Peninsula (light blue), Sumatra (green), Thailand (navy blue), and Myanmar (red). 64

Figure 18 Average clay mineral assemblages (%) of surface sediments in the Andaman Sea in the present time. The color shades represent four main clay contents; smectite (blue), kaolinite (red), illite (green), and chlorite (orange). Data of river draining samples of Malay Peninsula from Wang et al. (2011); data of river samples of Sumatra from Liu et al. (2012). Data of reference core of the Holocene period; MD77-169 (Colin et al, 1999), MD77-176, and MD77-186 (Colin et al, 1998; Joussain et al., 2016b). 66

Figure 19 Ternary diagram of the averaged clay mineral assemblages by three end members; illite+chlorite, kaolinite and smectite of the studying sediment groups. The clay mineral formation are indicated into various provenances as the difference shade; province 1- 4 of provenances surrounding the Andaman Sea. 67

Figure 20 Map of predominated surface circulations in the Andaman Sea driven by the northeast monsoon (red) and southwest monsoon (black) (modified after Brown, 2007) with sample locations. 70

Figure 21 Summary results of ADM2. Clay mineral assemblages (%) for <2μm particles non-calcareous clay; kaolinite, chlorite, illite, smectite, ratio of smectite/(illite+chlorite) (blue), illite chemical index, and illite crystallinity versus age (ka BP). Planktonic foraminifera (G. ruber) $\delta^{18}O$ curve of ADM 2 is displayed (green). Bar color displays MIS 2 stage. 72

Figure 22 Summary results of ADM6. Clay mineral assemblages (%) for <2μm particles non-calcareous clay; kaolinite, chlorite, illite, smectite, ratio of smectite/(illite+chlorite) (blue), illite chemical index, and illite crystallinity versus age (ka BP). Planktonic foraminiferal G. ruber $\delta^{18}O$ curve is displayed (green). Bar color displays MIS 2 stage. 73

Figure 23 Summary results of MASS-III-10. Clay mineral assemblages (%) for <2μm particles non-calcareous clay; kaolinite, chlorite, illite, smectite, ratio of smectite/(illite+chlorite) (blue), illite chemical index, and illite crystallinity versus age (ka BP). Planktonic foraminiferal G. ruber $\delta^{18}O$ curve is displayed (green). Bar color displays MIS 2 stage. 74

Figure 24 Summary results of MASS-III-07. Clay mineral assemblages (%) for <2μm particles non-calcareous clay; kaolinite, chlorite, illite, smectite, smectite/(illite+chlorite) ratio (blue), illite chemical index, and illite crystallinity versus age (ka BP). Planktonic foraminiferal G. ruber $\delta^{18}O$ curve is displayed (green). Bar color displays MIS 2 stage. 75

Figure 25 Ternary diagram of the averaged clay mineral assemblages by 3 end members; illite+chlorite, kaolinite and smectite of the studying sediment groups. The clay mineral formation are indicated into various provinces as the difference shade; four provenance provinces surrounding the Andaman Sea combined with the clay assemblages of four sediment cores. 77

Figure 26 Ternary diagram of the averaged clay mineral assemblages by 3 end members; (illite+chlorite, kaolinite and smectite). The clay mineral assemblages in the orange shade is presenting the study core distribution. ADM 2 is presented in a) and ADM 6 is present in the b) figure. The purple circle is representing the MIS 1 sediment, the red triangle is representing the MIS 2 sediment, and the green sign is representing the MIS 3 sediment. The

four provenance provinces surrounding the Andaman Sea in different shades are presented. 78

Figure 27 Ternary diagram of the averaged clay mineral assemblages by 3 end members; (illite+chlorite, kaolinite and smectite). The clay mineral assemblages in the orange shade is presenting the study core distribution. MASS-III-10 is presented in a) and MASS-III-07 is present in the b) figure. The purple circle is representing the MIS 1 sediment, the red triangle is representing the MIS 2 sediment, and the green sign is representing the MIS 3 sediment. The four provenance provinces surrounding the Andaman Sea in different shades are presented. 79

Figure 28 Major element variation of (% of total vol.); SiO_2, Al_2O_3, TiO_2, K_2O, CaO, K_2O/SiO_2 ratio (blue), K_2O/Al_2O_3 ratio (blue) versus age (ka BP) and planktonic foraminifera (G.ruber) $\delta^{18}O$ curve (green) are displayed. a) ADM 2 b) ADM 6. 83

Figure 29 Smectite/(illite+chlorite) ratio a) ADM2 b) ADM6, Major element ratio of K_2O/SiO_2 c) ADM2 d) ADM6, $\delta^{18}O$ (*G. Ruber*) curve e) ADM2 f) ADM6, g) global sea level (Waebroeck et al, 2002). Dash curve presents insolation curve calculated for September at 10^0N by using Analyseries software (Paillard et al., 1996). Shaded bars show the ages of Heinrich events H1, H2 (Hemming et al., 2004), Younger Dryas (YD; 13-11.5 ka) (Alley, 2000), Bølling/Allerød (B/A; 15–13.5 ka), respectively (Sijinkumar et al., 2010). 86

Figure 30 Smectite/(illite+chlorite) ratio a) MASS-III-10 b) MASS-III-07, Major element ratio of K_2O/SiO_2 c) MASS-III-10 d) MASS-III-07, $\delta^{18}O$ (G. Ruber) curve e) MASS-III-10 f) MASS-III-07, g) global sea level (Waebroeck et al, 2002). Dash curve presents insolation curve calculated for September at 10^0N by using Analyseries software (Paillard et al., 1996). Shaded bars show the ages of Heinrich events H1, H2 (Hemming et al., 2004), Younger Dryas (YD; 13-11.5 ka) (Alley, 2000), Bølling/Allerød (B/A; 15–13.5 ka), respectively (Sijinkumar et al., 2010). 89

Figure 31 Illustration of the paleoshoreline during; a) highstands at modern shoreline and lowstands at sea level dropped b) -40 m c) -70 m and d) -120 m during the LGM period (Awasthi et al., 2014)..... 91

LIST OF TABLES

Table 1 Drainage area, runoff, and observed suspended sediment discharge of major rivers flowing directly into the Andaman Sea. 29

Table 2 Summary of sediment materials 34

Table 3 Summary of sediment samples used in this study. 34

Table 4 ^{14}C AMS ages of ADM2 calibrated using Calib program version 7.0.2. 48

Table 5 ^{14}C AMS ages of ADM6 calibrated using Calib program version 7.0.2. 50

Table 6 ^{14}C AMS ages of MASS-III-10 calibrated using Calib program version 7.0.2. 52

Table 7 ^{14}C AMS ages of MASS-III-07 calibrated using Calib program version 7.0.2. 54

Table 8 Summary of ages of the studied cores in the southern Andaman Sea. 56

Table 9 Average clay mineral assemblages and illite chemical index of surface and core top sediments from different provinces surrounding the Andaman Sea with standard deviation values. 59

CHAPTER 1

INTRODUCTION

1.1 Rationales

Fluvial sediments eroded from drainage systems are transported and mostly deposited on the continental shelf and slope of the marginal seas (Liu et al., 2016). Marginal seas connect continents with open oceans, hence they are significant geological units located in the transition zone extending from the continents to the oceanic lithosphere. The marginal seas are areas where the lithosphere deforms and sediment accumulates. Thus, geological research on marginal seas is associated with key scientific issues, such as source to sink characterization, global structural dynamics, oceanic environmental processes, and global climate system impacts. Geological research on marginal seas is a well-established scientific discipline that seeks to understand at advanced levels the continental margins. Consequently, marginal seas are the last sediment pathway to the ocean. Sediment formation on the seafloor is due to sediment transfer from the continental crust to the oceanic crust. The deposition process has significant effects on the sedimentary sequences that can be preserved to record global and regional sea level changes, climate change, lithosphere deformation, oceanic circulation, and biogeochemical cycles. Therefore, the continental margins play an important role in land-sea interaction processes. The earth's continental margins respond to external forcing such as climate and internal forcing such as tectonic; the sediments found in the seabed of the marginal seas provide a long-term record of the interactions between these external and internal forces (P. A. Allen & Allen, 2013).

The study of marine geology related to the complete spectrum of sediment processes from source to sink is known as the sediment routing system (Philip A. Allen, 2008). Sediment is moved from a source to a sink - from the erosional engine of mountainous regions to its eventual deposition - by the sediment routing system as shown in Fig. 1, which diagrams the overall sediment dispersal system. Erosional and depositional areas are connected in the sediment routing system. The long term evolution of erosion and deposition locations are connected by sediment fluxes on short time scales and variations in the erosional products are directly related to changes in precipitation over the continent (source areas) (Ahmad et al., 2005). Sediment fluxes are associated with physical, biological and chemical processes, each of which impacts the transport of particulate sediment. The source to sink system provides a particularly important historical archive of past and present global change. Hence, the study of marine sediments also plays a role in understanding the processes of environmental change.

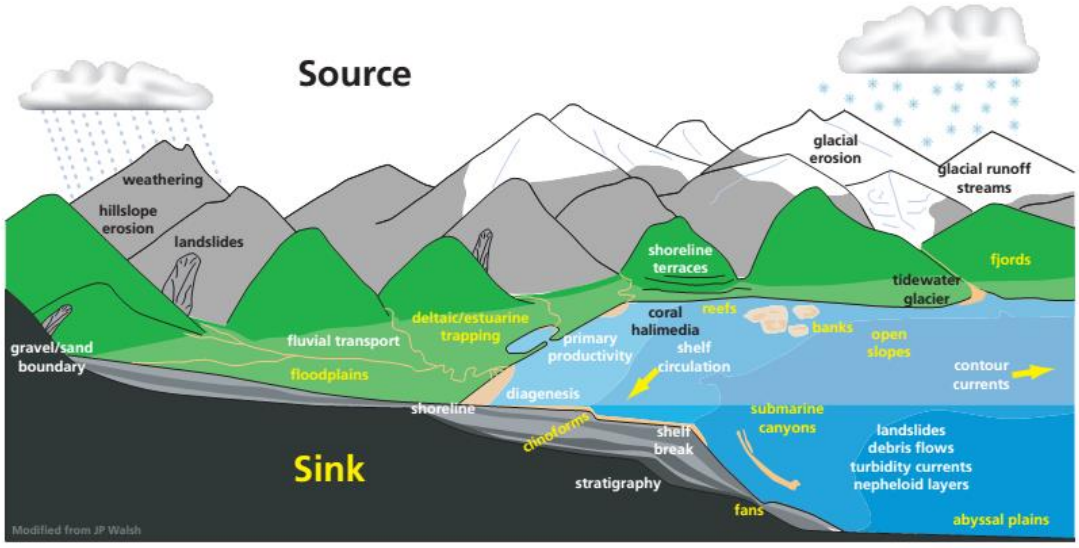

Figure 1 Schematic of a generalized sediment dispersal system showing the source to sink system. Sources are indicated by black text, sinks are yellow, processes are shown in white italics, and locations in white regular (National Science Foundation, 2004).

Marginal seas are ideal areas to study sediment source to sink transport processes; semi-enclosed systems are especially useful because the sediment budget and transport pathways can be more easily defined. The Andaman Sea is a unique marginal sea and is considered a semi-enclosed system due to it being surrounded by continents and islands. The Andaman Sea is located in the northeastern Indian Ocean but is obviously separated from the Bay of Bengal and the Indian Ocean by the oceanic ridge. The Andaman Sea offers a good place for studying the source to sink system among global marginal seas (Wang and Li, 2009; Liu et al., 2016). The terrigenous sediments in the Andaman Seaconvey various inputs of continental and oceanic transport, making the Andaman Sea an excellent area to establish the relationship between erosion and climate (Joussain, 2016b) (Fig. 2).

Sediments are defined as solid fragmental materials that originate from weathering of rocks and are transported by, suspended in, and deposited by many factor such as wind, water, ice, etc. During transportation to the depositional site, sediment may experience geochemical changes that cause sediment composition to differ from its parent rock (Sompongchaiyakul, 1989). The degree of this change depends on the depositional environment and the original sediment composition.

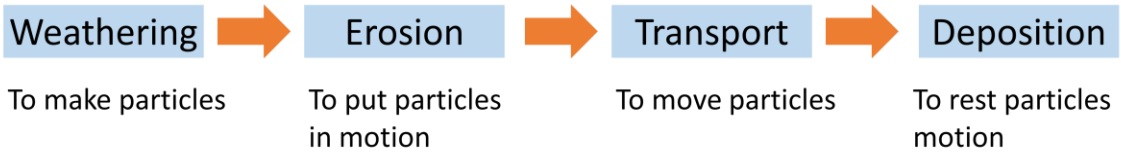

Figure 2 The sediment dispersal pathway from its originated source through the process to sink environments (the sediment routing system).

Provenance analysis in the past was centered on the general mineralogical properties of sand and sandstone samples, and on the specific content of distinctive heavy minerals. Heavy minerals, in particular, acted as

fingerprints for source areas and so could be used to reconstruct the parent rocks in eroding source regions (Philip A. Allen, 2008). Now, geochemical methods are better suited for provenance study; clay mineralogy is regularly studied to reconstruct paleoenvironmental evolution at different timescales. Clay mineral assemblages also provide information on the weathering environment; the relative formation of particular clay minerals depends on the balance between physical erosion and chemical weathering in the source regions before they are eroded and transported to the ocean (Chamley, 1989; Thiry, 2000).

Paleoclimatology is the study of past climates. Since it is not possible to go back in time to see what climates were like, scientists routinely use the imprints created during past climates, known as proxies, to interpret paleoclimate. Over the different time scales, long term variations can indicate the weathering history and on short time scales can investigate variations in the erosional products which are directly related to the changes in precipitation variation.

A major component of precipitation in the study Andaman Sea (the study area) is termed the Indian monsoon (or South Asian monsoon). The Indian monsoon results from differential land-sea heating and induces seasonal variations in precipitation and runoff (Webster, 1987). The Indian monsoon plays an important role in sediment transportation and also the Andaman Sea productivity. Sediments deposited in the Andaman Sea basin have recorded past environmental changes including not only the runoff fluctuation from the major rivers but also the Asian monsoon variability (Ali et al., 2015).

Clay mineralogy and grain-size sedimentology studies have been utilized to constrain the sedimentary sources, the dynamics of sediments transport to the Andaman Sea, and the degree of chemical weathering of the Andaman Sea sediments. These studies have utilized a variety of approaches (e.g., XRD analyses, laser siliclastic grain-size analyses) to reconstruct the

intensity of erosion, the dynamics of sediment transport and diagenesis processes (Bouquillon et al., 1989; 1990; France-Lanord et al., 1993; Fagel et al., 1994; Colin, 1997; Colin et al., 1999; Joussain et al., 2016b). Moreover, major element contents of sediments can be used to assess the state of chemical weathering of detrital sediments (Lupker et al., 2013; Joussain, 2016b) and/or the degree of chemical weathering of sediments exported from the sources at the present time and in the past (Galy and France-Lanord 2001; Colin et al., 1998; Lupker, et al, 2012; 2013). Therefore, it is possible to reconstruct by these investigation (clay mineralogy, grain-size, and element geochemical composition of marine sediment cores, located off river mouths) the sedimentary sources of river basins and the state of chemical weathering of sediments transferred to the ocean (Colin et al., 2006; 2010; Sirocko et al., 2000; Liu et al., 2004; 2005; Zhao et al., 2011; Joussain et al, 2016a). This, in turn, is related to paleoclimatic and paleoenvironmental changes of the Andaman Sea. Consequently, changes in monsoon intensity should therefore modify both sediment transfer and its weathering signatures.

1.2 Review of previous study

The Andaman Sea basin is one of the important active back-arc basins of the world (Raju et al., 2004; Curray, 2005). According to related studies, much of the Andaman Sea basin in general is considered a confined area. The Andaman Sea is located between the Irrawaddy delta coast of Myanmar, which extends 1,200 km southward to Sumatra and 650 km width in the east – west from the Malay Peninsula to the Andaman Islands. The Andaman Sea occupies a unique position as a marginal basin in Southeast Asia geography (Khan and Chakraborty, 2005) between the Burma–Java subduction margin in the region of subduction of the Indian plate beneath the Eurasia plate. Accordingly, it caused clockwise rotation of the subduction zone and increase in

obliquity of the convergence. This convergence is partitioned into two components comprising both trench subduction and forces parallel to the trench, which generate strike-slip motions along the major fault systems (Spencer, 2007). Curray (2005) observed that the rate of strike-slip motion in the Andaman Sea increased and extensional basins opened obliquely by the combination of back-arc extension and the strike-slip motion with more oblique convergence due to earth's rotation. In terms of timing of tectonic activity, the region has been significantly affected by at least three major geological events over the last 50 Ma. Approximately 50 Ma changes in the plate boundaries from the collision of India with Eurasia resulted in mountain building that led to major changes in both habitats and climates and was accompanied by significant changes in drainage systems, forcing huge volumes of sediment to move southward (Hall, 1998; Brown, 2007). The second event occurred ~25 Ma, the plate boundaries and motions changed once more, possibly due to the collision between the north Australian margin and arcs to the north. This tectonic event was probably very important in terms of biogeography, because it led to new links between Australia and Southeast Asia across areas which included many shallow marine habitats (Brown, 2007). The last event is more complex and/or contentious. Many studies concluded that the Andaman Sea showed active spreading only during the past 4–5 Ma, while others argue that spreading took place in two phases, one in the middle Miocene (~11 Ma) and another in the late Miocene–early Pliocene (4–5 Ma). Khan and Chakraborty (2005) confirmed that their model favored middle Miocene (~11 Ma) spreading and opening of the Andaman Sea; Hall (2002) referred to the last evolution as strongly contested in recent times. Accordingly, tectonic and lithological settings on land form the various topographies and generate interactions between sources and sinks sediment routing system. Therefore, the interaction on land responds to external forcing (e.g., climate) and internal forcing (e.g., tectonic) as can be determined by the study of terrigenous sediments.

The assemblage of bedrocks found on the Andaman Sea are well described by the surrounding regions of the Indo-Burma ranges. The catchment rocks of the Irrawaddy delta system consist of Cretaceous-Cenozoic flysch of the Indo-Burman ranges, Eocene-Miocene-Quaternary sediments of the Myanmar Central Basin, Late Precambrian, and Cretaceous-Eocene metamorphic/basic/ ultrabasic rocks of the eastern Himalayan syntaxis (Bender, 1983; Robinson et al., 2014; Licht et al., 2013; Awasthi et al., 2014; Ali et al., 2015). The catchment rocks of the Salween consist of magmatic rock and Precambrian to Tertiary sedimentary, igneous and metamorphic rocks of the Shan Plateau/Sibumashau block (Bender, 1983). The main islands of the Andaman Islands (North/Middle/South) are almost entirely made up of mafic and ultramafic rocks of the Cretaceous ophiolite sequence and sedimentary rocks derived from them (flysch deposits). The bedrock of the Malay Peninsula consists mainly of Paleozoic–Mesozoic granite and granodiorite and Paleozoic sedimentary rocks and minor Mesozoic (mainly Jurassic–Cretaceous) sedimentary rocks and sparse basic volcanic rocks develop in the central part of Malay Peninsula (Liu et al., 2012). Sumatra is covered mainly by Quaternary (mainly Holocene) intermediate to basic volcanic rocks in mountainous ranges and slope of the southwestern island and by late Tertiary sedimentary rocks in the plain of the northwestern island (Liu et al., 2012). Accordingly, the lithology of parent rocks in drainage basins (Liu et al., 2009) play a significant role in the weathering processes (Liu et al., 2012). Consequently, the related geological studies in the surrounding area of the Andaman Sea explained the tectonic activity may become one of major controlling factors on the weathering in these regions. Moreover, the available bedrock data in these regions can designate the origin and provenance of the sediment. However, there are only a few studies on multiproxy analyses of sediment cores from the Andaman Sea [e.g., Colin et al., 1998, 1999, 2006; Fontugne and Duplessy, 1986; Rashid et al., 2007, Kurian et al., 2008, Sijinkumar et al., 2010, Awasthi et al., 2014; Ali et al., 2015, Cao et

al., 2015b] and only one provides a semi continuous record for the last 280 ka [Colin et al., 2006]. Therefore, the use of multiproxy studies is still required to develop the sedimentary history in the Andaman Sea.

A comprehensive study of high resolution terrigenous based proxies in the Andaman Sea would help to explain changes recorded in the sediment. The study of sediments by multiproxy analyses of the Andaman Sea are mostly focused on deep sea sediments; these sediments were derived from a combination of processes during sedimentary cycles such as sedimentary source variations, sediment dynamics of transfer from land to sea, dynamics of sediment transport in the ocean (oceanic currents), and other related processes (Joussain, 2016b). The massive quantity of sediment produced from these processes is carried by rivers into the Indian Ocean, dispersed by ocean surface currents, and deposited in the deep sea (Awasthi et al., 2014). Therefore, deep-sea clastic sediments from the northeastern Indian Ocean (particularly in the southern Andaman Sea) provide important archives of past monsoon fluctuations as a function of changes in sediment provenance, tectonic activity in the source regions, and changes in ocean circulation and dispersal patterns. These temporal changes can be investigated by multi-proxy approach, combining mineralogical (clay mineral), sedimentological (gain size), and geochemical (major element contents and isotopic ratios) analyses to constrain all sedimentary processes. Clay mineral assemblages in marine sediments are a significant proxy to differentiate source possibility, propagation of water masses and to investigate ocean systems. In addition, clay mineralogy is suggested to differentiate the source of terrigenous sediments and marine sediment and to demonstrate geological conditions such as weathering processes (Gingele et al., 2001). Moreover, the fined-grained clay minerals can be used to determine the distance from the sediment original source and settlement pattern. The distribution in the main group of clay minerals (i.e.,smectite, illite, kaolinite and chlorite) can be used to illustrate sedimentological processes. The clay minerals in soils are

generally produced from weathering of parent rocks, including physical weathering, which leads to rock fragmentation, and chemical weathering. The provenance of sediment, investigating the intensive chemical weathering is identified form different provenance from both clay mineralogical and geochemical results in the surface sediment (riverine) regardless of their various lithological and tectonic settings in the southern Andaman Sea (Liu et al., 2012; Liu et al., 2016). In addition, the chemical weathering intensity increases gradually suggested that the monsoon climatic condition with constant warm temperature and abundant precipitation throughout the year is the principal forcing factor on the chemical weathering (Liu et al., 2012). The major element is used to examine the geological sediment from various sources especially major river dispersal. The major element for bulk and clay-fraction sediment is resulted to quantify both the intensity of chemical weathering and their various lithogical and tectonic settings (Liu et al., 2012). Moreover, the siliciclastic grainsize, combined with major elements, useful for constraining in order to constrain sediment transport dynamics (Joussain, 2016a). Therefore, the terrigenous sediments from land convey mixed signals of continental environment and oceanic transport, making the Andaman Sea a preserved study area of the land-sea interactions.

The Andaman Sea is dominated dispersed by the surface currents, these currents carry fine-grained sediments from the Ganges in the Bay of Bengal into the Andaman Sea and then spontaneous contributions from the Irrawaddy and Salween along their pathway and allocate these within the Andaman Sea. Therefore, the sediments deposited in the Andaman Sea record the erosion and weathering history of the Indo-Burman Ranges (Colin et al., 1999) as the main source contribution. There are few studies of circulation in the Andaman Sea but there is general agreement that during the summer monsoon surface currents enter the Andaman Sea from the Bay of Bengal through the Channel (between Myanmar and the Andaman Islands) and the Ten Degree Channel (south of the

Andaman Islands) and generally flow toward the south east forming a clockwise circulation, and exiting through the Great Channel between the Nicobar Islands and Sumatra (Rizal et al., 2012). These dispersals recognized to a variation of the prevailing surface circulation pattern influenced by the relative changes of monsoons intensity. The Indian monsoon is further divided into two major components of the Indian monsoon; the South West (SW) or summer monsoon and the North East (NE) or winter monsoon (Rodolfo, 1969b; Brown, 2007). The surface sediment distribution is mainly sourced form Irrawaddy discharge such a study of grain size distribution of Rao et al., (2005) showed the conclusion the surface distribution is controlled by the local turbidity current and the modern fine-grained sediments of outer shelf sands of Irrawaddy River are deposited probably during the Holocene transgression. Moreover, more investigation of organic matter associated with fine-grained sediment deposition in the inner shelf of Andaman Sea is well explained the control factor is a strong tidal current and confirmed the provenance source is from Irrawaddy river input by Ramaswamy et al., (2008). While the offshore sediment of recent studies (Ramaswamy et al., 2004) showed the sediment influx from the major rivers is transported along the shelf by monsoon driven currents and carried to the deep seafloor through submarine canyons by surface sediments. As their outcomes, the Irrawaddy continental shelf and the Gulf of Martaban are covered by a modern inner-shelf mud belt while the outer shelf is covered with relict sands and carbonates (Rodolfo, 1969) that the inner shelf (the Martaban canyon) incises the continental shelf and may serve as the conduit for transport of sediments to the deep Andaman Sea. The surface or riverine sediment study are not for only tectonism, landform, and climate study (Liu et al., 2007) but also describing of lithology of parent rocks in drainage basins (Liu et al., 2009) which play a significant role in the weathering processes (Liu et al., 2012; Liu et al., 2016). Therefore, the modern deposition of surface sediments is a key to understand their paleoenvironment and paleoclimate in the present time.

The reconstruction of paleoenvironment and paleoclimate change in the Andaman Sea in the glaciation period are developed by multiproxy study. As the results as example study by Cao et al., (2015b) about grain-size, major elements and Sr–Nd isotopes study in the sediment core. This results showed the common source of the Andaman Sea is from the Irrawaddy River by the Sr–Nd isotopes, the sensitive grain-size population indicated the control factor is under the sea-level change in the last glaciation while the present time the control factor of grain size is influence by the current transport driven by the Indian Summer Monsoon, and chemical weathering by major element (K/Al) and terrigenous input (Ti/Ca) coupled with sensitive grain-size revealed that the Indian Summer Monsoon was weak during glacial time and then strong in the Holocene. Moreover, the paleoclimatology study by Colin et al., (1998; 1999) found the long and short term of climatic variation in sediment record and showed strongly effected for the sedimentation in central Andaman Sea is by the seasonal reversals. Besides the period of glacial and interglacial that has been recorded in the result of oxygen isotope ($\delta^{18}O$) and dating by Carbon-14, the reconstructions of major hydrological sea surface current is documented. Hence, the microfossils benthic foraminifer are wildly used as paleoceanography proxies for study paleotemperature, ice volume, water masses movements and paleoproductivity (Wefer et al., 1999; Rohling and Cooke, 1999). Benthic foraminifera are common in marine sediments and dominate to preserve and represent for oceanographic and palaeoceanographic studies (Murgese and DeDeckker, 2005). Not only the paleo-recording is showed the sea level changing in term of differentials of sediment erosion and remobilizing within 23 ka and the paleoclimatic record in element analysis by Rashid et al., (2007) showed the sedimentation rate during the Holocene and last glaciation within 10.07 cm./ka and 17.8 cm./ka respectively and influenced to the sedimentation here is under the monsoon system but also the rare earth element variation in central Andaman Sea is descripted also related to the sea level change in glacial and interglacial

transition that covering a record of past 40 ka. (Alagarsamy et al., 2010). Moreover, the palaeoclimatic studies in Andaman Sea found the reconstruction of long-term East Asian paleo-monsoon intensity variations using proxies like grain size, magnetic susceptibility or clay mineral distribution (Boulay et al., 2005) to find the correlation of the summer monsoon during glacial periods which showed the monsoon intensity was weaker, whereas the winter monsoon was strong in the present time. Consequently, the modern monsoon study indicates that the Indian monsoon (or the south Asian monsoon) is characterized by seasonal changes in wind direction and moisture, giving rise to the summer monsoon and the winter monsoon (Webster, 1994). However, the understanding in the Indian monsoon changed in the past and its variation controls is poorly known.

For these reasons, the Andaman Sea is one of the interesting area attention in the paleoenvironmental and sedimentological studies. Few research conducts in the Andaman Sea is not well expressed the complex of the environmental changes in this area. This study will allow to find the understanding in the continental provenance and reconstruct the paleoenvironmental changes under the Indian monsoon.

1.3 Objectives and significance of this study

In the present study, high-resolution terrigenous records from sediment cores (four sites) in the southern Andaman Sea are presented. Clay mineralogy, X-ray fluorescence (XRF) element core scanning, and XRF elemental geochemistry are performed to investigate the variations of terrigenous inputs to the southern Andaman Sea since the last glaciation. The main research objectives are;

1) To reveal clay mineral assemblages in surface sediments of the Andaman Sea for understanding possible transport process at the present time.
2) To understand the clay mineral variation since the last glaciation and determine the provenance source sedimentary dynamics during the transport process.
3) To reconstruct the Indian monsoon evolution based on grain size, elemental geochemistry, and clay minerals.
4) To explore the possible mechanism of marine environmental evolution driven by climate change since the last glaciation.

CHAPTER 2

GEOLOGICAL AND ENVIRONMENTAL BACKGROUNDS

This Chapter is to introduce the geological setting, climate condition and oceanography, and river discharge surrounding the Andaman Sea. The Andaman continent and the serve respectively as the "source" and "sink" of terrigenous sediments studied in the present work. Focusing of this southern Andaman Sea on the continental shelf, because it is mostly covered by sediments that represented the "sink" area from the surrounding "source" along the continental shelf.

2.1 Geological setting

The Andaman Sea basin is one of the important active basins of the world which locates in the northeast of Indian Ocean. Generally, the Andaman Sea comprises of; areas extends north to south from Myanmar to Sumatra, and east to west from the Malay Peninsula to the Andaman and Nicobar islands. Accordingly, the Andaman Sea is active basin it could be divided by the different of tectonic characteristics into three parts (Jintasaeranee et al., 2012); the southwestern part (active N-S fault systems), the western part (volcanic areas), and the eastern part (distinctly smooth flat areas). The southwestern part is dominated by N-S trending fault systems (Raju et al., 2004) as Fig. 3. The western part has been separated by corresponding to the Andaman-Nicobar backarc spreading ridge (Rodolfo, 1969a) connected to the central basin. The central basin expressed of the ridge from the Bay of Bengal which covered 600,000 km^2, average water depth at 1,100 m to 4,400 m maximum in the western side (Dutta et al., 2007). The average depth of the Andaman Sea is about 870-1100 meters (Gebregiorgis, 2017). Moreover, the western part is dominated by volcanic constructs connected of backarc spreading activities (Rodolfo, 1969b). The East Andaman Basin and the Mergui Basin formation consequences from backarc spreading extensional tectonics, active throughout the area (Chakraborty and Khan, 2009; Curray, 2005; Schwab et al., 2012). The rifting part moved from the Mergui Basin over the East Andaman Basin during Oligocene to Pliocene, due to oblique changing of convergent margin of Australian or Indian plate and the Eurasian or Southeast Asian plate (Curray, 2005). Consequence, the Mergui ridge separates two contiguous basins, in the west is the East Andaman Basin and the Mergui Basin in the eastern and southeastern part of Andaman Sea which they are extended in NNE–SSW trending (Schwab et al., 2012). Thus, the sedimentation evolution is linked to typical rifting stages (Doust and Noble, 2007; Doust and Sumner, 2008; Jha et al., 2010; Schwab et al., 2012). Furthermore, the sediment had been filled in the southwest sub-basin of the Andaman Sea (Curray, 2005).

The third part, the eastern and the southern margin of Andaman Sea are between by the Burmese Archipelago and the Sumatra Islands (Jintasaeranee et al., 2012).

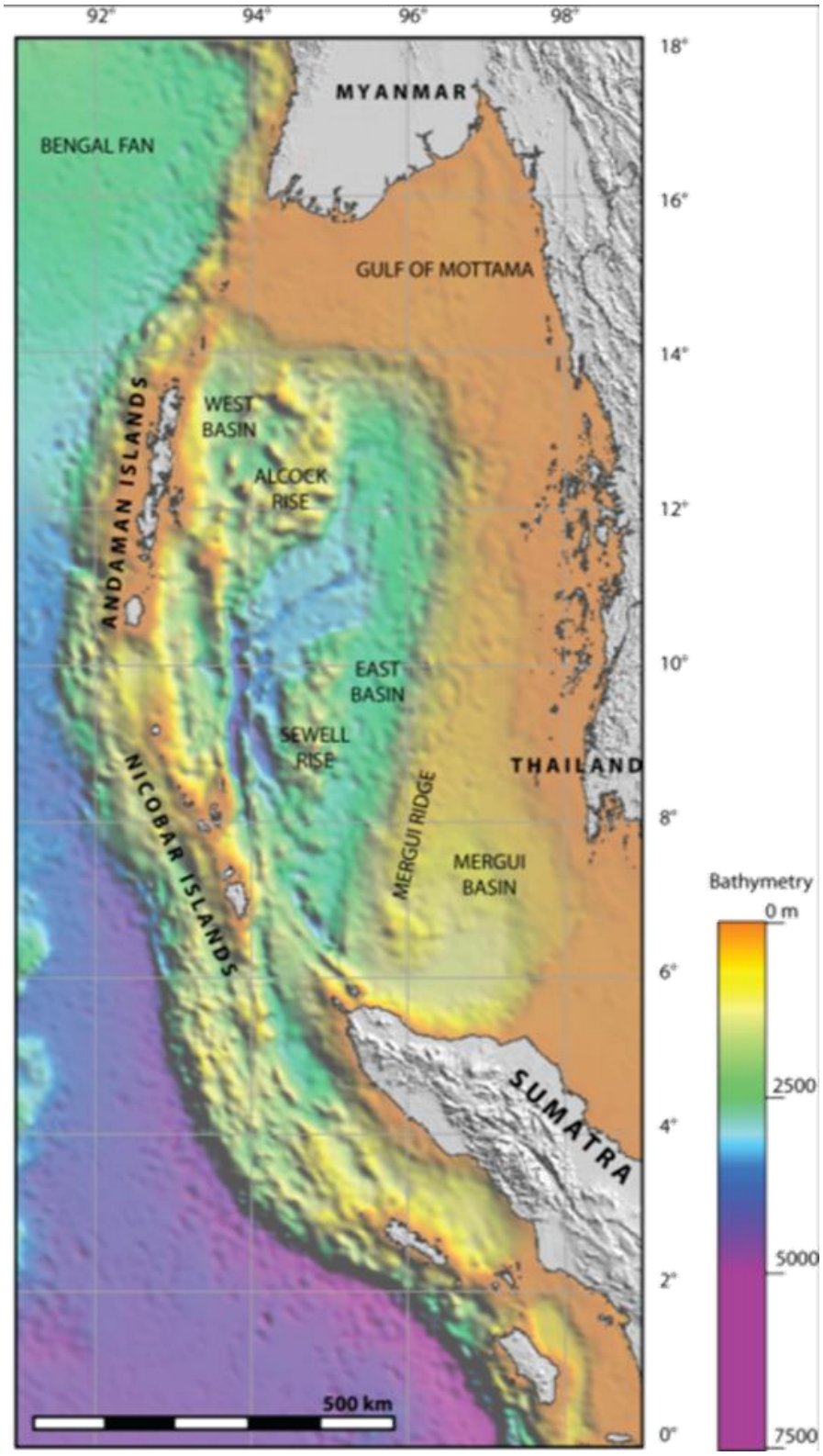

Figure 3 Bathymetric map of the Andaman Sea

The eastern Andaman Sea particularly the studied area which is considered a semi-enclosed sea extend to the Mergui Basin in southeastern Andaman Sea (Curray et al., 2005). The eastern continental shelf extends from the norther part off Irrawaddy and Salween delta along the eastern part to the south which connected to Malacca Strait (Rodolfo, 1969b). The eastern Andaman Sea extends southward from Irrawaddy delta to Sumatra and the Malacca Strait for 1,200 km (Rodolfo, 1969b) which is particularly smooth and mostly cover the flat area along the continental shelf (Raju et al. 2004). The sediment in the eastern is well flat-laying on the sea floor covers of least 4,600 m in the thickness of the sediment layers (Curray, 2005). Sediment distribution of this area is strongly dependent on tidal currents and seasonally reversing monsoon currents (Ramaswamy et al., 2004; Rao et al., 2005).

In addition, the various topography in Andaman Sea has been mentioned to obviously control the sedimentation mechanism and is significantly considered to study the sedimentation, the sediment deposition pattern in this area. Therefore, the sediment supply process here is well in examination the evolution of Andaman Sea. According to the sediment in Andaman Sea has been supplied from the southeast of the Bay of Bengal, south of Myanmar, west of Thailand and east of the Andaman Islands, India (part of the Indian Ocean) and Malacca strait, the Andaman Sea sediment also have been recorded for the major of terrigenous sediments input supplied from the major riverine inputs from the northern part while the other sediment are from the islands and strait.

2.2 Climate condition and Oceanography

Andaman Sea is significantly influenced by the South Asia monsoon (or Indian monsoon) (Rodolfo, 1969b; Rao et al., 2005; Robinson et al., 2007). This study will call Indian monsoon. Since the Indian monsoon (or South Asian monsoon) plays an important role in the sediment transportation and also the Andaman sea productivity, the sediments deposited in this basin have recorded the past environmental changes not only the runoff fluctuation from the major rivers but also the Asian monsoon variability (Ali et al., 2015). The Indian monsoon results from differential land-sea heating and induces seasonal variations in precipitation and runoff (Webster, 1987). Indian monsoon consists of two prevailing monsoon seasons; Southwest monsoon and Northeast monsoon (Fig. 4) as known as summer monsoon and winter monsoon. Andaman Sea is strongly affected by summer winds which dramatically drives the westerly current to the prevailing south-easterly current, resulting in the transportation of riverine sediment moving eastward along the inner shelf of Andaman Sea (Rodolfo, 1969b; Ramaswamy et al., 2004; Rao et al, 2005). On the contrary, the winter winds cause south-easterly currents to westerly currents. These variations have been recognized to a variation of the prevailing surface circulation pattern influenced by the relative changes of the summer and winter monsoons intensity (Joussain et al., 2016b). According to the monsoon driven, surface current variation through time significant controlled sediment provenances in Andaman Sea (Ahmed et al., 2005; Awasthi et al., 2014; Joussain et al., 2016b).

2.2.1 Climate conditions

Monsoon variation

The weather and climate condition of Andaman Sea are primarily influenced by the Southwest monsoon and Northeast monsoon and the short transitional periods between these two monsoons. The three monsoon seasons of Andaman Sea are as follows; 1) The summer monsoon (during June to September) is characterized by cloudiness, overcast skies, light rain almost daily, interspersed with rain squalls or thunderstorms, rainy season. 2) The winter monsoon brings less cloudy, scant rainfall, mild temperatures, and lower humidity weather during winter (December to March), cool season. 3) The transition period between the monsoons; hot season (spring) during April and May and autumn transition during October and November period is quite similar which are governed by the inter-tropical convergence. Mostly part of Andaman Sea is under influence by the Inter-Tropical Convergence Zone (ITCZ), that moves seasonally over the area (northwards in spring and southwards in autumn), with no well-defined weather pattern.

The influence of the ITCZ of the Andaman Sea on the climate pattern is lowest in summer (e.g., during the southwest monsoon period). Monsoon circulation in two hemispheres are characterized by seasonal migration of the solar zenith angle, which leads to annual migration of the equatorial trough ITCZ north and south of the equator (Fig. 4). The southwesterly monsoon winds bring abundant moisture from the warm waters of the tropical ocean to the Asian continent during boreal summer and displays a remarkably consistent annual cycle (Gebregiorgis, 2017). The amount of seasonal rainfall delivered by the monsoon winds.

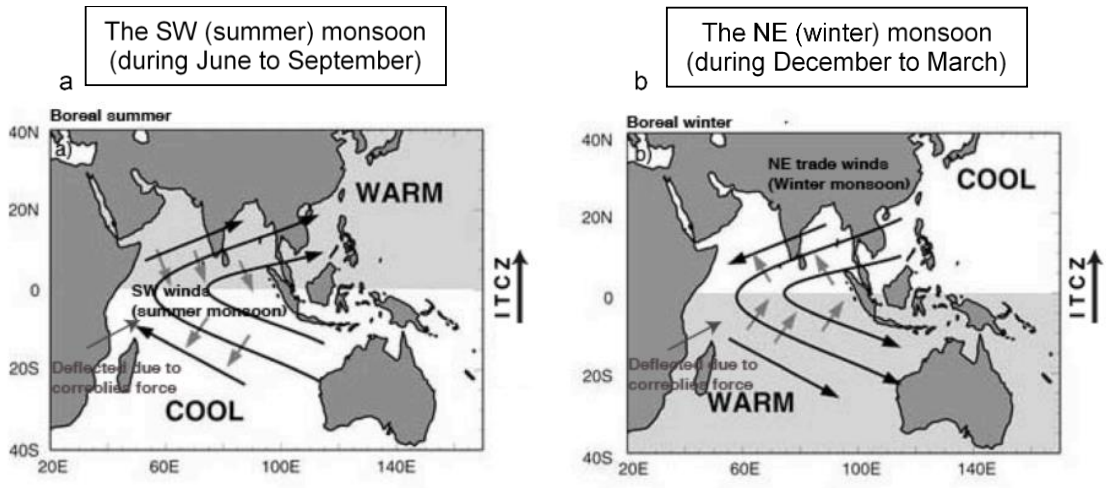

Figure 4 Overview of the South Asian Monsoon (SAM), the monsoon is a giant sea breeze that is fundamentally driven by differences of heat capacities between land and ocean, and following temperature differences between warmer land and cooler ocean surfaces. a) Winds generated after Southwest (summer) monsoon b) Winds generated after Northeast (winter) monsoon (modified from Loschnigg and Webster, 2000; Gebregiorgis, 2017)

2.2.2 Oceanography

The Andaman Sea locates under the effects of the South Asia monsoon or called “Indian monsoon” systems. Generally, winds of the SW monsoon (summer winds) blow steadily at rate more than twice of the NE monsoon (winter winds). Arrival of strong summer winds dramatically drive the westerly current to the prevailing south-easterly current resulting in the transportation of riverine sediment moving eastward along the inner shelf (Rodolfo, 1969b; Ramaswamy et al., 2004; Rao et al, 2005). On the contrary, the winter winds cause south-easterly currents to westerly currents. The north-westward current in the Malacca strait is generally restricted to the northern part of Sumatra. The sediments would have forced and transported by Sumatra streams

from the strait into the south Andaman Sea throughout the year as the density flows (Rodolfo, 1969b).

Surface Circulation

The Andaman Sea surface circulation study is limited, therefore, the oceanography information of Bay of Bengal will imply to understand the Andaman Sea circulation. The overview circulation of the Indian Ocean is strongly influenced by the seasonal reversal of the monsoon winds Tomczak & Godfrey (1994). The northeast monsoon is established the North Equatorial Current runs as a narrow current from the Malacca straits to southern Sri Lanka passing through the Andaman Sea. The transition from northeast to southwest monsoon is characterized by the easterly moving, intense Indian Equatorial Jet first described by Wyrtki (1973). While the southwest monsoon is fully established (July–September), the northern Indian Ocean is dominated by the eastern flow of the South West Monsoon Current which enters the Andaman Sea via the Bay of Bengal (Tomczak & Godfrey 1994).

A comprehensive review of oceanography of the Bay of Bengal and Andaman Sea is provided by Varkey et al. (1996) and combines actual observations by Varkey (1986) with results of a simulation model driven by climatological monthly mean winds (Potemra et al. 1991). Potemra's model was a four-layer isopycnal model that used the 200-m contour as the land boundary. Both Varkey et al. (1996) and Potemra et al. (1991) described surface circulation in the Andaman Sea as a double gyre with anticlockwise flow during the northeast monsoon and clockwise flow in the southwest monsoon. Earlier work by Soegiarto & Birowo (1975) and Soegiarto (1985) and simulations using the Ocean Circulation and Climate Advanced Model (OCCAM) do not reflect these gyres but do broadly agree on the predominant direction of current flow throughout the

year as shown in Fig. 5. This figure is probably an overly simplistic representation of current flow but is the best available at the present time. The earlier model used by Potemra et al. (1991) suggests surface flow enters the Andaman Sea south of the Nicobar Islands during the northeast monsoon and exits south of the Andaman. During the southwest monsoon flow enters from the Bay of Bengal, circulates clockwise and exits via the southern Andaman Sea.

The highly dynamic nature of the Andaman Sea is reflected in current flow at depth (>200 m) where Potemra et al. (1991) suggested that flow changes direction three times a year. In January, February and March flow is clockwise; between April and July it is anticlockwise; from August to October it becomes clockwise before reverting to anticlockwise in November and December. The water flowing is depended on the wind variations. Generally, Andaman Sea currents moves to the northeast generally persist longer and movement at greater speed because of the stronger southwest monsoons. An important vertical circulation in the Bay of Bengal and Andaman Sea is upwelling, sub-surface water is brought upward to the surface, and conversely downward occurs downwelling or sinking as well as at the nearshore or coastal zone.

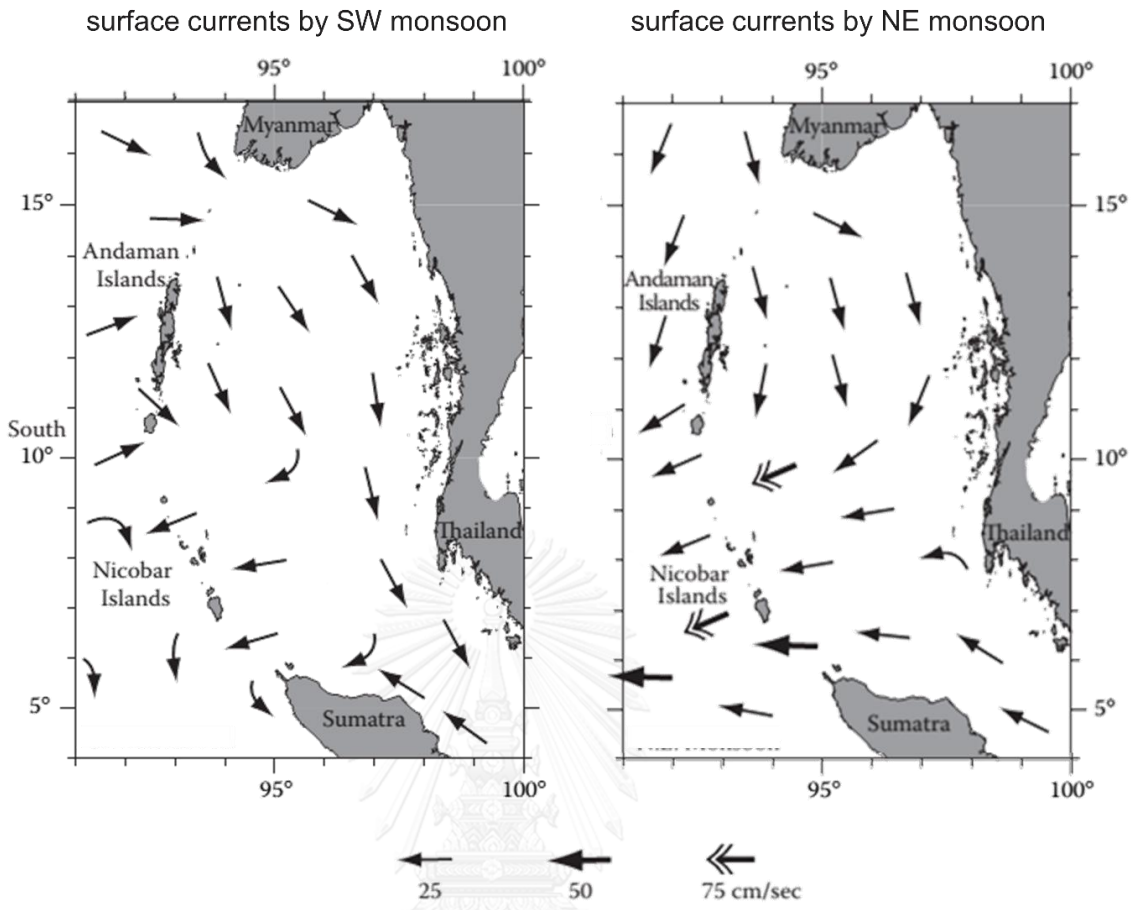

Figure 5 Surface currents in the Andaman Sea were driven by the northeast monsoon (December–May) and the southwest monsoon (June–November). Arrows represent the current strength (modified after Brown, 2007).

In addition, upwelling and downwelling are seasonal, which are created by monsoon winds that blow from the southwest during the summer, then reverse direction and come from the northeast during the winter. The persistence of the monsoon, especially from the southwest and the orientation of the coasts cause upwelling to occur along most of the east coast of India. That is why in the east coast of India the upwelling takes place in summer and down welling in winter, and in the eastern part of the Bay of Bengal and in Andaman Sea, upwelling occurs in winter and the downwelling in summer. However, the duration and intensity of vertical movement of water on both sides of the Bay of Bengal is not as great as on the Somali or North and South American coasts. But

it does have a profound effect on the food economy of the sea through its influence on chemical properties and biological populations. According to this reversibility, linking to climate, is one of an important factor to investigate the paleoclimate reconstructions.

Accordingly, Andaman Sea is relatively closed sea the water mass in Andaman sea had exchange to the area surrounding. The water masses of the Andaman Sea connect to the Bay of Bengal through various straits in the northern part, while others runs through the Andaman-Nicobar Islands in the west. Moreover, the Andaman Sea also connects with the Australian Mediterranean Sea through the Malacca Strait, between Sumatra and Thailand (Gebregiorgis et al., 2016).

The water mass of Andaman Sea is mixing water which are divided into 1) the surface water mass, 2) the sub-surface water mass, and 3) the deep water mass. The surface water mass is in the range about 150 m water depth. The water circulation is influenced by the monsoon winds into two prevailing monsoon; SW and NE. The upper layer, the surface water temperature at the first 50 m was relatively high at between 26-30 °C, which dominantly distributes in equatorial oceanic water mass. The sea surface temperature is quite stable during summer at ~30 °C and ~27.5 °C during winter. Thus, the water temperature is decreased to 5 °C below water depth of 1,500 m. In the surface water, salinity and water density of seawater are relatively low and fluctuate by the seasons due to the large amount of fresh water from the Irrawaddy, Salween and Kraburi input into the Andaman Sea during the monsoon season. During southwest monsoon the salinity of the Northern Andaman Sea is about 20 psu and offshore is about 32 psu. While during the northeast monsoon the salinity is quite stable, in the northern part is about 32 psu and offshore is about 33 psu. Furthermore, the water density is relatively low during the monsoon season (Source: U.S. Naval Hydrographic Office 1969) (Fig. 6). The second water layer is sub-surface water mass at water

depth at 150 m which was found the maximum of salinity at ~35 psu and then stable at 35 psu in depth between 150 to 500 m. The Andaman Sea is mostly dominated by this water mass due to this sub-surface covers range of water depth in 150 - 1,500 m. Accordingly, Andaman Sea is the semi-enclosed basin which the deep water mass is relatively stable. Therefore, salinity, the dissolved oxygen, temperature, and nutrients are constant at 1,500 m.

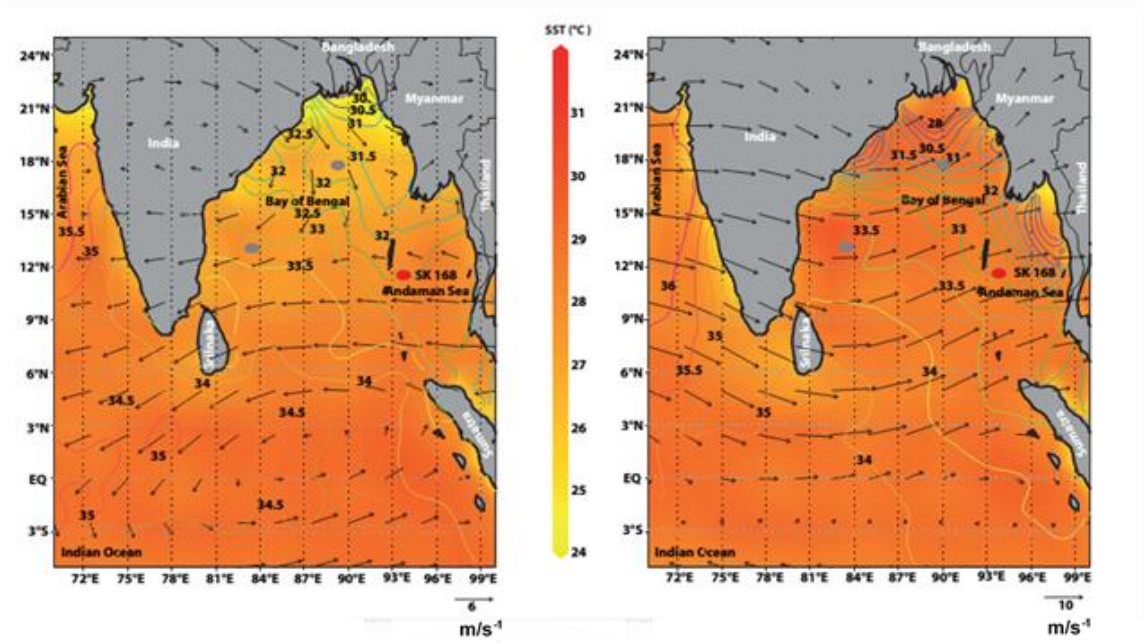

Figure 6 Sea surface temperature distribution in the Indian Ocean and eastern Arabian Sea. During winter influence present as left and summer as right. Contour lines represent annual sea surface salinities (SSS) (psu) from Levitus et al. (2010). Surface circulation pattern during winter and summer present by black arrows. Winter and summer SST (°C) ranges are shown in color gradient. (Modified after Gebregiorgis et al., 2016).

In general, the currents are characterized by the moving of water mass which is sum up of several occurred currents such as horizontal moving (surface current and deep water current) and vertical moving (upwelling and downwelling). The water mass movement in the Andaman Sea are four main types; density current, wind-driven current, tidal current, and oceanic current. The

density current is caused by the difference in density of water mass. Due to the difference in density, the distribution of hydraulic pressure does not correspond to the surface level. The sea level decreases when the density of water mass is high, reversely the sea level is higher when the water density is low. Thus, the sea water will move from high level to low level. Wind-driven currents are caused by the winds which effected on the sea surface and force the sea water move. In addition to, the Coriolis force effect by the orbital rotation the sea surface circulation in the northern hemisphere is forced rightward, while in the southern hemisphere, it slides leftward. The tidal currents caused by tides that crates the long wave movement which effects the water moving. Hence, the Andaman Sea tides is semidiurnal tide which raise up and down twice a day. Generally, the tidal current effect the ocean in the low drive forcing while it will be increasing the power at near the channel, the continental shelf, and the river mouth. The oceanic currents are caused by the movement of water mass from the river mouth to the sea by the different of water mass density. Due to fresh water has low-density from river and estuarine, lies above high-density of sea water, causing turbulent in the water masses caused turbulent current.

2.3 River discharge surrounding the Andaman Sea

The generally pathways for sediment transport into the Andaman Sea are transferred by the major river systems of Myanmar (the Irrawaddy, the Salween, and the Sittang) and much shorter rivers along the Myanmar shelf also contribute minor amounts of sediments to the eastern and southern Andaman Sea (Awashi et al, 2014). The derived sediment from the western slope of Indo-Burma-Arakan (IBA) ranges which receive some monthly highest summer monsoon precipitation (500 mm – 1 m/month) from June-September (Xie et al., 2006; Garzanti et al., 2013). These sediment input during the strong SW summer

monsoon are forced to transport into the Andaman Sea by the east flowing surface currents during the summer monsoon.

The main source of fine grained terrigenous sediment in the Andaman Sea is likely suggested that the supply from the Irrawaddy and Salween catchment (including Indo-Burman ranges and Central Myanmar basin) to deposit in Andaman Sea (e.g., Rodolfo, 1969b; Colin 1998; 1999; 2006, Awashi et al, 2014; Ali et al., 2015, Cao et al., 2015b) . According to the terrigenous input of Irrawaddy and Salween rivers provide the large amount loading more than 540 Mt (Robinson et al., 2007) as Fig. 7 and Table 5 into the Andaman Sea with the estimated discharge input 260-350 Mt per years (Ramaswamy et al., 2004; Rao et al., 2005). Andaman Islands that lies to the western is also one of potential source of sediment to Andaman Sea but there are no major rivers that could provide sediments to Andaman Sea on the Andaman Islands (Ali et al., 2015). The additional possible source of terrigenous input in the southern part from Malay Peninsula and Sumatra transported by the Malacca currents through the Great Channel (Rodolfo, 1969a), delivering fine grained terrigenous detritus to the deeper parts of the Andaman Sea basins (Keller and Richards, 1967). The estimated the total sediment load of Sumatra by Milliman et al. (1999) revealed amount of 780 Mt per year but it could provide <300 Mt per year to Andaman Sea due to Sumatra provides about 460 Mt per year to South China Sea (Liu et al., 2012; 2016). The southwestern of Thailand contributed less in the loading by the short and narrow rivers of <5 Mt per year (Liu et al, 2016). Furthermore, the river discharges over the Andaman Sea provide the input from land to sea, annually discharging is about 12,500 km^3 of freshwater and more than 20 x 10^9 tons of solid and dissolved material to the world ocean (Joussain, 2016a). According to the unique topography and orographic control on the Asian monsoon, the Himalayan system establishes the largest erosion system of the planet due to the annually supplies are more than a billion tons of sediments and dissolved materials to the oceans representing 10 to 12% of the dissolved and the sediments annual discharge

of all rivers to the ocean (Milliman and Meade, 1983; Milliman and Farnsworth, 2011; Joussain, 2016a).

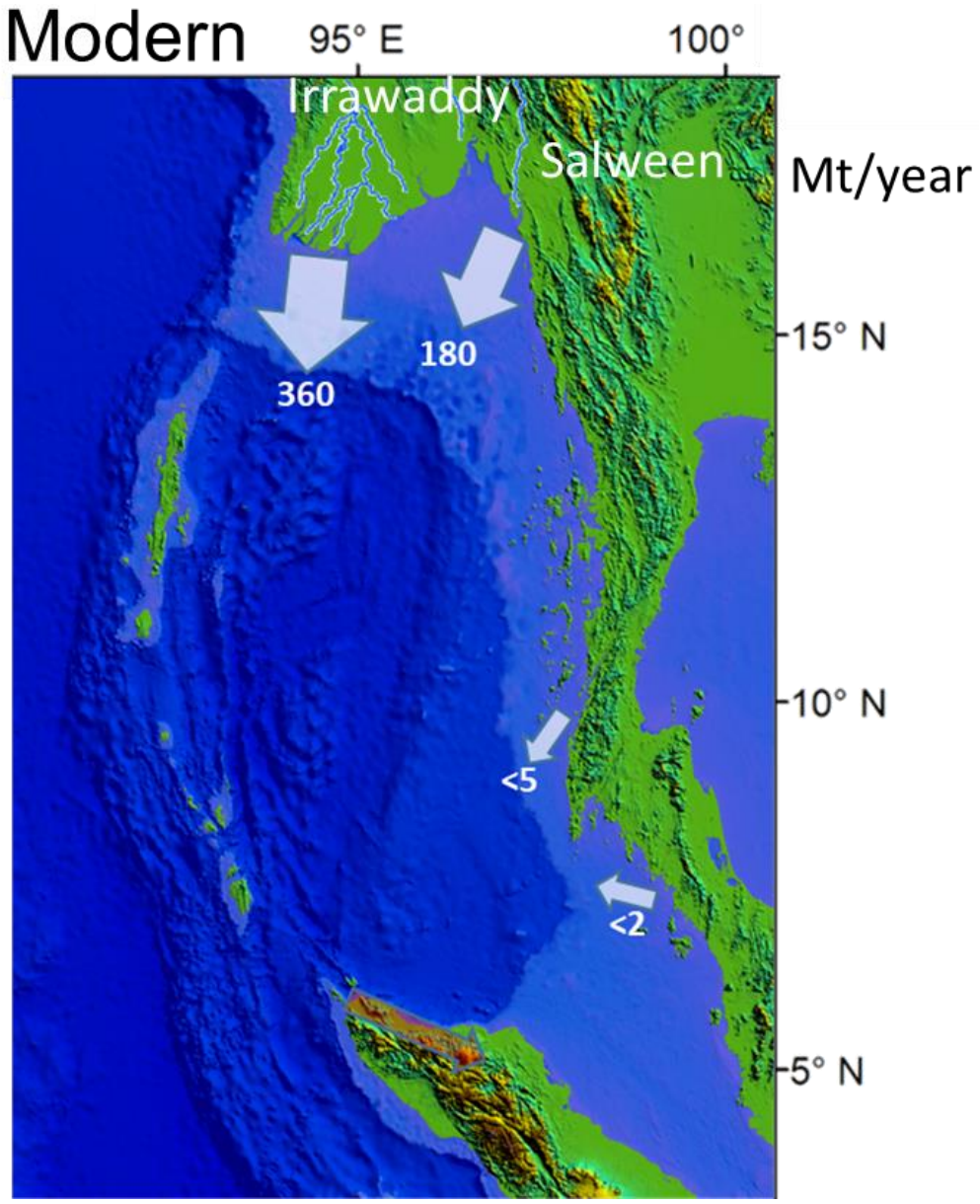

Figure 7 Fluvial drainage systems and their annual suspended sediment discharge to the Andaman Sea. White arrows with numbers indicate observed fluvial sediment discharge (in million metric tons, Mt, annually) from the Indochina Peninsula. See table 5 for detailed sediment discharge data of all major rivers.

Table 1 Drainage area, runoff, and observed suspended sediment discharge of major rivers flowing directly into the Andaman Sea.

River catchment name	Length (km)	Drainage area (10^3 km^2)	Runoff (km^3/year)	Suspended sediment discharge (Mt/year)	Data source
Myanmar					
Irrawaddy	2,300	430	430	360	Robinson et al., 2007
Sittang	560	35	50	-	
Salween	2,800	270	210	180	Robinson et al., 2007
Great Tenasscrim	450	15	-	-	
Malay Peninsula					
Muda	-	7.4	3.6	0.1	Cao, 2015a
Perak	270	13	12	0.9	Cao, 2015a
Selangor	-	32	3	0.1	Cao, 2015a
Langat	160	2.5	1.8	0.6	Cao, 2015a
Murar	-	3.2	1.7	0.1	Cao, 2015a
Thai rivers	-	-	-	-	-
Sumatra					
Ashan	100	7.5	3	-	Cao, 2015a
Panai	230	12	-	-	Cao, 2015a
Burumum	310	16	-	-	Cao, 2015a
Rokan	280	16	-	-	Cao, 2015a

Andaman Sea sediment distribution is the one complex system by the variations since the Last glacial maximum (LGM) and Holocene period (Colin et al., 1999) with the mixing sources to deposit in the Andaman basin. The sediment transport was suggested by the current variations which controlled the sediment provenances (Ahmed et al., 2005; Awasthi et al., 2014; Joussain et al., 2016b). The terrigenous input to Andaman Sea was increased during the glacial periods (Colin et al., 2006) by the increasing of physical weathering while the sea level was at the low stand. Moreover, the sediment evolution could be implied the study through the weathering evident of the weathering processes;

chemical and physical weathering. The Southeast Asia region is the nice representative to study the weathering processes due to this region has the top high of denudation rates which is the most abundant area were covered by the weathering products (McLennan et al., 1993; Summerfield and Hulton, 1994; Awasthi et al., 2014). The weathering processes investigation by the surface sediment had been used to separate the chemical weathering such as the study in the South China Sea; the chemical weathering is found much in the volcanically topography likes island.

More recently, the outer shelf is classified as a zone of well-sorted relict sand and the shell-fragment and mud contents render the sediment poorly sorted deposited probably during the Holocene transgression with a rate of 20 mm/year. Sediment blanket the shelf is generally originated by transportation of sediment from the Irrawaddy Delta in the north pass through the Mataban Canyon. The transportation of the sediment is mostly controlled by topography of the basin with associated by both westerly current and high tidal regime (Rodolfo, 1969a). Satellite image agreed with the work that the turbidity front oscillates about 150 km in phase with spring-neap tide cycle. The area covered by the turbid zone increase up to more than 45,000 km^2 during spring tide. The sediment discharged by the Irrawaddy River is transport mainly eastward along the coast into the gulf of Mataban. In addition, water profiles of suspended sediment concentration (SSC) measuring along longitudinal profile in the Irrawaddy Delta from shallow water to ~250 m water depth with 30-40 m length cut off contour-lines indicated increasing of SSC with depth. Compared to surface water, the near bottom highly SSC indicated near bottom turbidity zone extend further southward. Re-suspension of sediment by strong tidal current, shallow bathymetry, and seasonal sediment influx from river are combination factors of high turbid water (Ramaswamy et al., 2004). This work is supported by recent study on sediment sampling (Rao et al., 2005) that complex fine-grained sediment in Irrawaddy Delta with annual 360 million- tons possibly served large sediment to the shelf

associated with the prevailing westerly current and a strong tidal regime of 7 m maximum tidal range.

On upper few meters of Mergui Terrace, the sediments are composed largely with well-sorted muddy sand, and only the shell-fragments and mud contents render the sediment poorly sorted. The Irrawaddy Rivers supply these sediments to the basin as river discharges (Rodolfo, 1969a). The riverine influx supports sediment over 360 million ton/year (Rao et al., 2005). Of approximately 70% of the sediment influx settles at the rivers delta, whereas the rest could has been delivered through Mataban Canyon to the deeper part and accumulated on seafloor far from their source (Ramaswamy et al., 2004). The sediment transportation through the deeper part might be accomplished by some types of gravity-controlled sediment and shapes of the basin (Rodolfo, 1969b; Rao et al., 2005). The graded beds up to few meters thick of surface-layer sediment and associated primary structures suggested that the deposition was primarily by turbidity currents. Sedimentation rate on the terrace is less than 10 mm/1000yr (Rodolfo, 1969b). A pelagic component of interbedded sediment such as foraminiferal ooze suggested that these sediments accumulated continuously and slowly (Saidova, 2008).

On Mergui Basin, sediments were studied from three wells drilling. The upper thin layer of Pliocene to present sediment on seafloor of about 180-240 m thick comprises with silty shales and fine-grained sandstones, whereas the lower layer of middle Miocene sediment of about 700-1000 m thick comprises with coral/algal limestones. The late-Miocene sediment in between the both layers revealed a thin layer of sediment turbidities (Polachan and Racey, 1993). Roldofo (1969a) shows additional data from sediment core of the Sumatra shelf basin that revealed a very thin volcanic clayey sand layer below the core top. The sediment layer was interpreted as a density current deposit along the Sumatra Margin of Malacca Strait.

CHAPTER 3

MATERIALS, METHODS, AND AGE MODELS

In order to reach the goals of this study as described in Chapter 1, sediment cores and surface sediments were analyzed using various analytical methods. The surface sediments retrieved from the Myanmar shelf and Thailand shelf in the Andaman Sea were analyzed to study provenance of recent sediments that fill in the southern Andaman Sea. The high-resolution terrigenous records from four sediment cores, ADM2, ADM6, MASS-III-10, and MASS-III-07 retrieved from the southern Andaman Sea, were analyzed to reveal the variations in sediment provenance since the last glaciation. Clay mineralogy, grain size, major elements, and carbonate contents were investigated on terrigenous fractions for four sediment cores and only clay mineralogy analyzed for the surface sediments. Oxygen isotopic ratios of planktonic foraminifers and total carbon contents were measured to establish the age models for these sediment cores. In the present chapter, sediment materials, analytical methods, and age model of sediment cores adopted to achieve the objectives will be presented in details.

3.1 Sample materials

To achieve the aims of this study, there are two groups of materials employed in this study. The first sample group is sediment cores that are two deep sea cores (ADM2 and ADM6) from The vulnerability of the coastal zones under Thai (PMBC)-Chinese (FIO-SOA) collaborative project and two shallow water cores (MASS-III-07 and MASS-III-10) from Morphodynamics and Slope Stability of the Andaman Sea Shelf Break under Thai-German project, which were recovered from the southern Andaman Sea by gravity corers. The second sample group is surface sediments that were collected from two regions including nearshore area off Myanmar shelf (MM) from Environmental Impact Assessment (EIA) for The Myanmar Block M9 Production Development and Offshore gas transmission pipeline and Thailand shelf (TH) from Changing of sediment stratigraphy and historical tsunami tracing by nearshore sediment of the Andaman Sea under Thai-German project, which were taken by grab samplers. The sampling locations are displayed in Fig. 8 and Table 2, more details are reported in Appendix A. The summary of these sediment samples and analysis resolution in this study are listed in Table 3. All analyses were performed at State Key Laboratory of Marine Geology of Tongji University, Shanghai, China.

Table 2 Summary of sediment materials

Sample	Sample location	Project name	Cruise	Remarks
Sediment core				
ADM 2 (gravity core)	the Andaman Sea shelf (Thai water)	PMBC-FIO	M/V SEAFDEC November 2012	Appendix A
ADM 6 (gravity core)	the Andaman Sea shelf (Thai water)	PMBC-FIO	M/V SEAFDEC November 2012	Appendix A
MASS-III-10 (gravity core)	the Andaman Sea shelf break (Thai water)	MASS	RV Charkratong tongyai January 2011	Appendix A
MASS-III-07 (gravity core)	the Andaman Sea shelf break (Thai water)	MASS	RV Charkratong tongyai January 2011	Appendix A
Surface sediment				
Myanmar surface sediments (grab sampler)	the eastern and central parts in the Gulf of Martabun, offshore of Myanmar	EIA	December 2009	Appendix A
Thailand surface sediments (grab sampler)	Nearshore of Thailand, Phang Nga province	TUNWAT	December 2008	Appendix A

Table 3 Summary of sediment samples used in this study.

Method	Sediment core								Surface Sediment	
	ADM 2		ADM 6		MASS-III-07		MASS-III-10		MM(1)	TH(2)
	Total samples	Res.	Total samples	Res.	Total samples	Res.	Total samples	Res.	Total samples	Total samples
Stable oxygen isotope	183	2 cm	212	2 cm	72	2 cm	72	2 cm	-	-
Carbon-14 dating	5	-	4	-	5	-	5	-	-	-
Bulk Carbonate content	183	2 cm	212	2 cm	-	-	-	-	-	-
XRF core scanning	-	-	-	-	158 cm	1 cm	150 cm	1 cm	-	-
Grain size	183	2 cm	212	2 cm	76	2 cm	72	2 cm	-	-
Clay mineralogy	183	2 cm	212	2 cm	76	2 cm	72	2 cm	39	22
XRF elemental geochemistry	183	2 cm	212	2 cm	-	-	-	-	-	-

MM (1) = Myanmar shelf and TH (2) = Thailand shelf

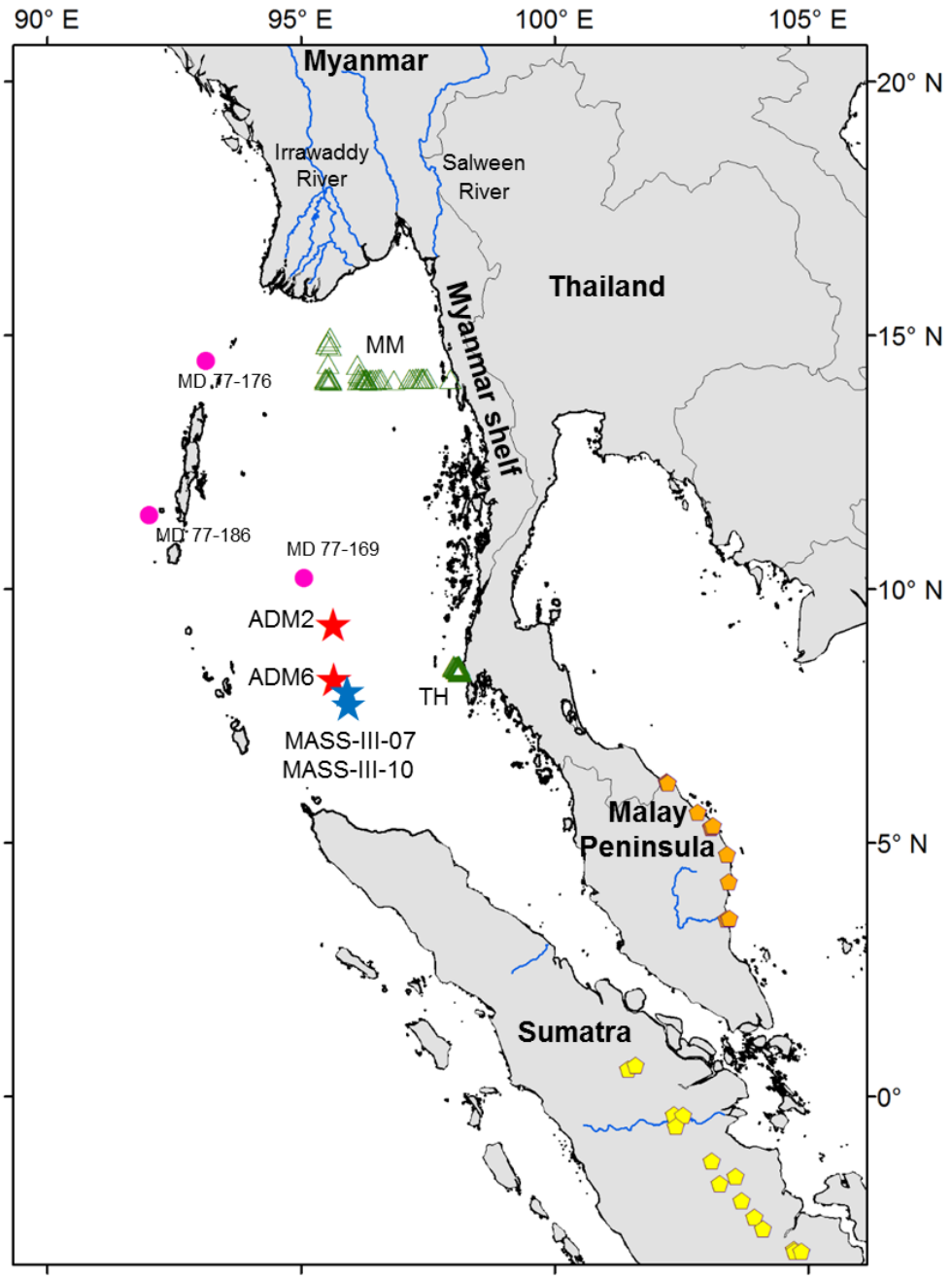

Figure 8 Sitemap of sediment sample locations in the Andaman Sea. The star signs are sediment cores and triangle signs are surface sediments used in this study. Circle signs represent the reference cores studied in the Andaman Sea and diamond signs are river and surface sediments conducted in the surrounding area.

3.1.1 ADM 2

Core ADM2 (09°16.53'N, 95°47.94'E; water depth 2,268 m, 3.85 m recovery) was collected in the upper and lower slope-break area off Thai waters in November 2012 by M/V SEAFDEC cruise. More sample location and details are presented in Appendix A. The core is located on the lower slope of the Andaman Sea, and so the terrigenous input could be dominated by fluvial sediments from land. The region is also dominantly influenced by surface currents (in water depth range of 500-1,500 m) indicating ADM2 is well-preserved core. Therefore, it is ideal to perform paleoenvironmental studies on sediment records in this region of the Andaman Sea. Core AMD2 is homogenously dominated by grey clays with several intervals rich in foraminifera, organic matter, and shell fragments without visible turbidity layers.

The lithology of upper layer of Core AMD2 consists of 75 cm thick olive grey silts that are mostly foraminiferal grains (Fig. 9, left). The interval of 75-100 cm consists of silty clay with a shell fragment layer (2 cm thick) at 100 cm. The sediment below 170 cm is dark grey clay with organic matter insert as well as shell fragments at 278 cm.

3.1.2 ADM 6

Core ADM6 (08°11.88'N, 95°39.55'E; water depth 1,890 m, 4.25 m recovery) (Fig. 8) was collected from the same cruise as Core ADM2. This core location is on upper slope of the Andaman Sea continental slope at 1,890 m water depth. Core AMD6 is homogenously dominated by green and grey clay with several intervals rich in foraminifera, organic matter, shell pieces, and shell fragments. A turbidity layer is found in the lower sequence below 380 cm, indicating that the majority of Core ADM6 is well preserved.

Lithographic descriptions of core AMD6 reveals obviously different color in the bottom layer as the turbidity layer as Fig. 9 (right). ADM6 is also consist of clay sediment in the upper part with some foraminiferal pieces (top to 100 m). The sediment layer below 100 cm is the grey clay layer with some shell pieces and organic matter layer showed at 188-200 cm. The lower part of core ADM6 below ~380 cm the sediment color is the light grey clay and then the light yellow clay in the deeper part, assuming these changing suggested the turbidity layer.

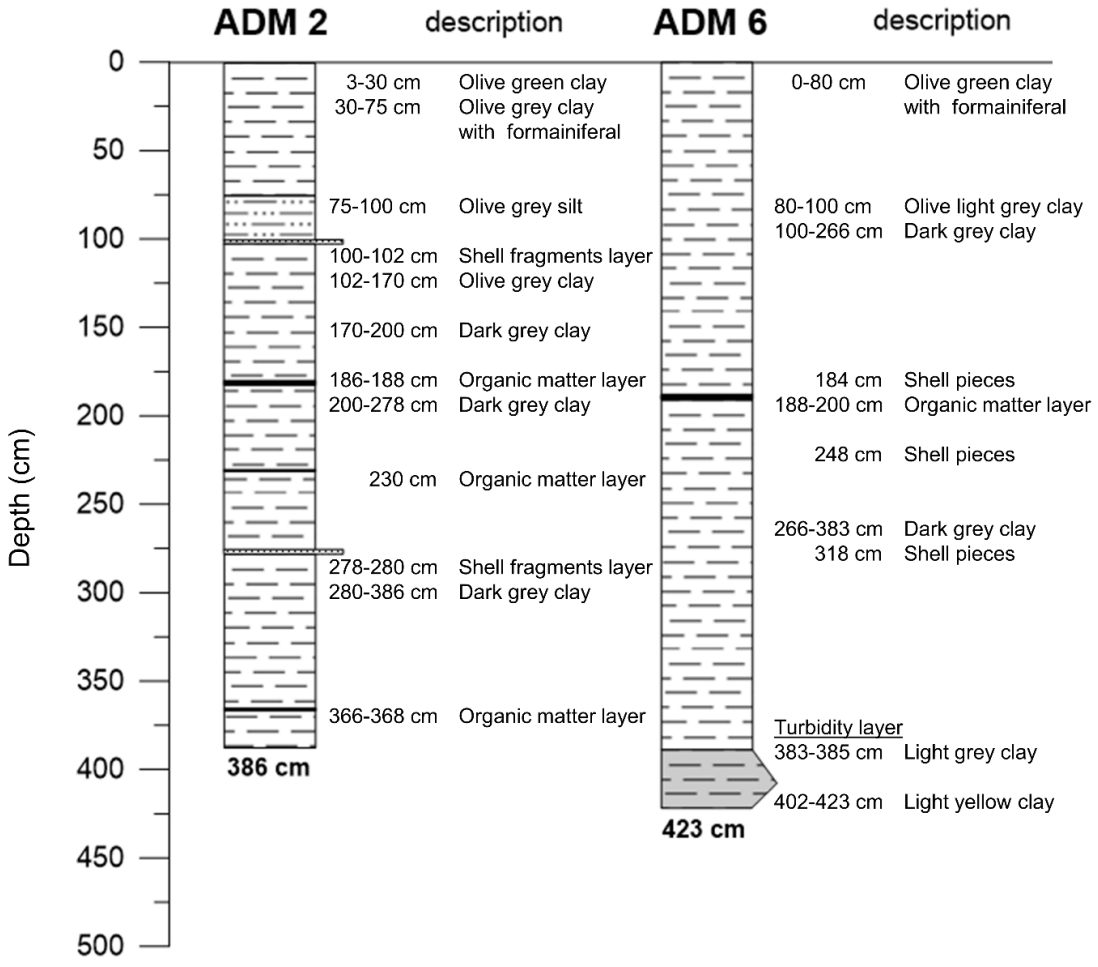

Figure 9 Lithographic descriptions of Cores ADM2 and ADM6

3.1.3 MASS-III-10

Core MASS-III-10 (8°06.92’ N, 95°51.74’ E, water depth 630 m, for 1.50 m recovery). MASS-III-10 is taken during the MASS-III cruise in January 2011 by the R/V Charkratong Tongyai. Due to MASS-III-10 site is located on the shallow water at 630 m water depth, as such this core may dominated by fluvial sediments more than ADM2 and ADM6 which taken from deeper water. Thus, MASS-III-10 is strongly influenced by the surface current. Sediment lithology of MASS-III-10 consists of silt layer in the top part and clay layer with several intervals rich in foraminifera, and shell fragment layers. No turbidity layer in the sediment sequence is found in MASS-III-10.

MASS-III-10, as Fig. 10 (left) present only two kind of the visible color along 150 cm recovery. The color found in core MASS-III-10 is dark brown in 6-18 cm and olive grey below 18 cm. The sediment textures in the upper (6-18 cm) consist of silt with mostly foraminifera while the lower layer below 18 cm consist of silty clay sediment.

3.1.4 MASS-III-07

Core MASS-III-07 (8°10.97’ N, 95°52.88’ E, water depth 600 m, 1.58 m recovery). Core MASS-III-07 is taken in the same cruise of MASS-III-07. This core is located on the shallow water at 600 m water depth, which is dominated by fluvial sediments from land and strongly influenced by the surface current. Sediment lithology of MASS-III-07 consists of three difference layers and no turbidity layer found in this core.

MASS-III-07, as Fig. 10 (right) the core recovery of 158 cm showed three parts by the color; 5-8 cm is light brown, 8-23 cm is olive grey, and below part is dark grey. The upper layer of core by 5-8 cm is mostly consist of sand, the 8-23 cm layer is finer sand and sandy silt, and the 23-158 cm layer consist of silt with mostly foraminifera.

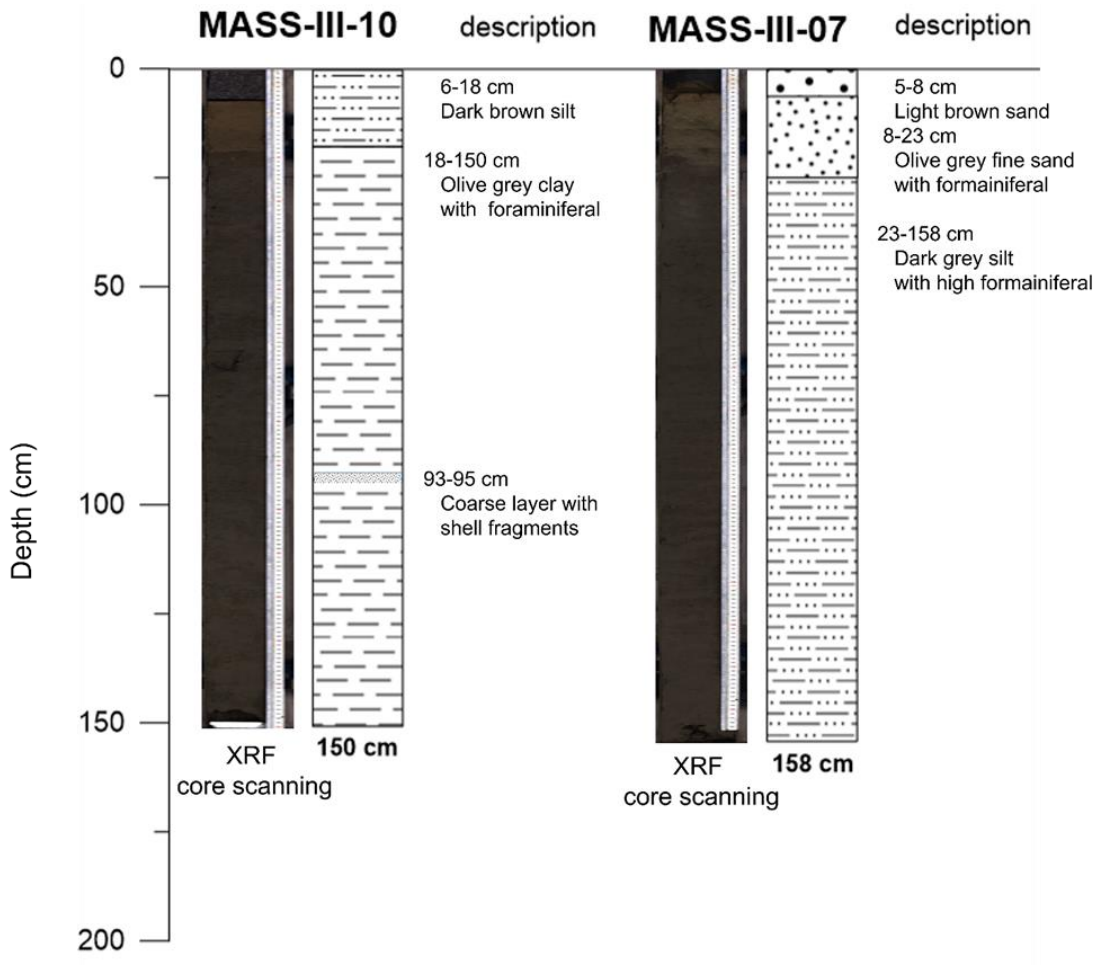

Figure 10 Lithographic descriptions of core MASS-III-10 and MASS-III-07 with the XRF core scanner image.

3.1.5 Myanmar surface sediments

Thirty nine samples were collected form nearshore of the Myanmar coast for 39 samples in December 2009. The sediment location is expanded between two major river systems which were actively supplying the sediments into the Andaman basin: the Salween River in the east and the Irrawaddy River in the west. Due to the environmental impact assessment (EIA) project on the gas transmission pipeline, the sampling were taken in the nearshore area around the pipeline developed station. The sampling station is located within the eastern and central parts in the Gulf of Martaban, offshore of Myanmar, approximately 300 km at south of Yangon and 240 km off west of Tavoy on the Myanmar coast. These sampling areas are developed by two river systems which were divided by the differential timing; the Salween River rapidly transported sediment to the Martaban basin while the Irrawaddy River deposited most of its sediments in the Central Basin. The sample sites were located in shallow water. Details location are presented in Appendix A.

3.1.6 Thailand surface sediments

The Thailand surface sediment are collected form nearshore of the Thai coast (Phang Nga coastal zone) for 22 samples during December 2008, proposing to find the evidence of territorial deposit in the nearshore of Thailand. The sediment location is located of Phang Nga province with no major river supply sediment form land to the sea.

3.2 Analytical methods

3.2.1 Stable oxygen isotope

The measurements of planktonic foraminiferal oxygen isotopic composition are performed on core sediments. The sediment preparation will be done by, heated samples by 50°C, measure dry weight, soak samples by deionized water, sieve samples by 63 μm pore size standard sieve, collect samples which are remained on sieve (>63 μm), dry the collected samples by 50°C, and preserved in the glass tube. The *Globigerinoides ruber* (white) specie of planktonic foraminifera are used in this study which are determined $\delta^{18}O$ values of foraminiferal shells; 8-14 good *G.ruber* shells in diameters range between 300-360 μm Measurements of the planktonic foraminiferal $\delta^{18}O$ values are performed in the State Key Laboratory of Marine Geology, Tongji University.

The calculation by Isotopic Ratio Mass Spectrometer (IRMS), the isotopic ratios ($^{18}O/^{16}O$) of the sample will be estimated to find the relationship with local environmental condition and to trace the monsoon variability record and paleotemperature (Rashid et al., 2007). The mean external reproducibility of carbonate standards was ~ 0.07‰ for $\delta^{18}O$. The cohesion and international PDB will be scaled by international standards NBS19 and NBS18 into line.

3.2.2 Carbon-14 dating

For the sediment cores, the chronology dating of Carbon-14 by Accelerator Mass Spectrometer (AMS) are used. The planktonic foraminifera species G. ruber (white) for 1,000 good shells and >250 μm in diameters are selected for each sample. The total sample number of ^{14}C dating are shown as table 3.1. Measurements of ^{14}C dating values by planktonic foraminifera; *G. ruber* are performed by the American Beta Laboratory for AMS analysis.

3.2.3 Bulk Carbonate content

Carbonate content determination is to use an acid test titration, to measure the volume of CO_2 gas produced by the reaction by using the gasometrical method. The titration produced carbonate and hydrochloric acid, can be informed of the quality of the carbonate content, and use the standard state volume of CO_2 for conversion the calculation which calculate the sample weight percentage of $CaCO_3$. Carbonate contents of bulk sediments can be calculated from the CO_2 volumes as stated by the equation: $CaCO_3 + 2HCl = CaCl_2 + CO_2 + H_2O$.

The sediment preparation are dry samples at 50ºC for 24 hours, pulverize in an agate mortar, take each grinded sample about 0.1 ± 0.005 g, prepare 3 mol/L a sufficient amount of concentrated hydrochloric acid (HCL) at condition by 20 ℃, and measure the sufficiently the volume of CO_2 produced in the reaction of gas volume (ΔV). The calculation will be based on; $CaCO_3\% = (100 * \Delta V) / (22414 * ml)$ to acquire the percentage content of carbonate sediments by error less than ± 2%

3.2.4 Clay mineralogical analysis

The set of samples is examined for clay mineralogy for <2μm particles non-calcareous clay (Holtzapffel, 1985). The clay minerals were analyzed by X-ray diffraction (XRD) using a PANalytical diffractometer which the clay mineral analysis was done under 3 conditions; normal, ethylene-glycol and heating at 490°C to identify the peak diagram by the semi-quantitative estimates of peak areas of reflections using MacDiff software (Petschick, 2000). In addition, the calculation of clay compositions are calculated the reflections of chlorite, kaolinite, illite, smectite, palygorskite, etc. which show the relative proportions of the total clay assemblage to differentiate the source of terrigenous sediments and marine sediment as well as the geological condition such as the weathering process (Gingele et al., 2001) and get the illite chemistry index value to refer the provenance input from the source variations. The clay assemblage calculation showed the relative clay mineral by the percentage of their total contents which accurate in the range 5-10% by Biscaye (1965).

The sample preparations are, sort samples by <63μm suspended sediment on behalf of the whole rock composition (Liu et al., 2009), remove deposits of calcium carbonate by 0.5% diluted hydrochloric acid (HCl), soak several repeatedly acid by deionized water, check pH until nearly 7, remove upper clear solution, preserve the non-calcareous clay fractions into vials. Then, to prepare the oriented-mounts samples the principle of settling time Stoke (Stokes' Law) will be used, extract 2 μm particles to represent sediment of clay minerals, and mixture a solution carefully oscillated to make homogeneously isolated. According to Stokes' Law, the solutions will be retained steady for 95 minutes and take these solution at the upper ~2 cm. which represent sediments of clay minerals < 2 μm, centrifuge the mixture at 4500 rpm (revolutions per minute) for 30 minutes, conduct the homogeneous mud to make the oriented mounts with the glass blade sheets.

To analyze clay mineral samples, measure by the PANalytical X'Pert PRO diffractometer which test conditions: CuKα radiation, Ni filter, tube voltage 45 kV, tube current 40 mA, scan range 3 ~ 30° 2θ, step size of 0.03° 2θ (a measuring time of ~1 second/step). The clay mineral blade sheets will be prepared for 3 sample condition: natural conditions, ethylene glycol conditions (at least 24 hours), heated conditions (490 °C heated for 2 hours). Clay minerals identification and interpretation of the main basis for XRD under three test conditions obtained by superimposing a comprehensive comparison of the spectrum, semi-quantitative parameters of each peak is calculated using MacDiff software (Petschick, 2000) on ethylene glycol curve. The calculation of the relative content of clay minerals mainly used various minerals (001) crystal face diffraction peak area ratio of smectite (including illite/ smectite mixed-layer minerals random) using 17 Å (001) crystal face, illite using its 10 Å (001) crystal face, kaolinite (001) and chlorite (002) using a 7 Å superimposed peaks. Their relative proportions by fitting of (002) kaolinite 3.58 Å / the (004) chlorite 3.53 Å peak area ratio determined, and the relative error of about ± 5% (Holtzapffel, 1985), the precision of replicate samples is analyzed ± 2% (2σ) (Liu et al., 2010). The relative proportions of smectite, illite, kaolinite, palygorskite and chlorite are specified in percentages of the total clay assemblage.

In addition, according to the glycol curve 5 Å and 10 Å peak area ratio calculated illite chemical index, when the ratio is greater than 0.40 for the Al-rich illite (muscovite), Representative strongly hydrolysis; if Mg and Fe substitution Erie when stone lattice Al, the ratio is reduced accordingly. Therefore, when the ratio is less than 0.15, the representative of illite-rich Mg-Fe (biotite) as a result of physical weathering (Esquevin, 1969; Petschick et al, 1996). The illite crystallinity you can use glycol curve 10 Å diffraction peak half-width of said lower values representative of mineral The higher the degree of crystallinity, may indicate the degree of weathering and chemical tracers source

and transport route (Chamley, 1989; Liu et al., 2010; Liu et al., 2008; Petschick et al., 1996).

3.2.5 X-ray fluorescence (XRF) element core scanning

The semi-quantitative elemental analysis is done by a high-resolution geochemical X-ray fluorescence spectrometry (XRF Core Scanner): Avaatech™ XRF Core Scanner. The measurement is directly scan the core cross-section and the relative content of elements (elements in the range of Aluminium-Al ~ Uranium-U). The XRF core scanning method is a relative fast analysis, continuously scan and non-destructive of the chemical composition on surface sediments scanning.

The core scanner measurement deal with the well prepared spitted cores then the sample preparations are carefully smooth the core surface, eliminate the cracks or pits, keep cores in horizontal, covered with a 4 μm special thin Ultralene® film, and eliminate the air bubbles and wrinkles which occur under film (Xie et al., 2007). Due to the XRF measurement is high resolution, the minimum test platform resolution can measure continuously by 0.5 mm but the irradiated surface of the sample rectangle is automatic adjusted in the range between 1 cm ~ 0.1 cm by the width fixed at 16 mm; therefore, this study use dimensions of the irradiated sediment surface at 1 cm × 1 cm. The data content of each element relatively detect in content to cps (counts per second) for 30s (counts per 30 second). The X-ray tube is excited to three different voltages (10 KV, 30 KV, and 50 KV) to obtain intensities of light (Al to Fe), median (Co to Mo), and heavy elements (Ag to U).

3.2.6 X-ray fluorescence (XRF) elemental geochemistry

The major elemental geochemistry by X-ray fluorescence analysis (XRF) using a PANalytical spectrometry - Axios MAX, to identify the different sources additionally to their clay mineral composition with element signatures for finding specific minerals. The detected major elements are mainly show the lithogenic contents of Si, Al, Fe, Mg, Ca, Na, K, P, S, Mn and Ti which the results will showed the percentage of element in the oxide form. This analysis is used to indicate the source of terrigenous input; if the sediment were transported from the same sources, if they are from the different sources but they have the similar contents and to find the relative proportion of different sources. This method will fuse the bulk sediment into the beads which were analyzed by the XRF. The beads preparations will start by the grounding the dried sediment (at 60 °C) ~1 g. to the fine powder, then rid the absorbed water in the samples by drying the powder at 120 °C at least 12 hours and preserved into dry condition. Besides, these sample, the reagents preparation will be done by very precious weighting of reagent powder by 7.000 g. ± 0.002 g. flux of lithium tetraborate (67%) and lithium metaborate (33%) anhydrous (heated at 600 °C) and prepare these into the 50ml ceramic crucible. Accordingly, the mixture between the samples and reagents, we will weigh the dehydrated powder sample by 700 mg. ± 0.2 mg. then add into the crucible of pre-weighted flux and homogenize the sample by stirring with a glass rod. Consequently, to do the glass beads, add the mixture powder into the platinum crucible and add two drops of mold dope (lithium bromine) and oxidant (Hydrogen peroxide). To do the melting of mixtures will be done at 1050 °C (by Electroheat Fusion Machine) then put the melting into the mold. Therefore, start the fusing the glass beads into the spectrometry by the automatic program.

3.3 Age Models

The ^{14}C AMS dating and oxygen isotope ($\delta^{18}O$) stratigraphy are obtained by planktonic foraminifer, *Globigerinoides ruber* (*G. ruber*), to establish age models of these studied cores. The ^{14}C dates obtained were converted into calendar ages using Marine09 calibration curve (Reimer et al., 2009) and were calibrated using Calib 7.0.2 (Stuiver et al., 1998) within 1σ level of errors.

The correlation of planktonic foraminiferal $\delta^{18}O$ record is performed semi-automatically by the Macintosh program "AnalySeries" (Paillard et al., 1996). The analyzing links the reference curve, Core MD77-169 (only core in the Andaman Sea providing a semi-continuous record for the last 280 ka) and the $\delta^{18}O$ curves of our cores. In addition, the accuracy of the time calibration was improved by well tuning of the extracted precession components of the $\delta^{18}O$ record to the precession components of Core MD77-169 that Colin et al. (1998, 1999) had well-tuned with the SPECMAP stack (Martinson et al., 1987).

3.3.1 Age model of Core ADM2

Five ^{14}C-AMS dates were obtained at Core ADM2 (Table 4) and the age covers the past 42 ka in the last glaciation. The ^{14}C dates were converted into calendar ages using Marine09 calibration curve (Reimer et al., 2009) and were calibrated using Calib 7.0.2 (Stuiver et al., 1998) within 1σ level of errors.

Table 4 ^{14}C AMS ages of ADM2 calibrated using Calib program version 7.0.2.

Depth (cm)	Foraminifera species	^{14}C AMS age BP	Average calibrated age (1σ, yrs BP)	Error 1 σ
ADM2				
18-24	*G. ruber*	2,080 ± 30 BP	1,652	99
134-136	*G. ruber*	10,660 ± 40 BP	12,005	183
168-170	*G. ruber*	13,240 ± 50 BP	15,285	192
260-264	*G. ruber*	25,200 ± 110 BP	28,813	266
364-368	*G. ruber*	37,780 ± 380 BP	41,827	560

The graphic correlation by using Analyseries between Core MD77-169 and Core ADM2 (the δ^{18}O curve) of core results is added to develop the age model. The result shows the age for 44 ka extends to the Marine Isotopic Stage (MIS) 3. The age model was established by linear interpolation, assuming a constant deposition rate between two adjacent tie points. By these calculated age scales, Core ADM2 presents continuous sedimentary record covering to mid-MIS 3, MIS 2 (glacial variation) and MIS 1 (interglacial variation) as Fig. 11.

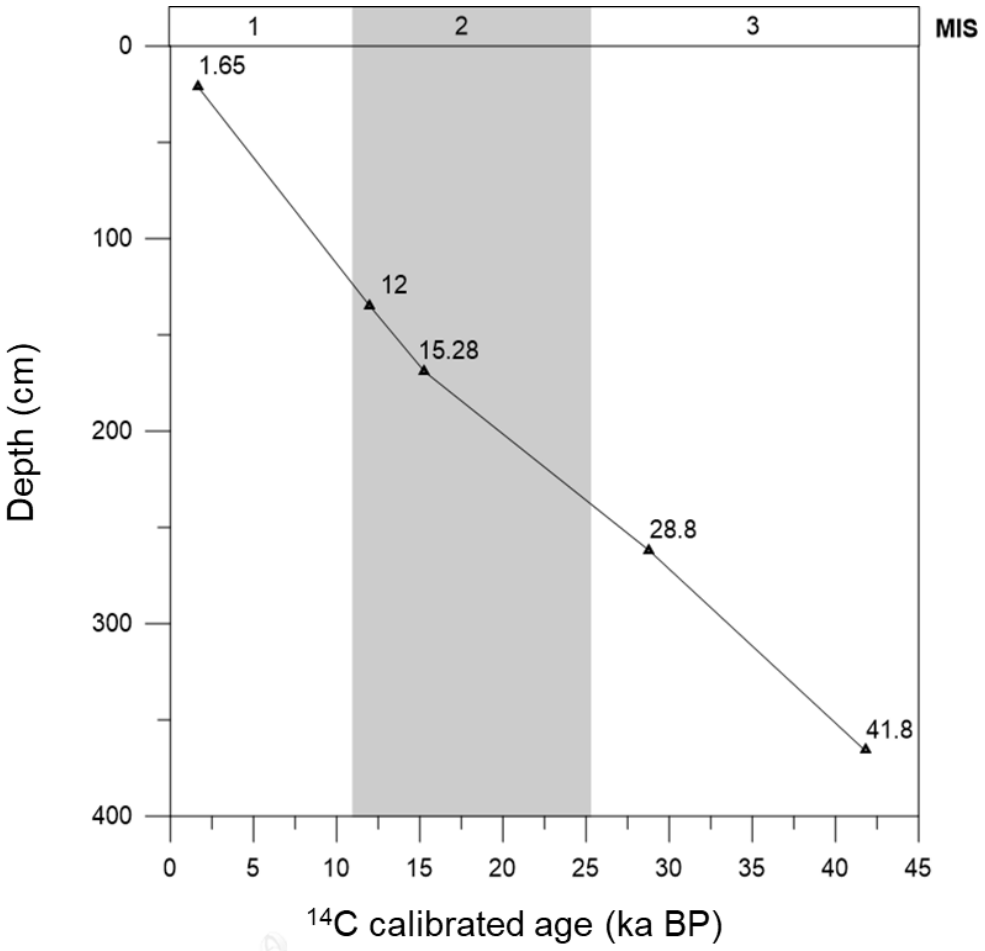

Figure 11 Age model of Core ADM2 based on 14C dating, showing by depth (cm) vs age (ka). The tilted triangles presents age controlled points, which were obtained from the oxygen isotope stratigraphy. Color shade presents the Marine Isotopic Stage (MIS) 2.

3.3.2 Age model of Core ADM6

Four ^{14}C-AMS samples were obtained as Table 5 that ADM 6 revealed age covers since the last glaciation (22 ka). The ^{14}C dates obtained were converted into calendar ages using Marine09 calibration curve (Reimer et al., 2009) and were calibrated using Calib 7.0.2 (Stuiver et al., 1998) with 1σ level of errors. The graphic correlation by using Analyseries between core MD77-169 and core ADM6 (the δ^{18}O curve) covers ages for ~22 ka extend to the MIS 2. By these calculated age scales, ADM6 presented sedimentary record covering to MIS 2 (glacial variations) and MIS 1 (interglacial variation) as Fig.12. ADM6 mostly presented in Holocene (MIS 1) since mid of MIS 2. However, ADM6 is presented the turbidity layer at the bottom core that the last age control point will not be included in all ADM6 interpretation.

Table 5 ^{14}C AMS ages of ADM6 calibrated using Calib program version 7.0.2.

Depth (cm)	Foraminifera species	^{14}C AMS age BP	Average Calibrated age (1σ, yrs BP)	Error 1 σ
ADM6				
2-4	*G. ruber*	1,700 ± 30 BP	1,260	60
254-258	*G. ruber*	9,180 ± 30 BP	9,990	153
316-318	*G. ruber*	12,040 ± 50 BP	13,473	141
376-380	*G. ruber*	18,690 ± 80 BP	22,164*	271

* Remark this age will be removed in the interpretation due to the turbidity layer

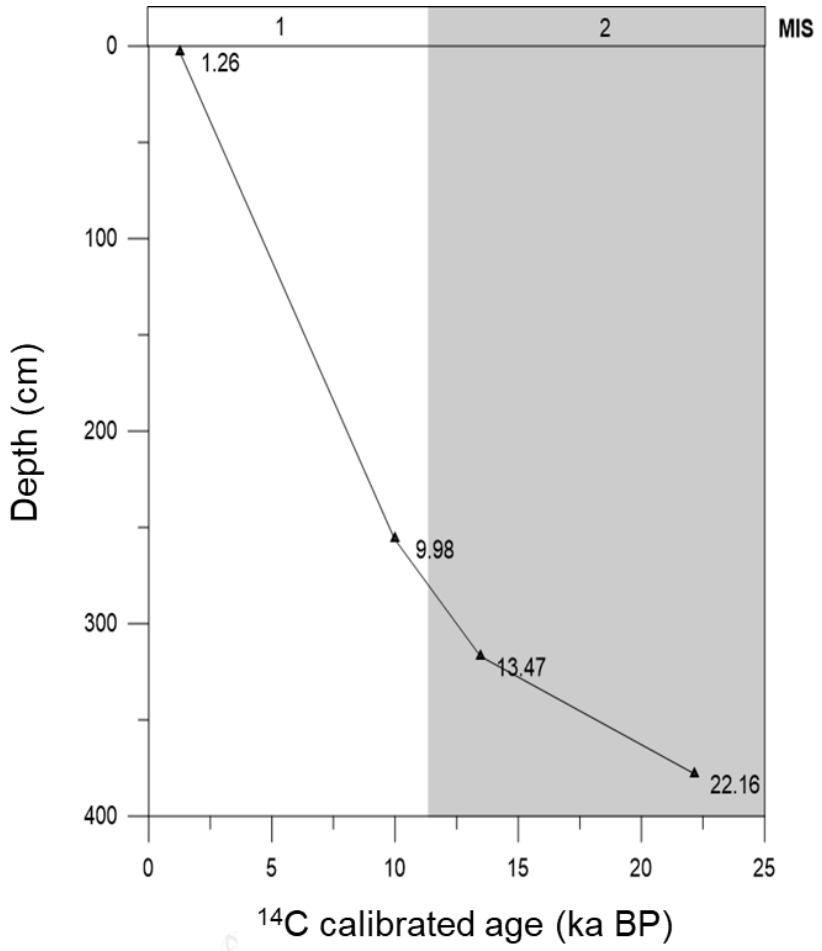

Figure 12 Age model of core ADM6 based on 14C dating, showing by depth (cm) vs age (ka). The tilted triangles presents age controlled points, which were obtained from the oxygen isotope stratigraphy. Color shade presented Marine Isotopic Stage (MIS).

3.3.3 Age model of core MASS-III-10

Five ^{14}C-AMS samples were obtained as Table 6. MASS-III-10 was revealed age covers since Late Glaciation around ~45 ka and Holocene which would transform to fit with the result analysis and correspond with the marine isotopic stages (MIS 3 and MIS 2 for glacial variations and MIS 1 for interglacial variation). The ^{14}C dates obtained were converted into calendar ages using Marine09 calibration curve (Reimer et al., 2009) and were calibrated using Calib 7.0.2 (Stuiver et al., 1998) within 1σ level of errors as well.

Table 6 ^{14}C AMS ages of MASS-III-10 calibrated using Calib program version 7.0.2.

Depth (cm)	Foraminifera species	^{14}C AMS age BP	Average Calibrated age (1σ, yrs BP)	Error 1 σ
MASS-III-10				
12	*G. ruber*	6,410 ± 40 BP	4,940	118
24	*G. ruber*	15,110 ± 60 BP	15,953	189
60	*G. ruber*	27,640 ± 130 BP	29,217	195
88	*G. ruber*	30,480 ± 180 BP	32,162	354
142	*G. ruber*	41,950 ± 690 BP	43,019	1,201

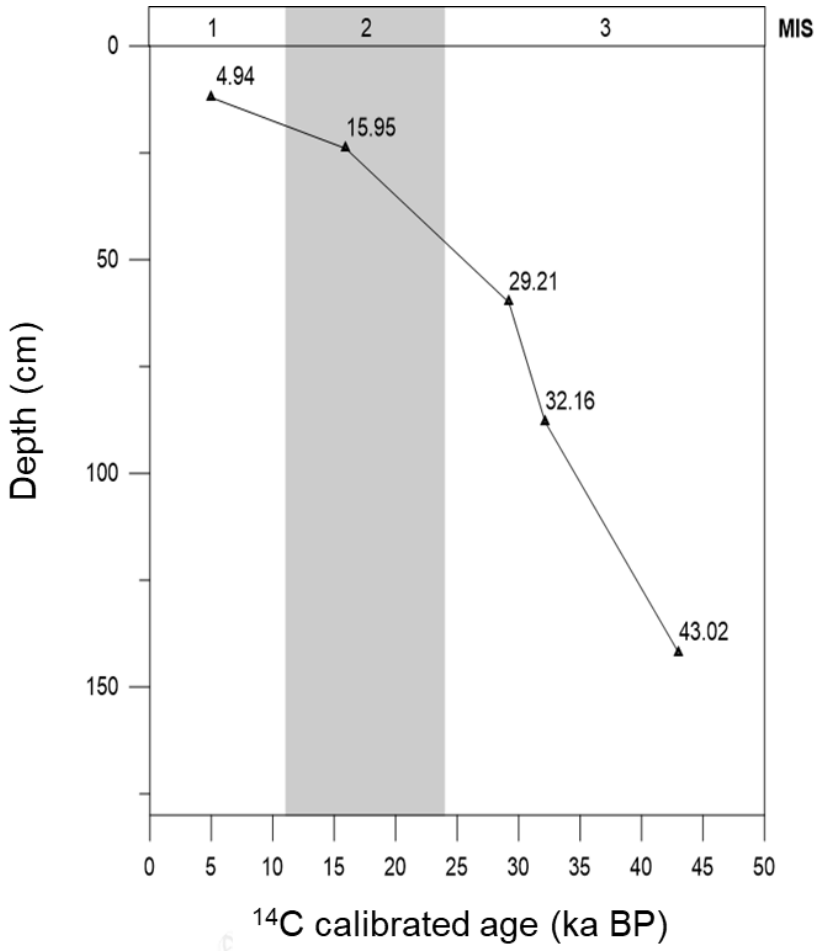

Figure 13 Age model of core MASS-III-10 based on 14C dating, showing by depth (cm) vs age (ka). The tilted triangles presents age controlled points, which were obtained from the oxygen isotope stratigraphy. Color shade presented Marine Isotopic Stage (MIS).

3.3.4 Age model of core MASS-III-07

MASS-III-07 obtained age cover 25 ka in the last glaciation. It was started by four ^{14}C-AMS samples but it is not continuous record for the last 25 ka. Therefore, two control points were selected to obtain this age model as Table 7. MASS-III-07 revealed age during 25-15 ka since the last glaciation and mostly correspond with the MIS 2 for glacial variations. The ^{14}C dates obtained were converted into calendar ages using Marine09 calibration curve (Reimer et al., 2009) and were calibrated using Calib program version 7.0.2 (Stuiver et al., 1998) within 1σ level of errors as well.

Table 7 ^{14}C AMS ages of MASS-III-07 calibrated using Calib program version 7.0.2.

Depth (cm)	Foraminifera species	^{14}C AMS age BP	Average Calibrated age (1σ, yrs BP)	Error 1 σ
MASS-III-07				
29	*G. ruber*	14,380 ± 60 BP	15,017	250
147	*G. ruber*	23,990 ± 120 BP	25,761	196

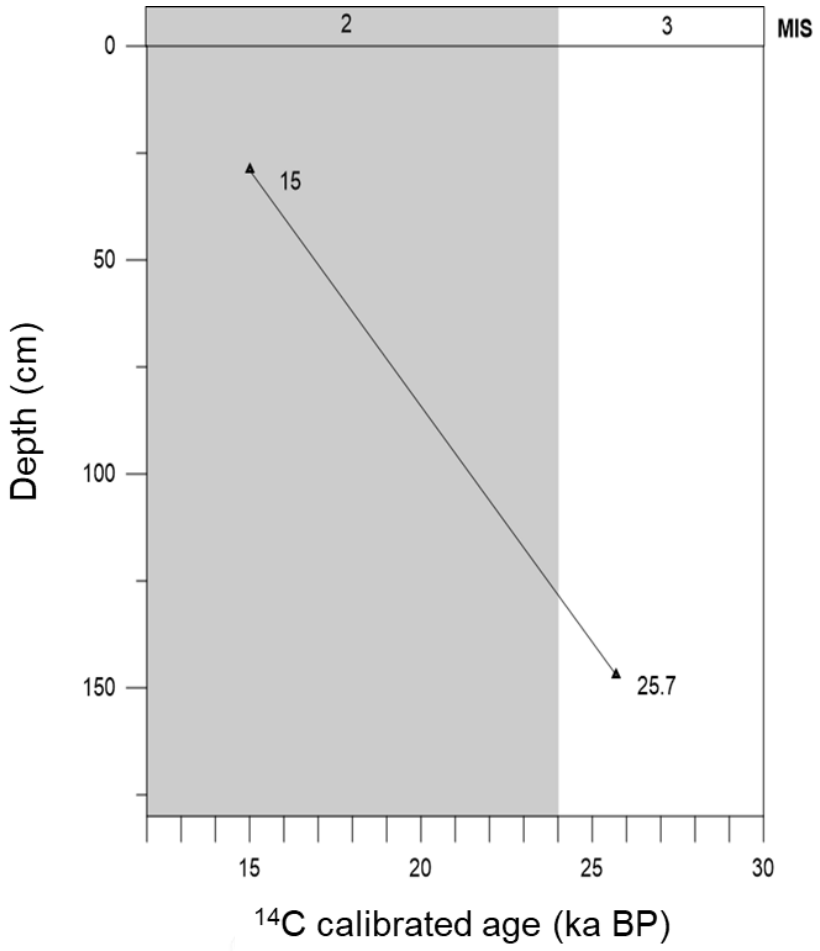

Figure 14 Age model of core MASS-III-07 based on 14C dating, showing by depth (cm) vs age (ka). The tilted triangles presents age controlled points, which were obtained from the oxygen isotope stratigraphy. Color shade presented Marine Isotopic Stage (MIS).

3.3.5 Summary of chronological frameworks

The age models of the four cores are summarized in Table 8. High-resolution planktonic foraminiferal oxygen isotope stratigraphy combined with ^{14}C AMS dates of four cores confirms their excellent quality of sedimentation rates. In comparison to MD77-169, ADM2 was characterized by lower sedimentation rates but ADM6 sedimentation rates was high. For the deep sea

cores, sedimentation rate of ADM2 displayed an average at 10.7 cm/ka for last 15 ka and at 7.7 cm/ka during 44-15 ka period. While ADM6 provided continuous sedimentary record with high average sedimentation rate of 28.9 cm/ka for the Holocene, and of 17.5 cm/ka for 15 ka (Fig. 15). MASS-III-10 sedimentation rates are low in the Holocene and MIS 3 (2.2 cm/ka and 4.0 cm/ka) and it is 9.9 cm/ka during 30-15 ka (glaciation time). MASS-III-07 showed the sedimentation rate of 12.3 cm/ka during 25-15 ka.

As the results of two deep sea core, presenting high sedimentation rate during the Holocene than the last glaciation, it may be suggested that this core was consistent with enhancing of southwest monsoonal effect since the beginning of Holocene (Morrill et al., 2003; Herzschuh, 2006; Awasthi et al., 2014). Additionally, the high sedimentation rate, presenting in core ADM6 it may be due to the high of hydrodynamic in this area. Moreover, ADM6 can be indicating the mixing zone as well as it was found the turbidity layer in the lower part of the core. Although the two shallow water cores are located in the same area but their sedimentation were showed the difference rates which are not stable in the downward evolution of the sedimentation rate. The sedimentation rate of core MASS-III-10 is quite stable, not much vary between 2.2 - 9.9 cm/ka but the core MASS-III-07 is higher (12.3 cm/ka). Core MASS-III-07 could be suggesting that it located in the disturbance zone and this core is effected by the slide of sediment. It may be because of NE monsoon driven influence on Sumatra current into the Andaman Sea may wash off some of the surface sediment that correspond well with losing of the core top.

Table 8 Summary of ages of the studied cores in the southern Andaman Sea.

Core	Cover age	MIS
ADM 2	44 ka to present	3, 2, 1
ADM 6	23 ka to present	2, 1
MASS-III-10	45 ka to present	3, 2, 1
MASS-III-10	25-14 ka	2

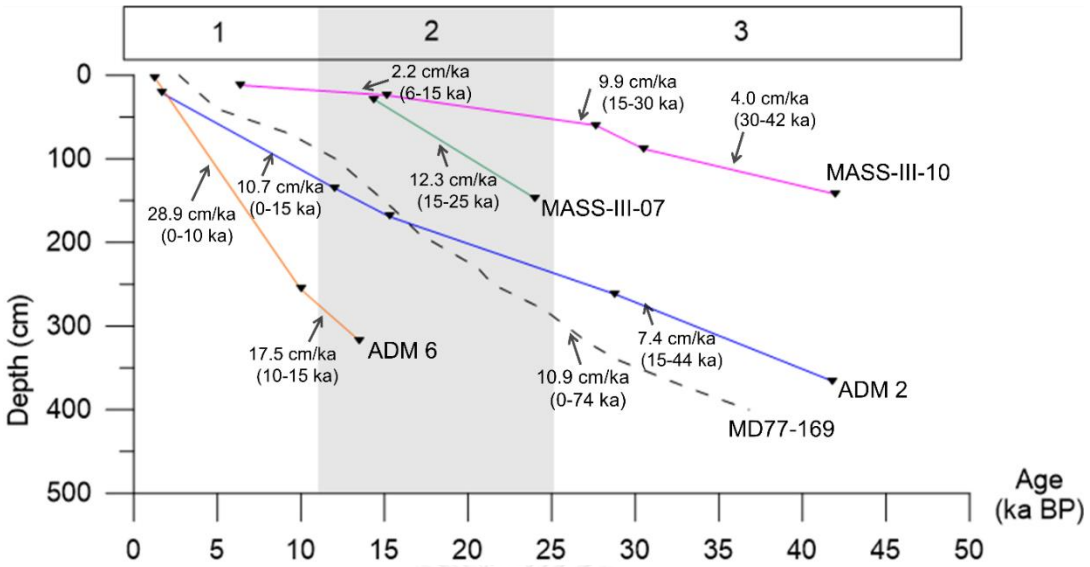

Figure 15 Time scale of ADM 2, ADM 6, MASS-III-10, and MASS-III07 are obtained by combining 14C AMS ages and correlation with core MD77-169 (Colin et al., 1998) as reference. The age model for these cores were established by correlating the δ18O obtained on G. ruber with core MD77-169 by using Analyseries software (Paillard et al., 1996). Depth (cm) versus age (50 ka) diagram showing variations in the sedimentation rates (cm/ka). The tilted triangles presents age controlled points and color shade presented MIS stage.

CHAPTER 4

CLAY MINERAL IN SURFACE SEDIMENT OF THE ANDAMAN SEA

The clay mineral assemblage in marine sediments has been widely used to identify sediment provenance, water mass circulation, and environmental change investigations. Clay mineral assemblage has been used in numerous studies to constrain and reconstruct variations in the sources of sediments and their link with transport of detrital fine-grained sediments processes. In particular, the distribution in the main groups of clay mineral which are smectite, illite, kaolinite and chlorite can be used to illustrate the sedimentological processes.

4.1 Composition of clay minerals in the provenance area

Generally, clay minerals are typical weathering products on the earth's surface that can be used to trace sediment sources and to indicate various intensities and processes of chemical weathering on the source rock. Clay mineralogy of surface samples from the Andaman Sea and the surrounding area were investigated to reveal source and transport of detrital fine-grained sediments. In total 61 surface sediments combined with 26 river sediments were analyzed for the clay mineral assemblage of Andaman Sea surface sediments. The relative abundance of clay minerals including kaolinite, smectite, illite and chlorite of surface sediments from Myanmar shelf (MM) and Thailand shelf (TH) together with the illite crystallinity and illite chemistry index were reported in Table 9.

Table 9 Average clay mineral assemblages and illite chemical index of surface and core top sediments from different provinces surrounding the Andaman Sea with standard deviation values.

Region	Sample Number	Averages contents (%) + Standard deviation				Illite chemical index	References
		Smectite	Kaolinite	Illite	Chlorite		
Surface sediment							
Myanmar shelf (MM)	39	44 ± 7.23	17 ± 1.43	13 ± 4.13	16 ± 2.96	0.437	This study
Thailand shelf (TH)	22	23 ± 12.78	47 ± 8.43	18 ± 5.19	11 ± 3.99	0.303	This study
Malay Peninsula	12	0 ± 0.49	80 ± 3.17	18 ± 3.94	2 ± 2.11	0.469	Wang et al. (2011)
Sumatra	14	18 ± 4.54	66 ± 7.23	8 ± 5.01	7 ± 4.97	0.701	Liu et al. (2012)
Core top sediment							
ADM2	-	71	11	10	8	0.373	This study
ADM6	-	67	11	13	9	0.395	This study
MASS-III-10	-	71	13	10	7	0.438	This study
MD77-169	-	47	7	36	10	-	Colin et al. (1999)
MD77-176	-	62	9	14	15	-	Joussain et al. (2016b)
MD77-186	-	86	4	7	4	-	

Three characteristic end-members in clay mineral compositions were characterized to identify the potential provenances of fluvial input. The clay mineral assemblages in the Andaman Sea and surrounding fluvial drainage basins are largely different between the different provenances. Therefore, the clay mineral compositions are grouped and present in four different provinces by the average mineral assemblages showing by pie-chart in Fig. 16. The provenance areas of the Andaman Sea based on this study can be divided into four provinces; Myanmar shelf, Thailand shelf, Malay Peninsula, and Sumatra.

Myanmar shelf: Province 1

The clay mineral assemblages of Myanmar shelf province (Province 1) from 39 nearshore surface sediments consist mainly of smectite (average 44%), kaolinite (17%), illite (23%), and chlorite (16%). The illite chemistry index, a proxy showing the degree of chemical weathering, in this province usually varies between 0.35 and 0.51.

Thailand shelf: Province 2

The clay mineral assemblages of Thailand shelf from 22 nearshore samples consist dominantly of kaolinite (average 47%), smectite (23%), illite (18%), and chlorite (11%). The illite chemistry index of Thailand shelf province showed moderate chemical weathering degree between 0.23 and 0.38.

Malay Peninsula: Province 3

The clay mineral assemblages of 12 samples from six rivers in Malay Peninsula of Wang et al. (2011) (Province 3) is dominated overwhelmingly by kaolinite (74-85%, average 80%), with moderate illite (17%) and scarce chlorite (2%). The illite chemistry index in Malay Peninsula usually varies between 0.41 and 0.55.

Sumatra: Province 4

The investigated surface river samples in Sumatra of Liu et al. (2012) (Province 4) are divided geographically into three sub-provinces, but for the overall comparison the average of all sub-provinces (14 samples) were used. Sumatra province contained the overwhelming content of kaolinite for 67%, moderate smectite (18%), minor illite (average 8%) and chlorite (average 8%). In Sumatra, illite chemistry index is usually high, among 0.48–0.94, without an obvious difference between the sub-provinces.

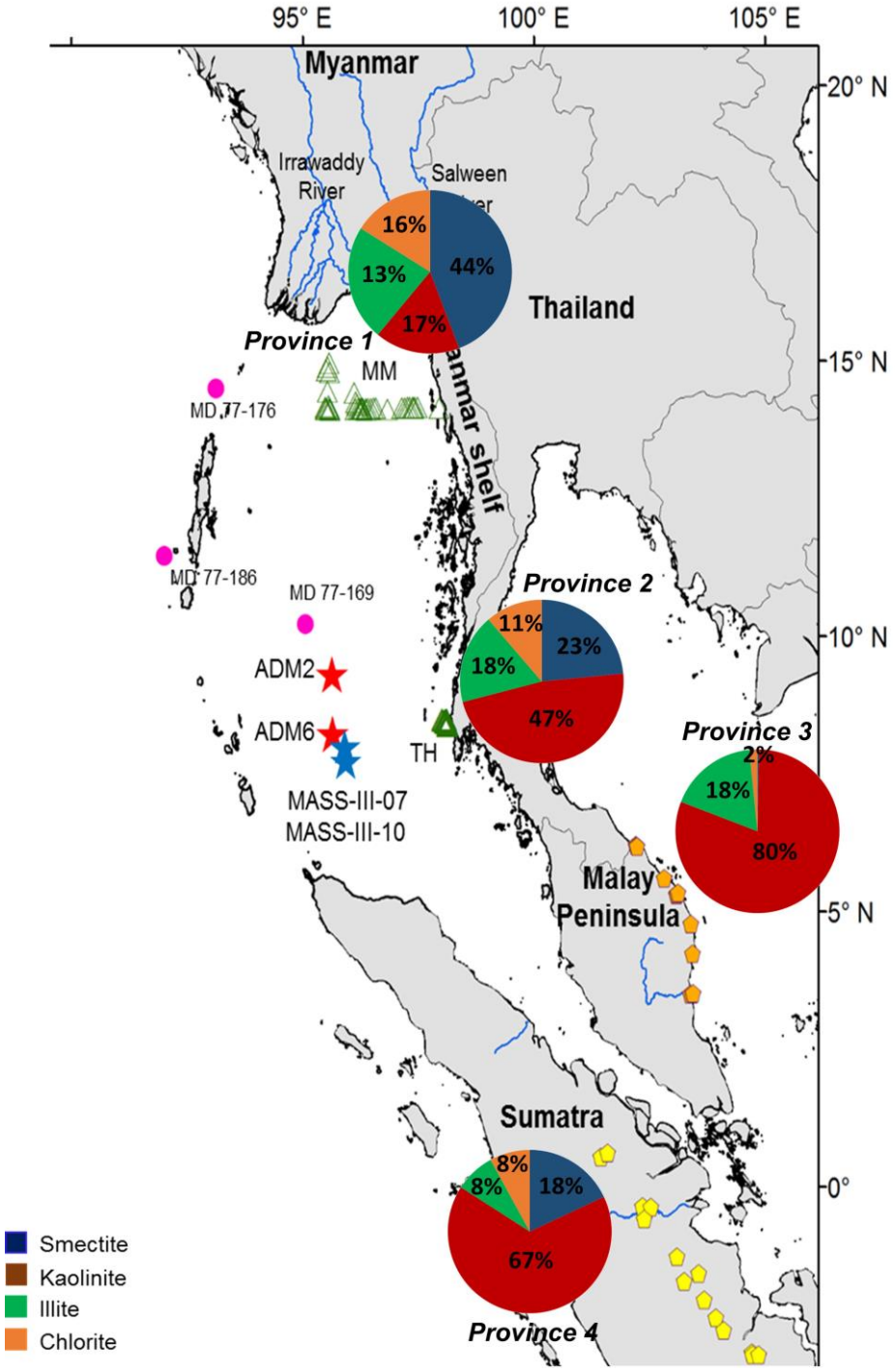

Figure 16 Average clay mineral assemblages (%) of four main clay contents; smectite (blue), kaolinite (red), illite (green), and chlorite (orange) by various provinces in the Andaman Sea and surrounding drainage basins. The data calculated from various provinces are listed in Table 9. Data of river draining

samples of Malay Peninsula from Wang et al. (2011); data of river samples of Sumatra from Liu et al. (2012).

In order to understand controlling factor of clay minerals in Myanmar shelf and Thailand shelf, the diagram of Velde, 1985 is plotted (Fig. 17). The figure indicated that the clay minerals of Myanmar shelf is controlled by lithology. Taking into consideration of lithological settings, the bedrock of the western part of the Andaman Islands consists mainly of Palaogene sedimentary rocks and volcanic rocks from island volcano (Awasthi et al., 2014). The northern part of the Andaman Sea is in different settings which include the Irrawaddy river delta consisting mainly of Quaternary deposits (Colin et al., 1998; 1999) with Neogene and Palaogene sedimentary rocks (Robinson et al. 2014; Awasthi et al., 2014) and the Myanmar shelf (included Salween river area) consisting mainly the Paleozoic and Tertiary sedimentary rocks. This rock can produce more smectite to the Andaman Sea. On other hand, the clay minerals of Thailand are mainly controlled by climate (Fig. 17). The humid and warm climatic conditions of southern Thailand can produce kaolinite, which can consider as an indicator of intense chemical weathering (Chamley, 1989).

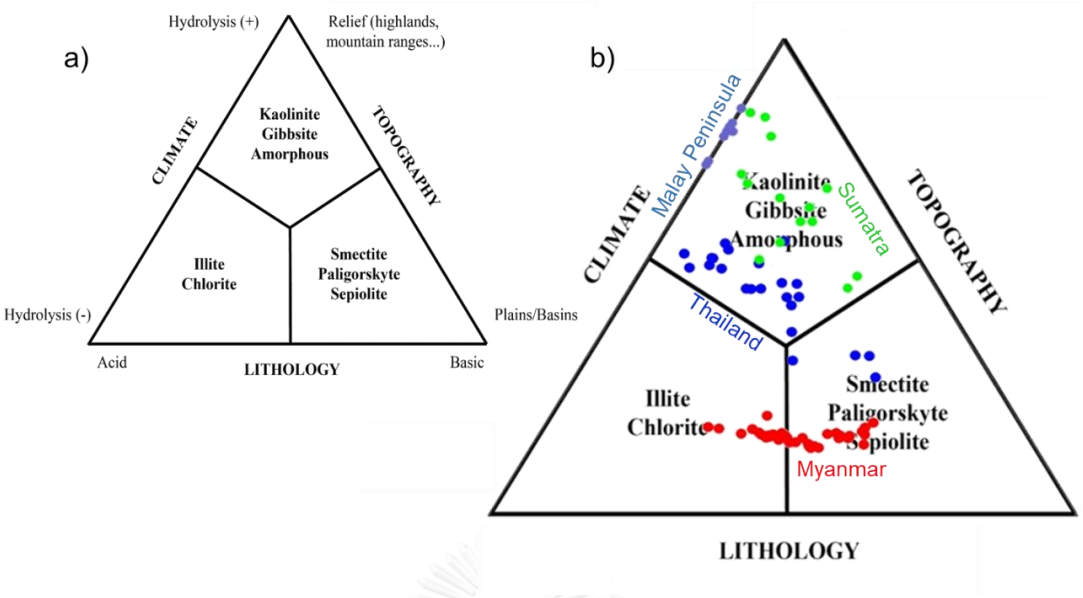

Figure 17 a) Clay ternary diagram which represents the influence on the clay assemblage of the climate, the topography and the lithology of the source rock (from Velde, 1985) b) Interpretation of control factor influence on the clay assemblages in the different provenance area; four potential provenance are plotted in the diagram as Malay Peninsula (light blue), Sumatra (green), Thailand (navy blue), and Myanmar (red).

4.2 Clay minerals in surface sediments

The clay mineral assemblages of the surface sediments obtained from different provenance area of Myanmar shelf, Thailand shelf, Malay Peninsula, Sumatra, and the Andaman Islands show two significant features (Fig. 18): (1) high smectite contents (47%) in Myanmar shelf and in all three provinces of the Andaman Island with extremely high values (>80%) in surface samples of core MD77-186; (2) kaolinite contents (generally >60%) in Sumatra with extremely high values (~80%) in Malay Peninsula, and >40% in Thailand shelf.

Andaman Islands: Additional potential province

The core top samples of sediment core derived from the Andaman Sea surrounding the Andaman Islands were added to illustrate the clay mineral in one of potential provenance area of the Andaman Sea. This provenance is divided geographically into three sub-provinces, all containing the overwhelming content of smectite. The core top sample of core MD77-169 (Colin et al, 1999) consists of major smectite (47%), moderate illite (36%), and minor kaolinite (7%) and chlorite (10%). Core MD77-176 and MD77-186 have similar clay mineral assemblage, consisting of major smectite (61 and 86%), minor kaolinite (9 and 4%), minor illite (14 and 7%), and low chlorite (15 and 4%).

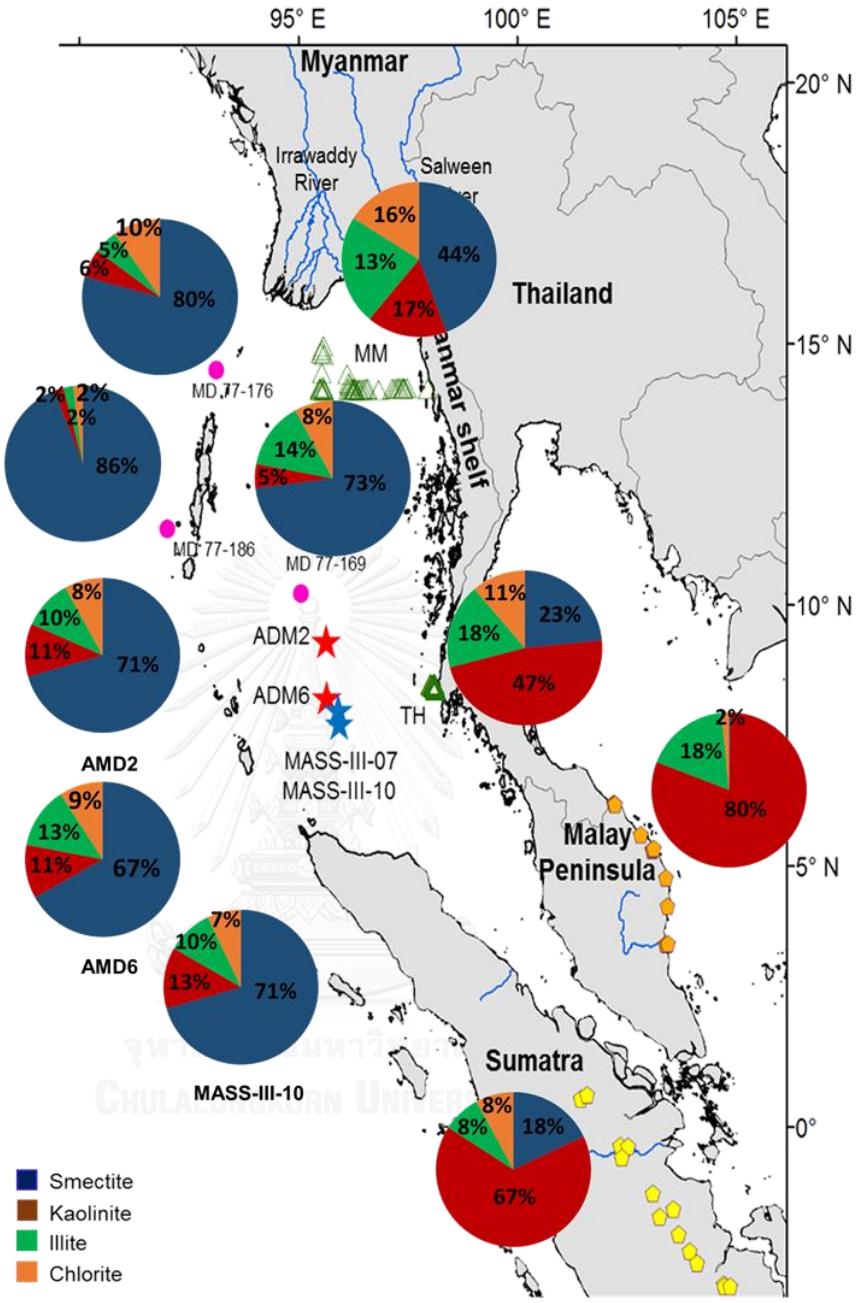

Figure 18 Average clay mineral assemblages (%) of surface sediments in the Andaman Sea in the present time. The color shades represent four main clay contents; smectite (blue), kaolinite (red), illite (green), and chlorite (orange). Data of river draining samples of Malay Peninsula from Wang et al. (2011); data of river samples of Sumatra from Liu et al. (2012). Data of reference core of the Holocene period; MD77-169 (Colin et al, 1999), MD77-176, and MD77-186 (Colin et al, 1998; Joussain et al., 2016b).

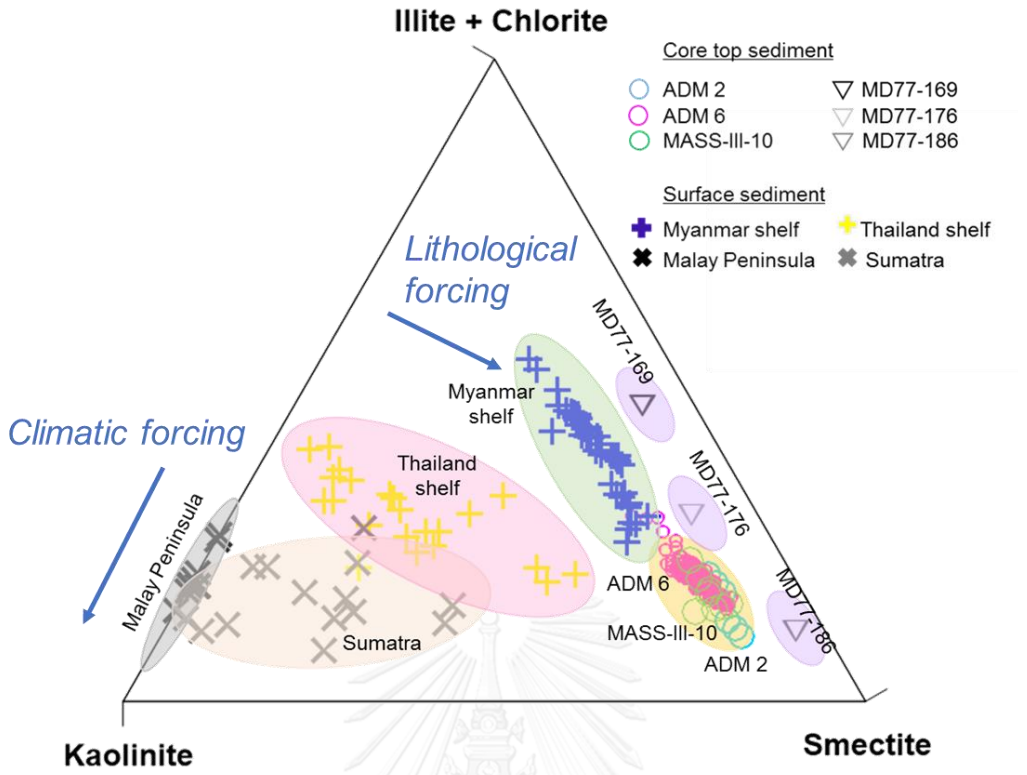

Figure 19 Ternary diagram of the averaged clay mineral assemblages by three end members; illite+chlorite, kaolinite and smectite of the studying sediment groups. The clay mineral formation are indicated into various provenances as the difference shade; province 1- 4 of provenances surrounding the Andaman Sea.

In summary, clay mineral assemblages in surface sediments of the Andaman Sea show progressive changes among three end-members of the provenances: Myanmar shelf sediments (major smectite and minor kaolinite, illite, and chlorite), Malay Peninsula and Sumatra sediments (principal kaolinite), and Thailand shelf sediments (predominant kaolinite and moderate smectite). The core top sediment samples were included to reveal clay mineral in the surface sediments in the present time. However, the three cores (core ADM2, ADM6, and MASS-III-10) were investigated in the Holocene sediments except core MASS-III-07 which revealed period since 25-15 ka in MIS 2, missing the Holocene period. The surface sediment of three sediments cores; ADM2, ADM6, and MASS-III-10 in the southern Andaman Sea showed similar

contents, consisting the high smectite (~80%) and minor kaolinite, illite, and chlorite. These are corresponded well the Myanmar shelf sediment as in Fig. 19, suggesting that the clay mineral in the core site are under lithological forcing. The Myanmar shelf sediments are situated in Irrawaddy inner-shelf which is dominated by terrestrial sediment delivered by the Irrawaddy-Salween Rivers (Ramaswamy et al., 2008). Accordingly, the terrigenous material in the Andaman Sea sediments is mainly composed of world-class large rivers such as the Irrawaddy River, Salween River. The Irrawaddy and Salween is the third largest river in the world in terms of suspended sediment discharge contributes annually more than 540 Mt of sediment (Robinson et al., 2007). The suspended detrital sediments from these rivers are major provenance of sediment to the southern Andaman Sea as clay mineral showed in the core top sediments of core ADM2, ADM6, and MASS-III-10. However, Malay Peninsula and Sumatra are suggested as minor sources of terrigenous sediment for the Andaman Sea (Liu et al., 2012). This is because there are no major rivers in the Malay Peninsula and Sumatra which are related to terrestrial sediment delivery to the Andaman Sea. While few rivers have developed on the peninsula, most of them debouch into the Gulf of Thailand and the South China Sea (Rodolfo, 1969b). Cao et al. (2015b) suggested that suspended sediment discharge contributes from Malay Peninsula by Malay river is less than 2 Mt/year. By estimation from catchment areas following the study of Liu et al. (2016) who studied riverine input to the Gulf of Thailand, suspended sediment from Thai rivers contributed to the Andaman Sea is estimated to be less than 5 Mt/year.

4.3 Modern ocean transportation process

Differential settling

The smectite contents of surface sediment and core top sediments are higher than riverine sediments that are in source area. This implies differential settling of smectite in surface sediments. Higher salinity can promoted the flocculation and deposition of smectite, and it lead to higher smectite content on deep sea. This is a common phenomenon found in several continental shelves adjacent to large rivers, for examples, the Niger River (Porrenga, 1967), the Amazon River (Patchineelam and de Figueiredo, 2000), and the Mekong River (Szczuciński et al., 2013; Xue et al., 2014).

Modern surface sediment transport

Although smectite contents on the surface sediments and core top sediments are controlled by differential settling, the spatial distribution of smectite in the southern Andaman Sea has a close relation to the local current systems that mainly controlled by the monsoonal winds (Fig. 20). The sediment transferring into the Andaman Sea is under the sub-surface current and is controlled by the seasonal reversal of two monsoonal winds. The smectite from the northern provenance can disperse clockwise into the Andaman Sea. The obtained smectite in these cores might result from particle fractionation as smectite dominates the smallest clay mineral size fraction (Kurian et al., 2008) that is consequently transported further away from the coastal source areas to the core site.

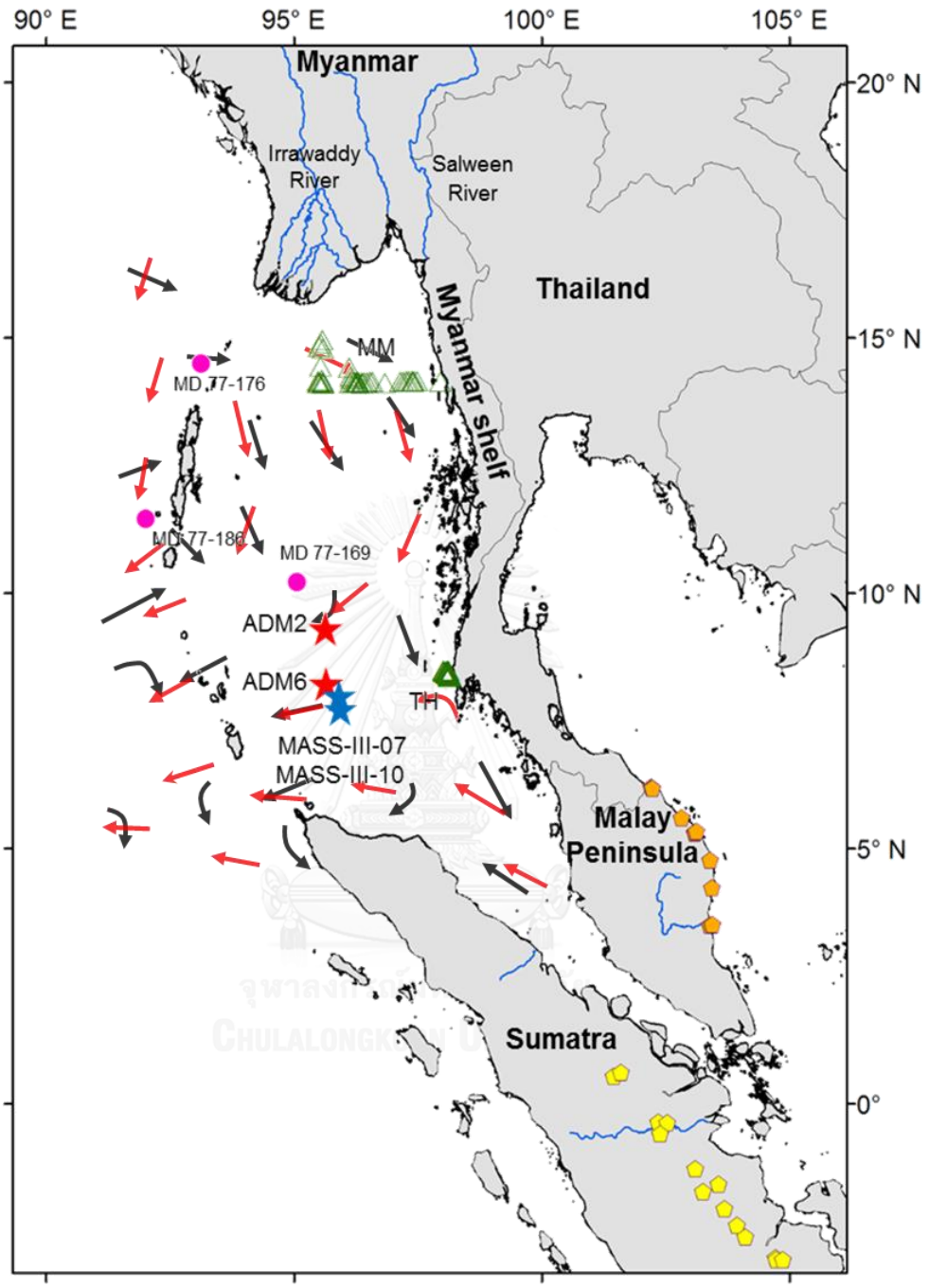

Figure 20 Map of predominated surface circulations in the Andaman Sea driven by the northeast monsoon (red) and southwest monsoon (black) (modified after Brown, 2007) with sample locations.

CHAPTER 5

CLAY MINERAL VARIATION SINCE THE LAST GLACIATION

5.1 Clay mineral assemblages

5.1.1 Characteristics of clay mineralogy records in sediment cores

Clay minerals of Core ADM 2

The relative abundance of several clay minerals including kaolinite, smectite, illite and chlorite in the studied core are plotted in Fig. 21. The clay mineral assemblage of core AMD2 since the Last Glaciation (44 ka) is mainly composed of smectite (51–78%, average 67%), illite (7–17%, average 11%), kaolinite (9–17%, average 13%) and chlorite (5–14%, average 9%). The kaolinite, illite and chlorite distributions showed similar trends and revealed the inverse trend from smectite distribution. The patterns of illite, chlorite, and kaolinite show increased contents in MIS 3 while decreased contents during MIS 2 and the Holocene. On the other hand, the smectite showed decreasing content at ~23 ka, and then increased to the Holocene.

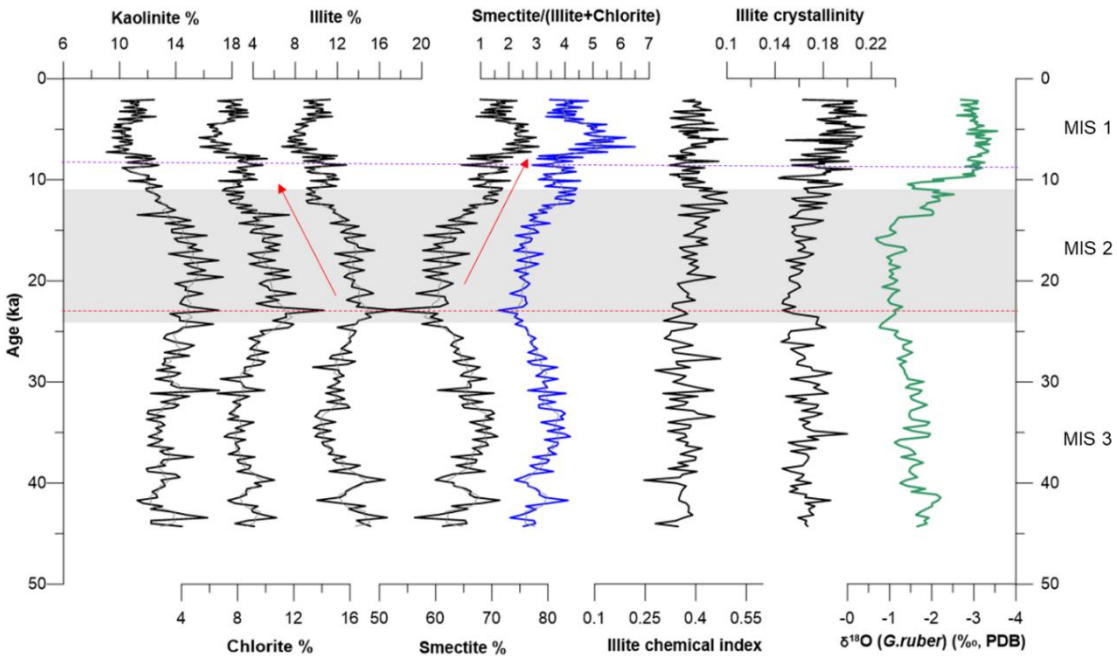

Figure 21 Summary results of ADM2. Clay mineral assemblages (%) for <2μm particles non-calcareous clay; kaolinite, chlorite, illite, smectite, ratio of smectite/(illite+chlorite) (blue), illite chemical index, and illite crystallinity versus age (ka BP). Planktonic foraminifera (G. ruber) $\delta^{18}O$ curve of ADM 2 is displayed (green). Bar color displays MIS 2 stage.

Clay minerals of Core ADM 6

Because of turbidity layer after 342 cm, the result of lower section of 342 cm were not involved in the interpretation in this study. The clay mineral assemblage of core ADM6 of the upper section of 342 cm that date back to 15 ka are plotted in Fig. 22. The sediments of core AMD6 is mainly composed of smectite (61–74%, average 69%), illite (8–13%, average 10%), kaolinite (10–16%, average 13%) and chlorite (7–11%, average 8%). The smectite variations in Holocene period is generally lower than glaciation. In the Holocene, smectite distribution shows several peaks and is low at ~8 ka then decreased in MIS 1 period. The kaolinite, ittite and chlorite patterns show the same trend, which are

slightly low during the Holocene, and reached upward to the peak at ~8 ka (Fig. 22).

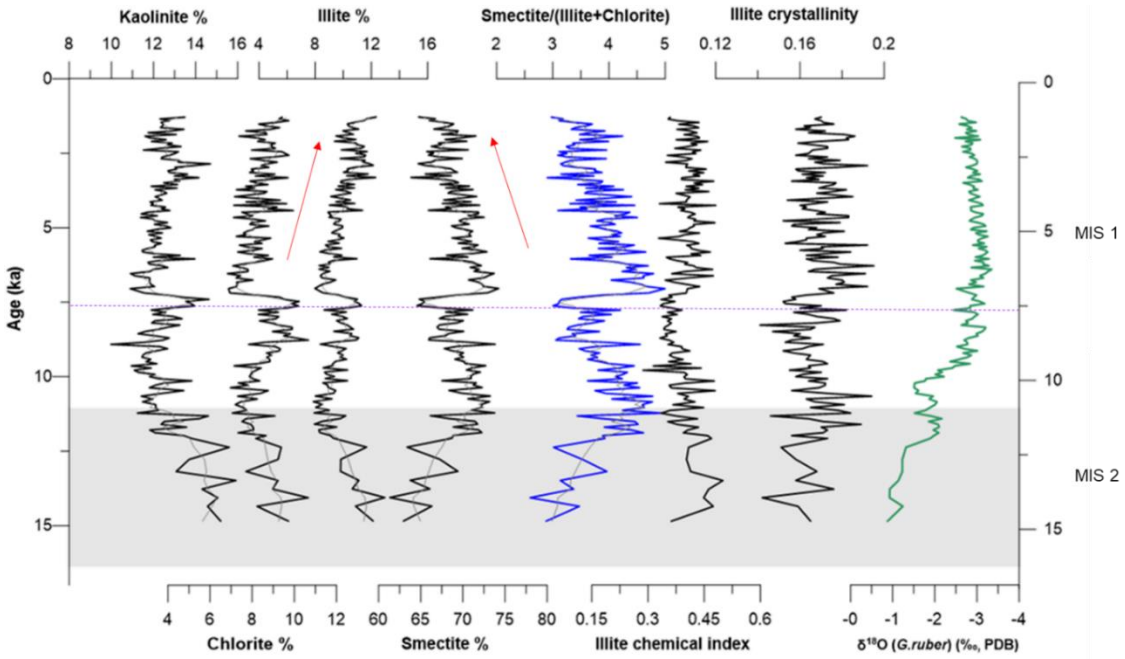

Figure 22 Summary results of ADM6. Clay mineral assemblages (%) for <2μm particles non-calcareous clay; kaolinite, chlorite, illite, smectite, ratio of smectite/(illite+chlorite) (blue), illite chemical index, and illite crystallinity versus age (ka BP). Planktonic foraminiferal G. ruber δ18O curve is displayed (green). Bar color displays MIS 2 stage.

Clay minerals of Core MASS-III-10

The clay mineral assemblageof MASS-III-10 over the last 45 ka are plotted in Fig. 23. The sediments of core MASS-III-10 contain of high smectite for 73% (65-79%)**,** moderate kaolinite for 12% (10-17%), and low illite and chlorite contents (<15%). In general, smectite distribution is inversely correlated to illite. The sediments during MIS 3 and MIS 2 are characterized by higher contents of smectite than during MIS1 ones, whereas illite is lower during

MIS1 than during MIS 3 and MIS 2. Meanwhile, kaolinite and chlorite display a short range since 45 ka (Fig. 23).

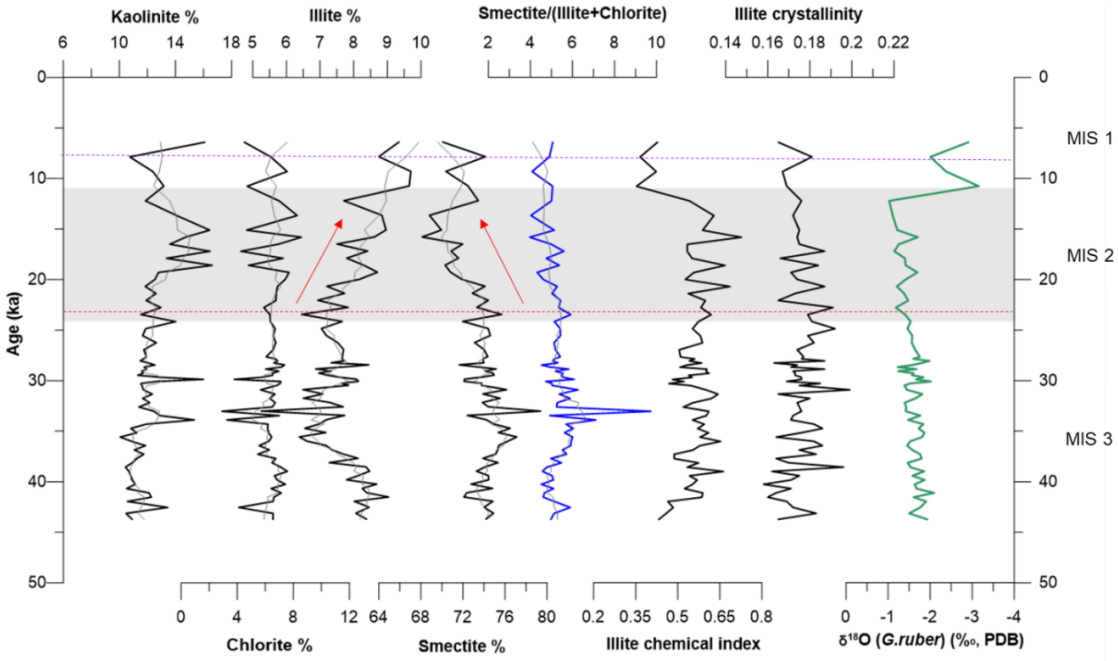

Figure 23 Summary results of MASS-III-10. Clay mineral assemblages (%) for <2μm particles non-calcareous clay; kaolinite, chlorite, illite, smectite, ratio of smectite/(illite+chlorite) (blue), illite chemical index, and illite crystallinity versus age (ka BP). Planktonic foraminiferal G. ruber $\delta^{18}O$ curve is displayed (green). Bar color displays MIS 2 stage.

Clay minerals of Core MASS-III-07

The relative abundance of kaolinite, smectite, illite and chlorite in Core MASS-III-07 are plotted in Fig. 24. The clay mineral assemblage of core MASS-III-07 over the last 25 ka is mainly composed of smectite (66–77%, average 72%), illite (7–11%, average 9%), kaolinite (10–18%, average 13%) and chlorite (4–9%, average 7%). The smectite distribution is inversely correlated to illite. The sediments during MIS 2 are characterized by higher contents of smectite than during MIS 1 ones, whereas illite is lower during MIS 1 than during

MIS 2. Meanwhile, kaolinite and chlorite display a short range though entire record.

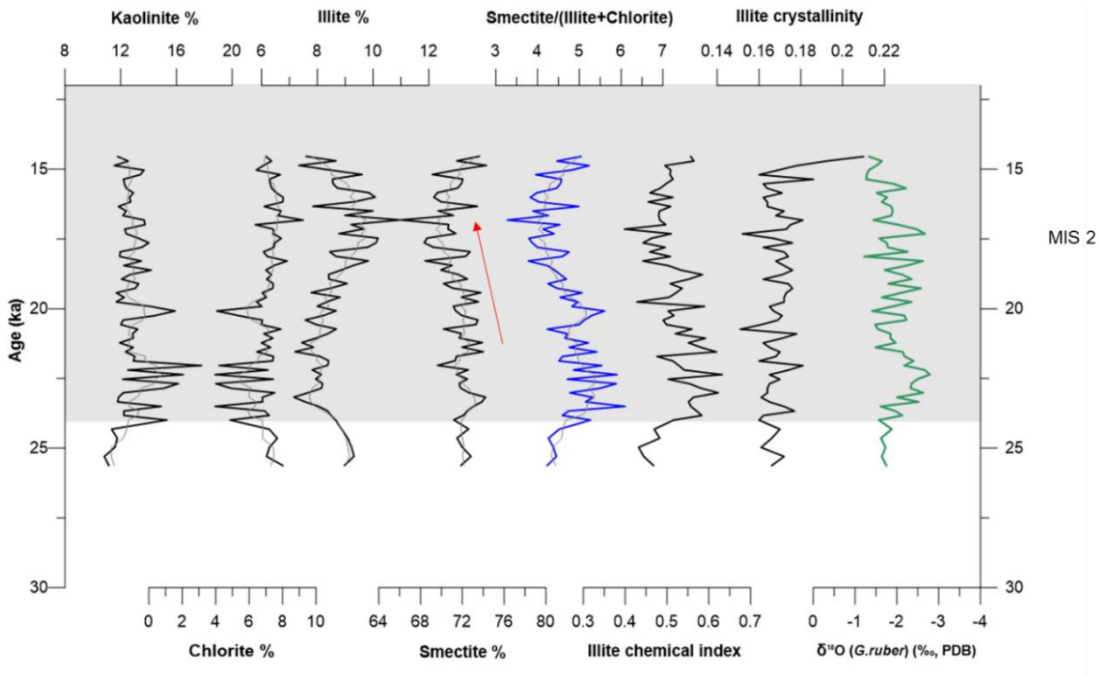

Figure 24 Summary results of MASS-III-07. Clay mineral assemblages (%) for <2μm particles non-calcareous clay; kaolinite, chlorite, illite, smectite, smectite/(illite+chlorite) ratio (blue), illite chemical index, and illite crystallinity versus age (ka BP). Planktonic foraminiferal G. ruber $\delta^{18}O$ curve is displayed (green). Bar color displays MIS 2 stage.

In the Andaman Sea, sea level changes occurring between glacial and interglacial stages may have had an important control on sedimentation in this area (Colin et al., 1998). Moreover, the strong 23 ka periodicity is largely dominating, suggesting relationship with the monsoon process and the sea level changes (Colin et al., 1998). Core ADM2 is dominant in smectite content. The smectite variation in this core showed the lowest at ~23 ka, suggesting the changing signal of the occurrence event. Core ADM 6 showed the lowest smectite content during ~8 ka while core MASS-III-10 and MASS-III-07 displayed slight variations along the core. During Holocene, the '8.2 ka' cold

event was recorded in Greenland ice cores (Kobashi et al., 2007). The cold climate in Greenland and the weak ISM occurred at ~8.2 ka BP according to $\delta^{18}O$ evidence from Greenland ice cores and the Asian speleothems (Kobashi et al., 2007; Thomas et al., 2007; Cheng et al., 2009).

5.2 Provenance Analysis

As mention in chapter 4, dominant smectite in surface sediment is influence by prevailing surface circulation and the differential setting of smetite. The well correspondent with the Myanmar shelf sediment suggesting that the clay mineral in the downcore (Fig. 25) are under lithological forcing similar to the core top sediment (Fig.19). It may suggest that the sediment dispersed to the core sites come from the Myanmar shelf which is the rest area of sediment eroded from Irrawaddy and Salween River.

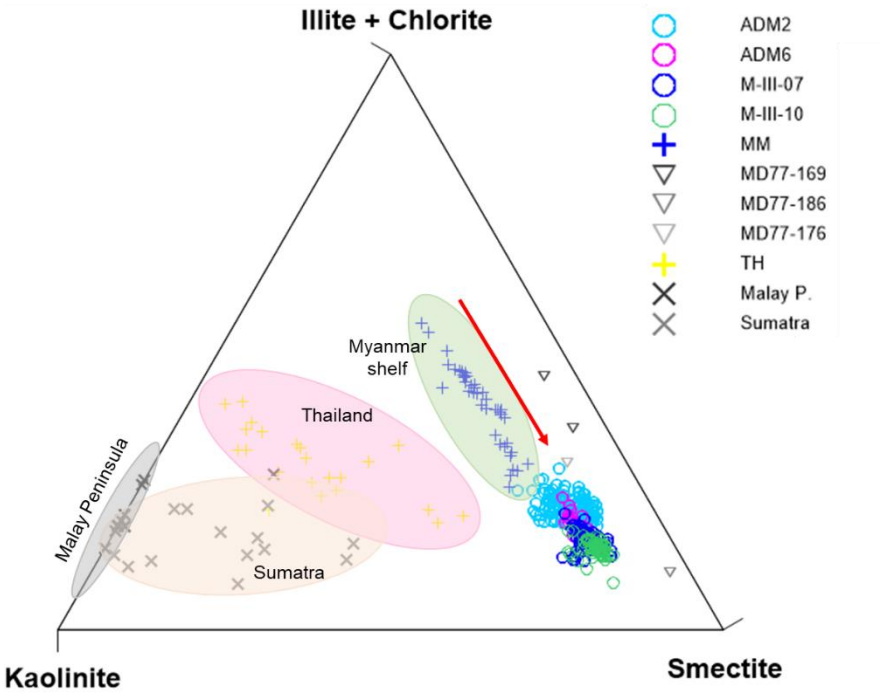

Figure 25 Ternary diagram of the averaged clay mineral assemblages by 3 end members; illite+chlorite, kaolinite and smectite of the studying sediment groups. The clay mineral formation are indicated into various provinces as the difference shade; four provenance provinces surrounding the Andaman Sea combined with the clay assemblages of four sediment cores.

The large variations downcore found in ADM2, ADM6, and MASS-III-10 while slight variation found in MASS-III-07 suggest the relative contributions from different sources area which may relate to the monsoon changing over the glaciation period and Holocene (Awasthi et al., 2014). The changing in the source contributions to the core location were most likely influenced by surface currents in sediment transportation as indicated by the variations of the sedimentation rate among the sediment cores. Although sedimentation rate in the deep sea can be affected by various processes such as dynamics of transportation from land, surface circulation pattern, local processes (turbidity by channel transportation and sea level changing especially in the northern Indian ocean, it was mostly affected by the physical weathering such as the continental erosion linked to the intensity of summer monsoon (e.g., Chauhan and Vogelsang, 2006; Awasthi et al., 2014, Cao et al., 2015b, Joussain et al., 2016b).

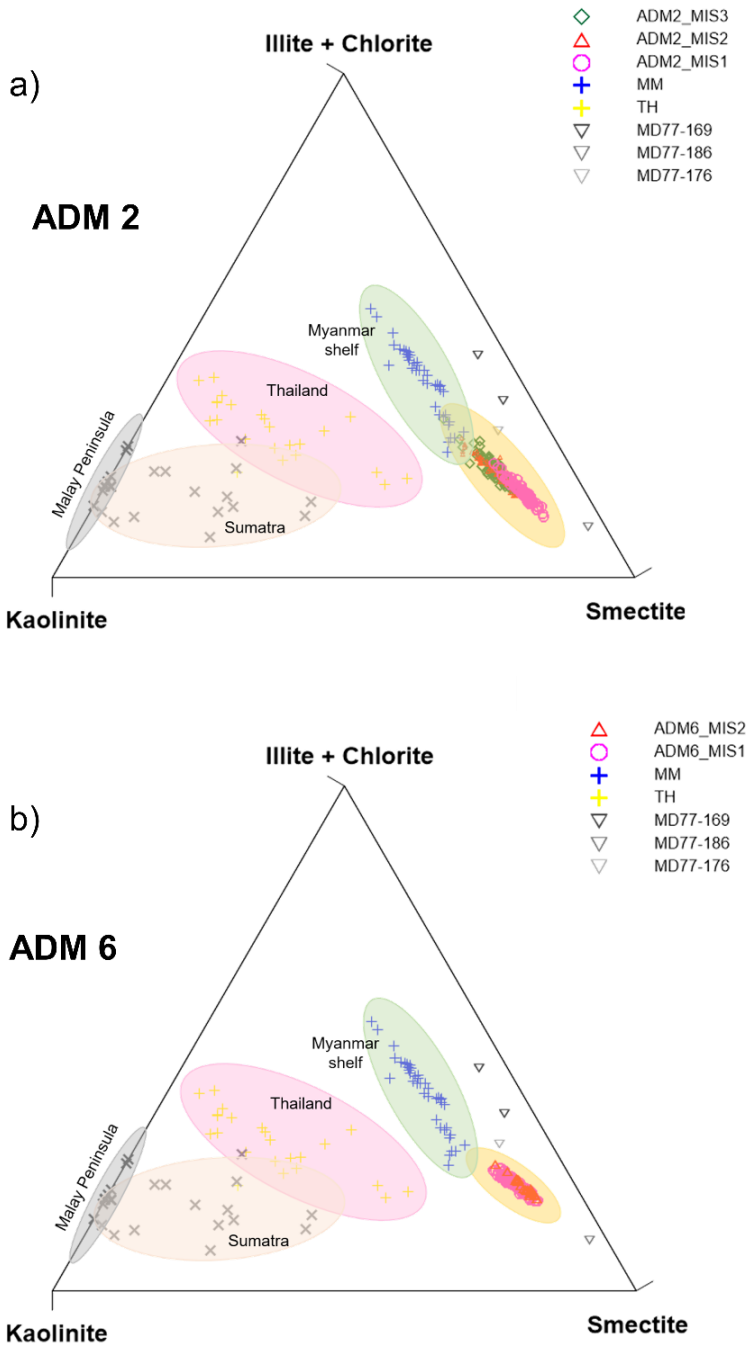

Figure 26 Ternary diagram of the averaged clay mineral assemblages by 3 end members; (illite+chlorite, kaolinite and smectite). The clay mineral assemblages in the orange shade is presenting the study core distribution. ADM 2 is presented in a) and ADM 6 is present in the b) figure. The purple circle is representing the MIS 1 sediment, the red triangle is representing the MIS 2 sediment, and the green sign is representing the MIS 3 sediment.

The four provenance provinces surrounding the Andaman Sea in different shades are presented.

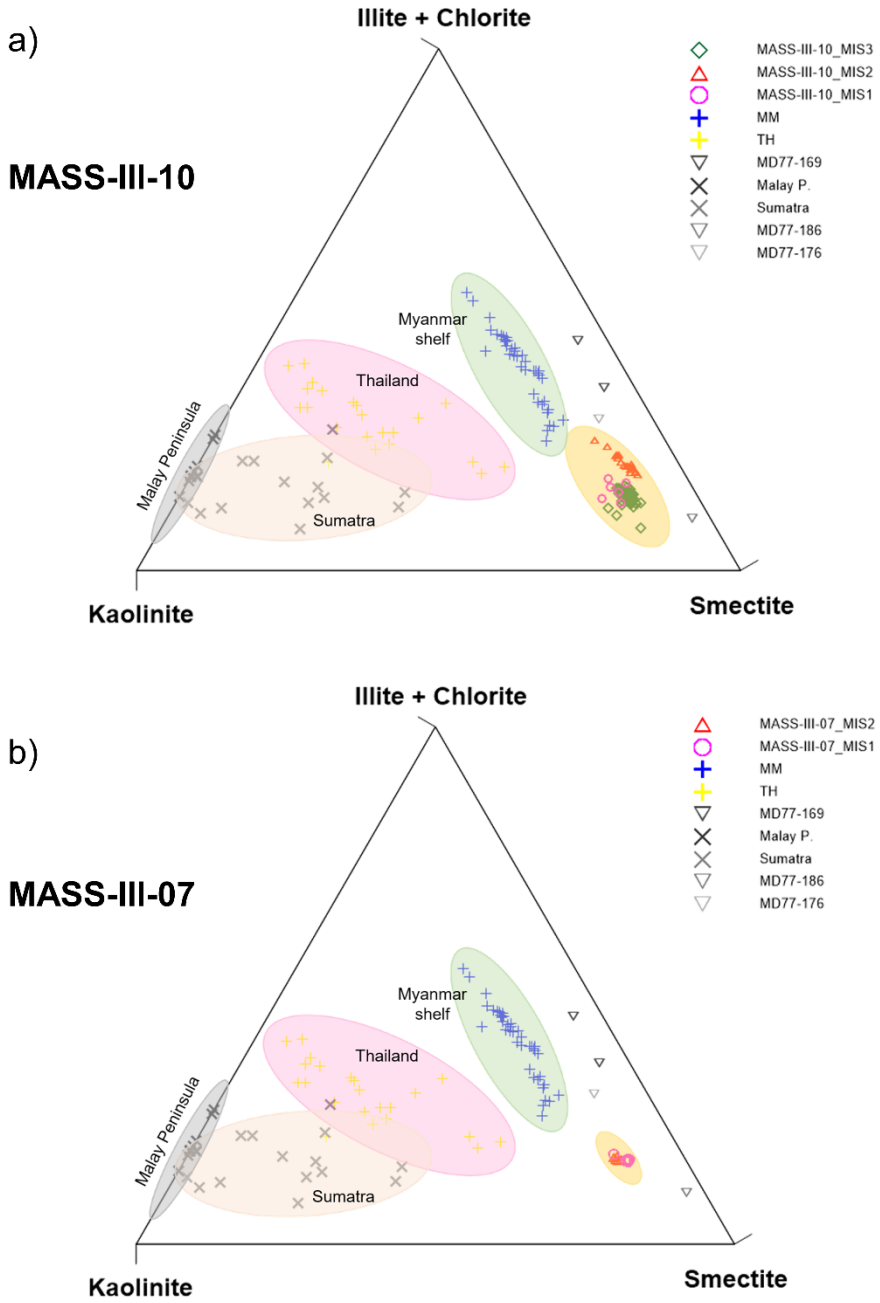

Figure 27 Ternary diagram of the averaged clay mineral assemblages by 3 end members; (illite+chlorite, kaolinite and smectite). The clay mineral assemblages in the orange shade is presenting the study core distribution. MASS-III-10 is

presented in a) and MASS-III-07 is present in the b) figure. The purple circle is representing the MIS 1 sediment, the red triangle is representing the MIS 2 sediment, and the green sign is representing the MIS 3 sediment. The four provenance provinces surrounding the Andaman Sea in different shades are presented.

From the provenance analysis of the Andaman Sea sediments, it may suggest that the Irrawaddy and Salween Rivers are the main source of the Andaman Sea sediments over the last 45 ka BP, consistent with previous studies (e.g., Colin 1998; 1999; 2006, Awashi et al, 2014; Ali et al., 2015, Cao et al., 2015b). However, Colin et al. (1999; 2006) have proposed that sediment inputs from northern Andaman Sea did not vary over the past 60 ka, whereas Ali et al. (2015) have suggested that little influence of source region changes on sediment composition over the past 60 ka. As Fig. 26 and Fig. 27 revealed the provenance of the sediment recorded in core ADM2, ADM6, and MASS-III-07 had no significant change in downcore variation. It can be concluded that the relative contributions of the provenances to the core sites did not vary through time since the last glaciation which fit well with Colin et al. (1999, 2006) conclusion. While MASS-III-10, in Fig. 27 (left), presented the variation during the glacial and interglacial periods suggesting the variation of contributions to this core site. This could be due to the changing of other controlling factors such as river discharge.

The sedimentation rate of both deep sea cores; ADM2 and ADM6 display similar pattern, i.e. high rate in Holocene and low in the glacial period. ADM2 showed the low sedimentation rate (7.4 cm/ka) during 44-15 ka which may occur because of the local processes, i.e. the sea level low stand during LGM by -120 m (Awasthi et al., 2014), effecting the sedimentation. Although ADM6 presented the low sedimentation rate during glaciation similar to ADM2, this core revealed much higher rate than ADM2 which was found 28.9 cm/ka for the

Holocene, and 17.5 cm/ka for 15 ka. Comparing between ADM2 and ADM6, the high sedimentation rate of ADM6 may be due to the different morphology whereby ADM6 was located shallower than ADM2 making it more sensitive to changing of sea level than ADM2. Moreover, the bottom of ADM6 was found the turbidity layer during 22-15 ka which corresponded well with the sea level changing pattern that may effect to the sedimentation in ADM6. The turbidity in ADM6 could suggest the high sediment input especially from the Irrawaddy sediment to Andaman Sea (Awasthi et al., 2014). The shallow water cores which taken from continental slope; MASS-III-07 shows high sedimentation rate (12.3 cm/ka) than MASS-III-10 (2.2 - 9.9 cm/ka). Although these two shallow water cores are located in the same area, their sedimentation rates were different. The high sedimentation rate of core MASS-III-07 suggested that the core location may be existed in the disturbance zone, of which may be influenced by the NE monsoon driven on Sumatra current into the Andaman Sea. The current may wash off some of the surface sediment that corresponded well with losing of the top of core.

CHAPTER 6

ENVIRONMENT RECONSTRUCTION OF THE ANDAMAN SEA

6.1 Element geochemistry variation

The major elements were measured on bulk sediment of core sediment samples from ADM2 and ADM6 to assess the state and degree of chemical weathering. The percentage of SiO_2, Al_2O_3, Fe_2O_3, MgO, CaO, Na_2O, K_2O, P_2O_5, SO_3, MnO and TiO_2 were measured and grouped into 3 geomorphic units. ADM 2 and ADM 6 consisted of high amount of SiO_2, Al_2O_3 and CaO (> 60%) of their total contents, low amount of Fe_2O_3, MgO, Na_2O and K_2O (12%) and small percentages of P_2O_5, SO_3, MnO and TiO_2. Fig. 6 presented results of terrigenous (SiO_2, Al_2O_3, TiO_2, K_2O) and biogenic component (CaO) of both cores. ADM2 revealed several peaks, the terrigenous input was low in LGM and rapidly increased in Holocene after 10 ka (Fig. 28a). Major element distribution of ADM6 (Fig. 28b) was similar to ADM2 distribution. The variation in Holocene of ADM2 and ADM6 revealed the high components at ~8 ka which corresponded well with the clay mineral changing.

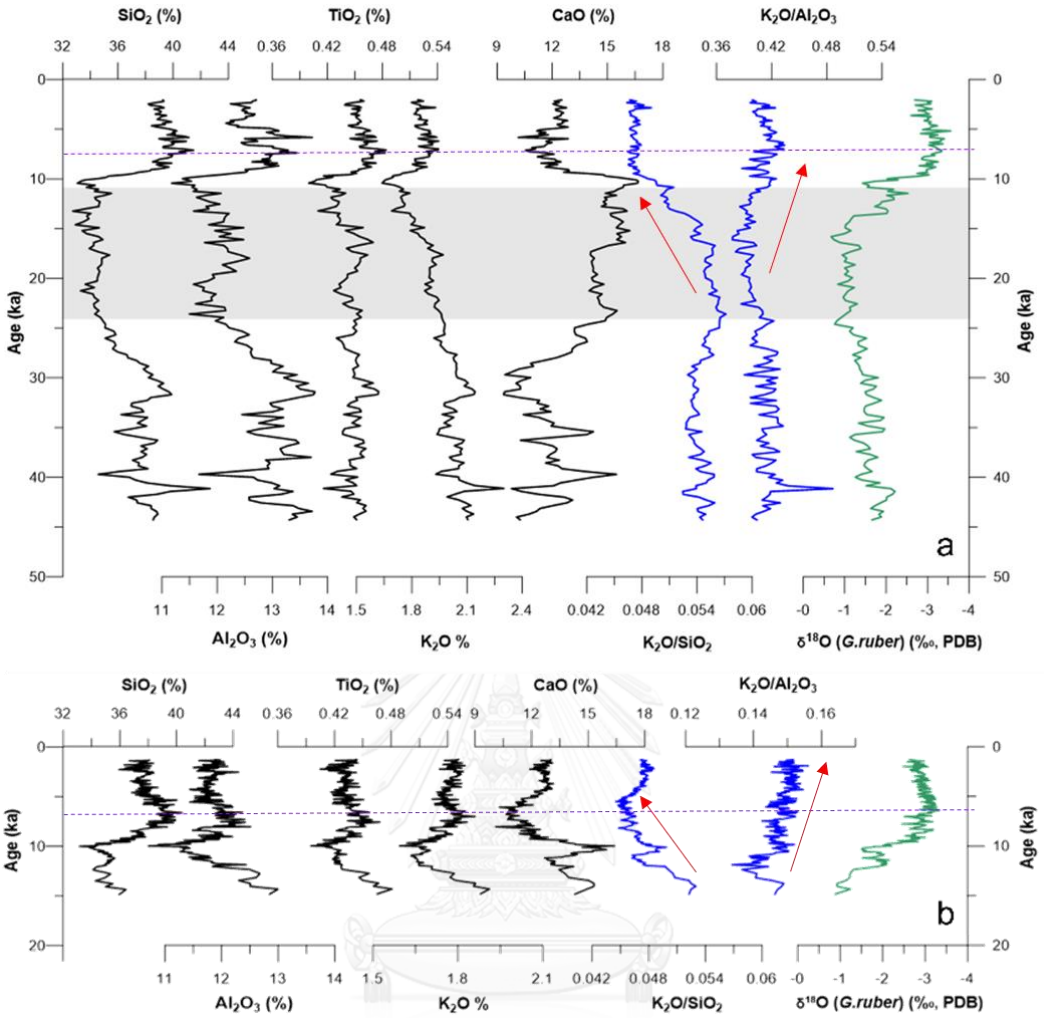

Figure 28 Major element variation of (% of total vol.); SiO_2, Al_2O_3, TiO_2, K_2O, CaO, K_2O/SiO_2 ratio (blue), K_2O/Al_2O_3 ratio (blue) versus age (ka BP) and planktonic foraminifera (G.ruber) $\delta^{18}O$ curve (green) are displayed. a) ADM 2 b) ADM 6.

The K_2O/Al_2O_3 and K_2O/SiO_2 ratios of bulk sediments are usually studied to recognize the sediment sources. For more identification of sources, the correlation of K_2O/Al_2O_3 and K_2O/SiO_2 were obtained to reflect the changing of chemical weathering from provenance sources. The K_2O/Al_2O_3 and K_2O/SiO_2 ratios displayed moderate positive correlations in the bulk sediment indicating that the mineralogical were controlled by contents of SiO_2 and Al_2O_3. These

results suggest that the enrichment of Si and Al during chemical weathering occurred in the sedimentation in the Andaman Sea. In order to examine the changes within terrigenous fraction, K_2O/Al_2O_3 ratio is employed because of Al is resilient to leaching while K is more mobile during chemical weathering, K_2O/Al_2O_3 ratio can trace the chemical weathering degree of bulk sediments. K_2O/Al_2O_3 ratio indicates rainfall-induced physical erosion in source areas. The trend of K_2O/Al_2O_3 of both deep sea cores presented the decreasing trend from MIS II to Holocene, implying the decreasing of chemical weathering intensities and the changing of the rainfall by the summer monsoon (Colin et al., 2006).

6.2 Paleoclimate reconstruction

6.2.1 Comparison of major elements to clay mineral variation

In addition, the ratio of K_2O/Al_2O_3 from major element compositions reversely related to the chemical weathering, K_2O/Al_2O_3 decreases when the chemical weathering increases. K_2O/Al_2O_3 ratios from core ADM2 and ADM6 showed moderate negative correlations with smectite (note the reversed axis of K2O/Al2O3 ratios in Fig 29.) displyaing obvious decline of K_2O/Al_2O_3 ratio during Holocene while smectite content incresed. This may suggested that during the Holocene the clay mineralogy was mainly controlled by the increasing of summer monsoon intensity which in turn affected the major sources of sediment inputs to the Andaman Sea. In Glaciation period, the K_2O/Al_2O_3 ratio variation might not be related to the intensity of the monsoon but could correspond well with low stand of sea level by the global sea level variation (Waebroeck et al, 2002). Moreover, during sea level lowstand, smectite was transported by the surface current as showing by its low value, whereas illite and chlorite which were mainly eroded by physical weathering increased. Therefore, the terrigenous input of Andaman Sea may be affected by both monsoon

intensity and sea level change. This is in agreement with the sedimentary responses to summer monsoon observed in the same area (Cao et al., 2015b).

Additionally, the changes in the mineralogical ratio; smectite/(illite+chlorite) could indicate the intensity of chemical weathering. Moreover, illite and chlorite are primary clay minerals while smectite is review as secondary, the ratio of smectite/(illite + chlorite) could also be used to reveal the glacial-interglacial variation of clay mineral deposition. This ratio will reflect the balancing of physical erosion (illite + chlorite) and chemical weathering (smectite) (Ali et al., 2015). As illustrated in Fig. 29, the ratio of ADM2 and ADM6 showed similar pattern in Holocene and ADM2 showed low ratio during last glacial period, illite and chlorite contents were significantly increased while smectite contents trend to decrease.

Core ADM2 presented the lower value of smectite/(illite+chlorite) in the glacial early of stage 2, indicating increasing of physical weathering which could imply high physical erosion of the highland Indo-Burma ranges in Irrawaddy catchment led to the release of large amounts of illite+chlorite into Andaman Sea (Joussain et al., 2016b). Coupled with the sea level lowstand during LGM, the materials on the continent could be transferred to the Andaman Sea more than during the Holocene. This is confirmed by the lower smectite/(illite+chlorite) ratio of core ADM2. During the Holocene, higher smectite/(illite+chlorite) ratios of both cores responded to the interglacial period and reflect high monsoon intensity and also reflect the stronger summer monsoon as previously studied in this area (Colin et al., 1999; Ali et at., 2015).

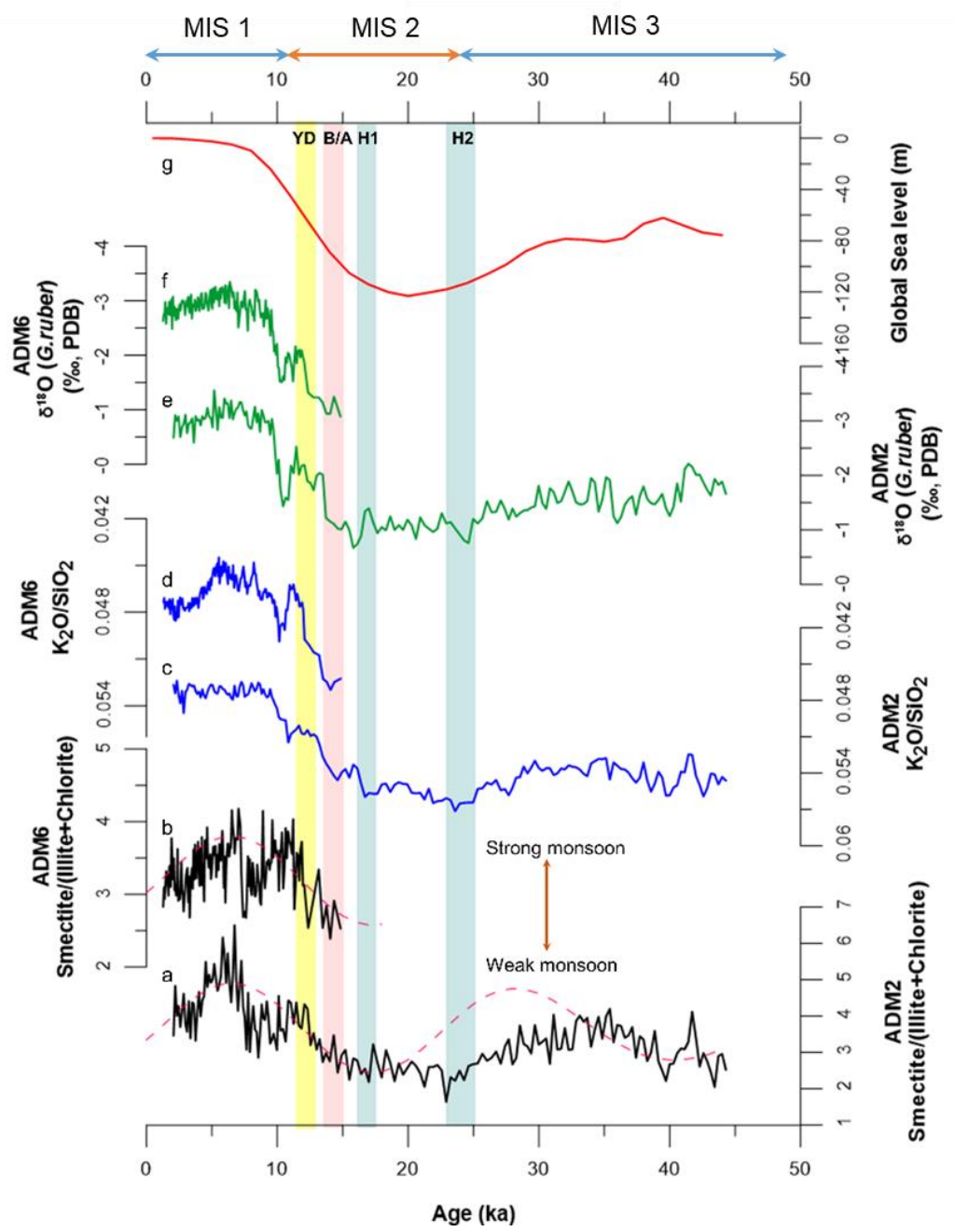

Figure 29 Smectite/(illite+chlorite) ratio a) ADM2 b) ADM6, Major element ratio of K_2O/SiO_2 c) ADM2 d) ADM6, $\delta^{18}O$ (*G. Ruber*) curve e) ADM2 f) ADM6, g) global sea level (Waebroeck et al, 2002). Dash curve presents insolation curve calculated for September at 10^0N by using Analyseries software (Paillard et al., 1996). Shaded bars show the ages of Heinrich events H1, H2

(Hemming et al., 2004), Younger Dryas (YD; 13-11.5 ka) (Alley, 2000), Bølling/Allerød (B/A; 15–13.5 ka), respectively (Sijinkumar et al., 2010).

Moreover, the changes in the smectite/(illite+chlorite) ratio were related with the precessional changes of the earth's orbit at 23 ka and also correlated with the mineralogical characteristics. The calculated September solar radiation at 10ºN was used as a proxy for clay mineral variation since the maximum rainfall occurs in August and it takes approximately one month for maximum runoff and hence sediment input to occur (Colin et al., 1999). The intensity of the 23 ka periodicity significantly associates with the relationship between the clay mineralogy and the low latitude solar forcing, as well as the Asian summer monsoon intensity. The insolation curve calculation for September using Analyseries software (Paillard et al., 1996) demonstrated the summer monsoon intensity variations (Boulay et al., 2005) which maximum of insolation corresponds to the peak of smectite/(illite +chlorite) ratio. The smectite/(illite +chlorite) ratio of ADM2, ADM6, MASS-III-10, and MASS-III07 with September insolation in Fig. 29 and Fig. 30 showed that during Holocene the ratio corresponded well with the maximum of insolation, indicating that the clay mineral changing due to the increasing of chemical weathering intensity in the Andaman Sea. This correlation imply that the terrigenous input to Andaman Sea were mainly controlled by the increasing of summer monsoon intensity over the Irrawaddy catchment (Colin et al., 1999; Rashid et al., 2007; 2011). Moreover, the stronger summer monsoon during Holocene provided stronger rainfall, suggesting the increasing of chemical weathering of Irrawaddy catchment illustrated by increasing of kaolinite and smectite to Andaman Sea (Colin et al., 2006). However, the amount of both cores presented low contents of kaolinite which may be due to the clay mineral transformations of secondary lithological forcing processes on the chemical weathering (Egli et al., 2001; Liu et al., 2012).

The same interpretation with ADM2 and ADM6 can be obtained from Core MASS-III-10 and MASS-III-07 using the ratio of ln[K/Al] (Fig. 30). The ratio of *ln*[K/Al] decreases when the chemical weathering increases in late of MIS 2. During the Holocene the clay mineralogy was mainly controlled by the increasing of summer monsoon intensity in the Andaman Sea, but it is not clear in the Holocene variation in these shallow water cores. In the Glaciation period of MASS-III-10 and MASS-III-07, the *ln*[K/Al] ratio variation are not related to the sea level curve (Waebroeck et al, 2002) but corresponded well with the insolation curve. The mineralogical ratio; smectite/(illite+chlorite) indicated the intensity of chemical weathering. The smectite/(illite+chlorite) ratio of MASS-III-10 and MASS-III-07 (Fig.30) showed the similar pattern in MIS 2. Core MASS-III-10 presented the lower smectite/(illite+chlorite) in the early of MIS 2, indicating increasing of physical weathering which in turn implied the high physical erosion of the highland Indo-Burma ranges in Irrawaddy catchment (Joussain et al., 2016b) similar to the results obtained from the deep sea cores.

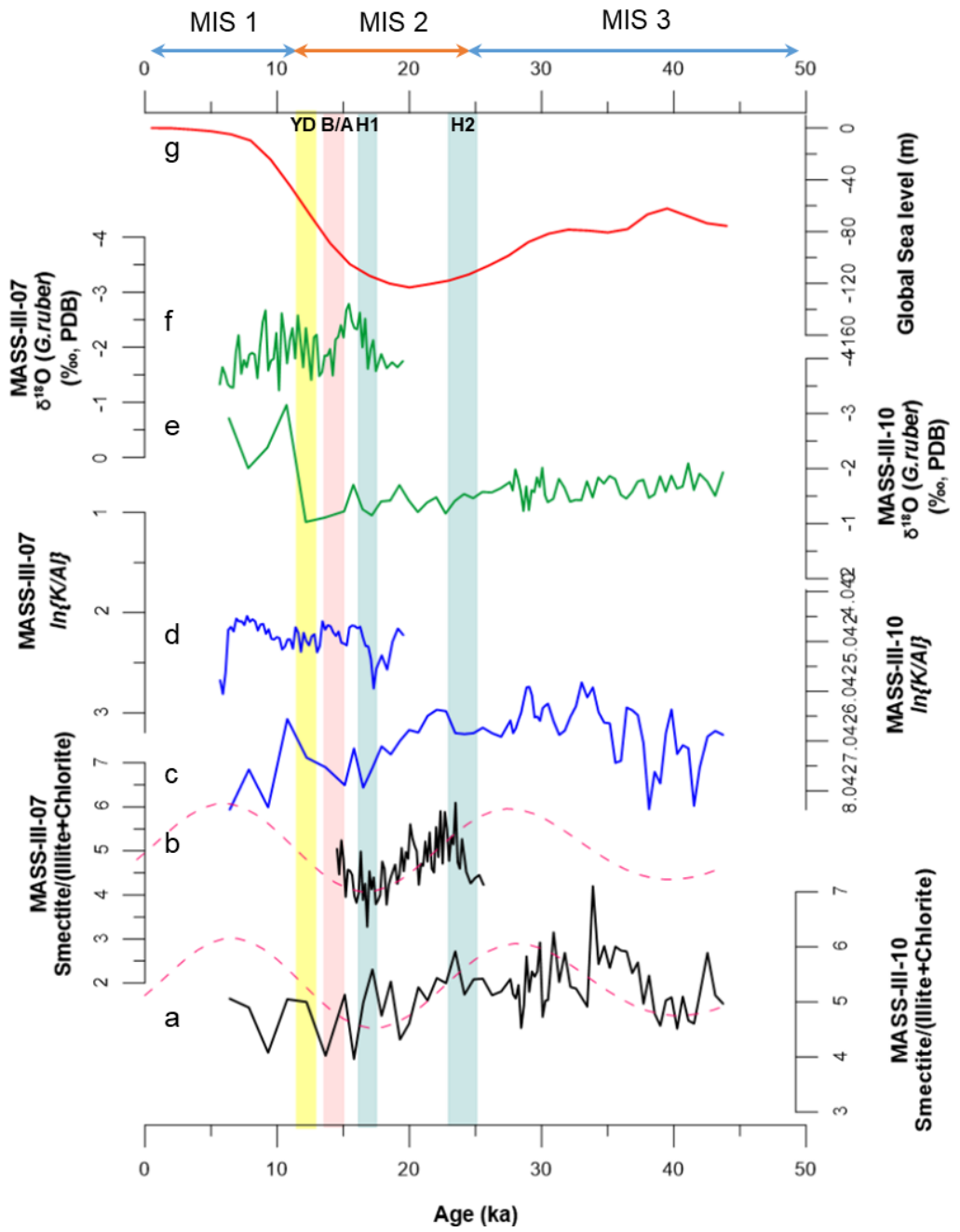

Figure 30 Smectite/(illite+chlorite) ratio a) MASS-III-10 b) MASS-III-07, Major element ratio of K_2O/SiO_2 c) MASS-III-10 d) MASS-III-07, $\delta^{18}O$ (G. Ruber) curve e) MASS-III-10 f) MASS-III-07, g) global sea level (Waebroeck et al, 2002). Dash curve presents insolation curve calculated for September at 10^0N by using Analyseries software (Paillard et al., 1996). Shaded bars show the ages of Heinrich events H1, H2 (Hemming et al., 2004), Younger Dryas (YD; 13-11.5

ka) (Alley, 2000), Bølling/Allerød (B/A; 15–13.5 ka), respectively (Sijinkumar et al., 2010).

6.2.2 Sedimentation control factors

As the location of the cores are adjacent to major rivers in the northern Andaman, it is necessary to evaluate the influences of global sea level changes during glacial-interglacial transitions (Zhao et al, 2011). During sea-level lowstands, large quantities of fluvial sediments can be deposited on the exposed continental and remobilized sediments were then redeposited in the deep sea. Fig. 31 illustrated the paloeshoreline during highstands (present) and lowstands (glaciation) from Awasthi et al. (2014). The sea level dropped within 120 m during the LGM (Awasthi et al., 2014). The sea level changing event at ~23 ka largely affected oceanographic system in the Andaman Sea which contributed the evolution of sedimentary environment (Colin et al., 1998; 2006)

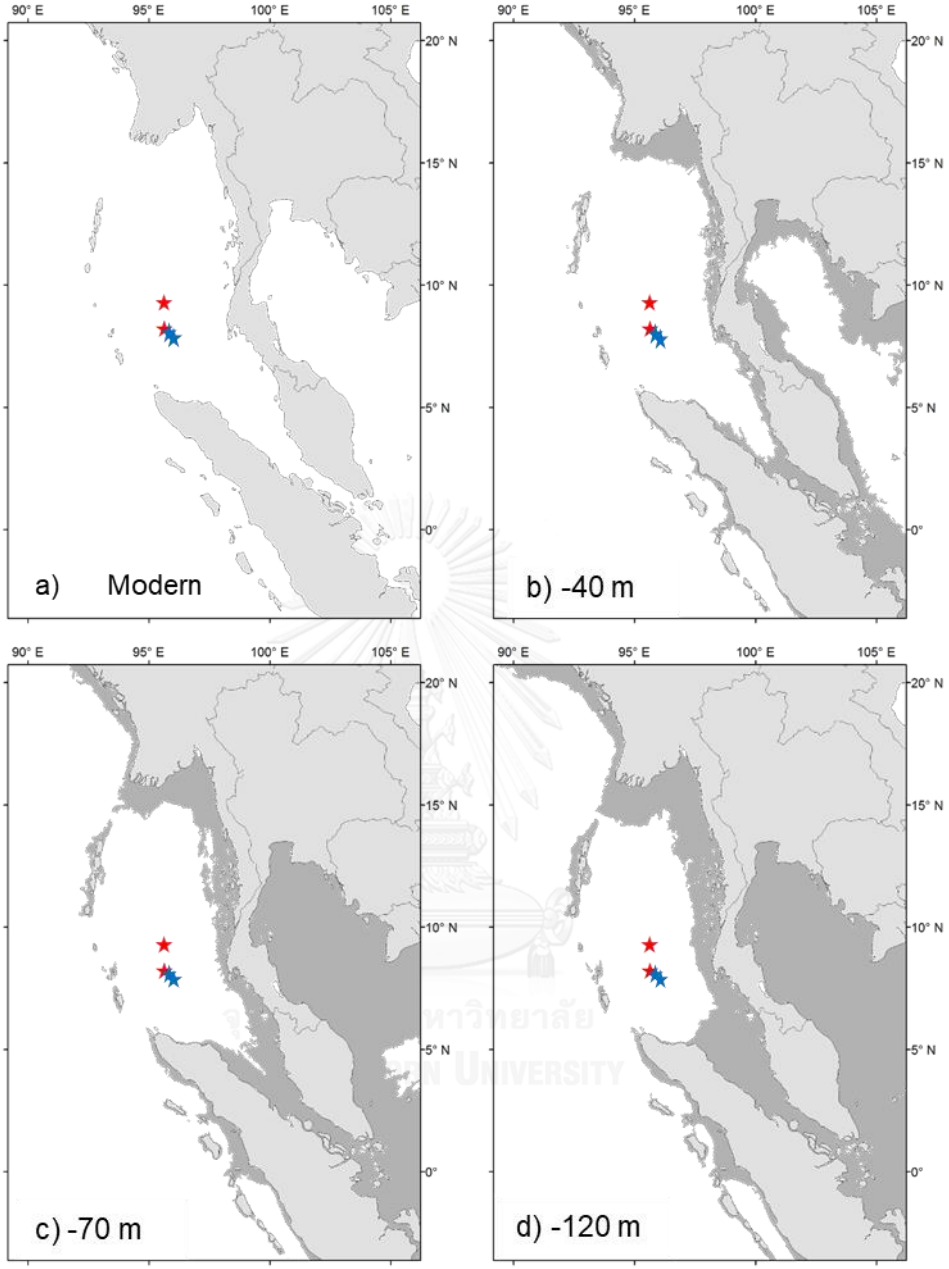

Figure 31 Illustration of the paleoshoreline during; a) highstands at modern shoreline and lowstands at sea level dropped b) -40 m c) -70 m and d) -120 m during the LGM period (Awasthi et al., 2014)

CHAPTER 7

Conclusions and Prospective

7.1 Conclusion

The marine sedimentary from four sediment cores recovered from the southern Andaman Sea and two surface sediment samples groups form Myanmar shelf and Thailand shelf have been investigated. The four cores were divided into deep water cores; ADM2 (2,268 m), ADM6 (1,890 m) and shallow water cores; MASS-III-07 (600 m), and (MASS-III-10 (630 m). They have been studied to identify provenance sources, to determine deposition pattern, and to infer the paleoenvironmental evolution of Andaman Sea sediments. To achieve the study aims, the sediments were examined by clay mineralogy, XRF elemental geochemistry, and grain size compositions. In order to establish the precise age model for these cores, ^{14}C Accelerator Mass Spectrometry (AMS) dating and oxygen isotope stratigraphy obtained by planktonic foraminifera (*G. ruber*) were combined. The conclusions are presented as follows;

Clay mineral in Surface sediment of the Andaman Sea

The clay mineral assemblage of Myanmar shelf is mainly composed of smectite (average 44%), kaolinite (average 17%) and chlorite (average 16%), and illite (average 13%). Meanwhile, the clay minerals of Thailand shelf consist of kaolinite (average 47%), smectite (average 23%), illite (average 11%). In comparison to other potential provenance area, the clay mineral assemblages of the surface sediments show two significant features: (1) high smectite contents (47%) in Myanmar shelf and in the all three provinces of the Andaman Island with extremely high values (>80%) in surface samples of

core MD77-186; (2) kaolinite contents (generally >60%) in Sumatra with extremely high values (~80%) in Malay Peninsula, and >40% in Thailand shelf.

In order to understand controlling factors of clay minerals in Myanmar shelf and Thailand shelf, ternary diagram was used for the provenance analysis. This indicated that the clay minerals of Myanmar shelf are controlled by lithology. Due to the fact that north of the Andaman Sea, in part of Myanmar on Irrawaddy river delta, consists mainly of Quaternary deposits with Neogene and Palaogene sedimentary rocks and the Myanmar shelf (included Salween river area) consists mainly the Paleozoic and Tertiary sedimentary rocks. These rocks can produce more smectite to the Andaman Sea. On the other hand, the clay minerals of Thailand are mainly controlled by climate. The humid and warm climatic conditions of southern Thailand can produce kaolinite, which can be considered as a proxy for intense chemical weathering.

Smectite was found to predominate in the core top surface of the studied cores. Smectite contents of surface sediment and core top sediments are higher than riverine sediments that are in source area. These results imply differential settling of smectite in surface sediments. Higher salinity can encourage the flocculation and deposition of smectite, leading to higher smectite content on deep sea. Although smectite contents on the surface sediments and core top sediments are controlled by differential settling, the spatial distribution of smectite in the southern Andaman Sea has a close relation to the local current systems that mainly controlled by the monsoonal winds. The sediment transport into the Andaman Sea is influenced surface current which is controlled by the seasonal reversal of two monsoonal winds. The smectite from the northern provenance can disperse clockwise into the Andaman Sea. The obtained smectite in these cores might result from particle fractionation as smectite dominates the smallest clay mineral size fraction that is consequently transported further away

from the coastal source areas to the core site. The modern transportation process are under surface circulation effect due to the similar pattern of surface circulation by SW and NE monsoon supplying the sediment into the Andaman Sea and differential setting of dominated smectite.

Clay mineral variation since the Last Glaciation

Clay mineral variation in the sediment cores taken from the southern Andaman Sea revealed no significant change in downcore variation. This indicates that the relative contributions of the sources did not vary through time since the last glaciation. The clay mineral variations over the last glaciation of two cores; ADM2 and MASS-III-10 are related to the sea level and monsoon control factors, core ADM6 is under the monsoon influence, while core MASS-III-07 shows unclear controlling factor.

The deep sea cores; core ADM2 is characterized by lower sedimentation rates in comparison to core ADM6. The high sedimentation rate of core ADM6 may be resulted from high hydrodynamic condition in this area. In addition, the mixing layer can be indicated in the lower part of the core ADM6. The shallow water cores taken from continental slope; MASS-III-07 shows high sedimentation rate (12.3 cm/ka) than MASS-III-10 (2.2 - 9.9 cm/ka). Although these two shallow water cores are located in the same area, their sedimentation rates were different. The high sedimentation rate of core MASS-III-07 suggested that the core location may be existed in the disturbance zone, of which may be influenced by the NE monsoon driven on Sumatra current into the Andaman Sea. The current may wash off some of the surface sediment that corresponded well with losing of the core top.

Environment Reconstruction of the Andaman Sea

The clay mineral variation since the last glaciation and the element ratios implied the paleoclimate in the Andaman Sea. In conclusion, the deep sea cores; ADM 2 and ADM 6 displayed two signals to imply the paleoenvironmental control factors. ADM 2 revealed the first controlling factor is sea level changing and also associated with the monsoon variation while ADM 6 covering 15 ka revealed the controlling factor is monsoon variation especially in Holocene. The shallow water cores showed additional controlling factors such as river discharge and sea floor morphology changing.

7.2 Perspectives

In summary, this study based on the clay mineralogy, major element composition of detrital sediments allows us to understand the modern and glaciation sediment recording in the Andaman Sea, the modern transport processes, and paleoclimate controlling factors. It is because of the limitation of material and methods, suggestion for further research are listed;

Firstly, the provenance analysis of this study is based on only the clay minerology. This study used the assumption that all clay compositions are produced as the primary mineral thus the interpretation based on the dominant mineral are not precise in the provenance identification. More precise provenance proxies, such as Sr & Nd isotopic method, could provide high significant to answer the provenance of the Andaman Sea.

Secondly, the sediment transport processes in the Andaman Sea was assumed to be affected by only the surface circulation. This is due to the lack of information on ocean circulation in this area. The conclusion of modern transport of surface sediment is based on one research on the circulation pattern resulted from the monsoon winds, lacking of any field observation. Moreover, the ocean circulation in the glaciation period is not well documented thus it was

assumed that the last glaciation and the present have the same pattern of the ocean circulation.

Thirdly, the interpretations about paleoenvironmental evolution are based on the assumption that mineralogical and elemental compositions of sediment cores covering the last 45 ka are not significantly altered by past environmental changes.

APPENDIX

Appendix A

The materials of this study were divided for two groups;

- Core sediment: 2 gravity cores of a maximum 4 m. recovery [(1)] in the deep water area and 2 gravity cores of a maximum 2 m. recovery [(2)] from shallow water from the Andaman Sea shelf-break area off Thai water boundary.
- Surface sediment: nearshore surface sediments are collected from two sites from Myanmar shelf (MM) [(3)] and Thailand shelf (TH) [(4)] by grab sampler.

Remarks; all sediment collections are supported by the research project as following lists below;

(1) THE VULNERABILITY OF THE COASTAL ZONES, under Thai (PMBC) – Chinese (FIO-SOA) collaborative project leaded by Dr. Somkiat Khokiattiwong (PMBC) and Prof. Dr. Xuefa Shi (FIO-SOA)

(2) MORPHODYNAMICS AND SLOPE STABILITY OF THE ANDAMAN SEA SHELF BREAK, under Thai-German cooperative project leaded by Dr. Anond Snidwongs (SEA START RC) And Prof. Dr. Sebastian Krastel (IFM-GEOMAR)

(3) ENVIRONMENTAL IMPACT ASSESSMENT (EIA) FOR THE MYANMAR BLOCK
M9 PRODUCTION DEVELOPMENT AND OFFSHORE GAS TRANSMISSION PIPELINE, collaborated project by Dr. Penjai Sompongchaiyakul, (CU)

(4) CHANGING OF SEDIMENT STRATIGRAPHY AND HISTORICAL TSUNAMI
TRACING BY NEARSHORE SEDIMENT OF THE ANDAMAN SEA, under Thai-German cooperative project leaded by Dr. Penjai Sompongchaiyakul (CU) and Dr. Klaus Schwarzer (University of Kiel)

A-1 Locations of Surface Sediment form nearshore of the Myanmar shelf.

Station no.	Referred Station Name	Latitude (N)	Longitude(E)
1	KP10	14˚ 11.45'	96˚ 08.37'
2	KP20	14˚ 11.68'	96˚ 13.93'
3	KP30	14˚ 11.90'	96˚ 19.49'
4	KP40	14˚ 12.12'	96˚ 25.05'
5	KP50	14˚ 12.34'	96˚ 30.61'
6	KP60	14˚ 12.55'	96˚ 36.17'
7	KP70	14˚ 12.77'	96˚ 41.73'
8	KP80	14˚ 12.97'	96˚ 47.29'
9	KP90	14˚ 13.18'	96˚ 52.85'
10	KP100	14˚ 13.39'	96˚ 58.40'
11	KP110	14˚ 13.59'	97˚ 03.96'
12	KP120	14˚ 13.80'	97˚ 09.52'
13	KP130	14˚ 13.99'	97˚ 15.09'
14	KP140	14˚ 14.19'	97˚ 20.64'
15	KP150	14˚ 14.39'	97˚ 26.20'
16	KP160	14˚ 14.58'	97˚ 31.76'
17	KP170	14˚ 14.77'	97˚ 37.31'
18	KP180	14˚ 14.96'	97˚ 42.88'
19	KP190	14˚ 15.15'	97˚ 48.44'
20	ZIP-1	14˚ 20.04'	96˚ 01.69'
21	ZIP-2	14˚ 14.28'	96˚ 02.77'
22	ZIP-3	14˚ 16.71'	95˚ 55.77'
23	ZIP-4	14˚ 14.16'	95˚ 59.02'
24	ZIP-5	14˚ 11.94'	95˚ 53.00'
25	ZIP-6	14˚ 11.88'	95˚ 56.75'
26	ZIP-7	14˚ 08.86'	95˚ 54.22'
27	ZIP-8	14˚ 10.27'	95˚ 59.41'
28	ZIP-9	14˚ 04.38'	95˚ 54.20'
29	ZIP-10	14˚ 07.81'	95˚ 58.49'
30	ZPP	14˚ 11.57'	96˚ 02.82'
31	ZWP-1	14˚ 11.14'	96˚ 02.82'
32	ZWP-2	14˚ 11.70'	96˚ 02.30'
33	ZWP-3	14˚ 09.53'	95˚ 56.80'
34	ZWP-4	14˚ 01.47'	95˚ 49.11'
35	SPH-1	14˚ 10.51'	96˚ 03.80'
36	KKN-1	14˚ 23.95'	96˚ 01.43'
37	Zawtika-1	14˚ 08.26'	95˚ 51.42'
38	Zawtika-8	14˚ 11.74'	95˚ 48.53'
39	Reference	14˚ 04.17'	96˚ 11.25'

A-2. Locations of Surface Sediment form nearshore of the Thailand shelf.

Station no.	Referred Station Name	Latitude (N)	Longitude(E)
1	AS01	08° 37.77'	98° 13.33'
2	AS02	08° 38.35'	98° 13.67'
3	AS03	08° 38.86'	98° 14.03'
4	AS04	08° 40.74'	98° 12.18'
5	AS05	08° 42.19'	98° 13.02'
6	AS06	08° 42.17'	98° 9.15'
7	AS07	08° 41.42'	98° 7.048'
8	AS08	08° 46.69'	98° 6.99'
9	AS09	08° 46.55'	98° 8.00'
10	AS10	08° 46.67'	98° 8.65'
11	AS11	08° 47.09'	98° 9.55'
12	AS12	08° 47.44'	98° 9.92'
13	AS13	08° 47.39'	98° 10.16'
14	AS14	08° 47.57'	98° 10.88'
15	AS15	08° 47.81'	98° 11.35'
16	AS16	08° 47.97'	98° 11.55'
17	AS17	08° 47.46'	98° 12.07'
18	AS18	08°38.85'	98° 12.98'
19	AS19	08° 39.60'	98° 12.21'
20	AS20	08° 40.85'	98° 12.56'
21	AS21	08° 45.67'	98° 13.47'
22	AS22	08° 45.63'	98° 12.37'

Appendix B

同濟大學
TONGJI UNIVERSITY

A dissertation submitted to
Tongji University and Chulalongkorn University
in conformity with the requirements for
the degree of Doctor of Science

PROVENANCE OF DETRITAL SEDIMENTS IN THE SOUTHERN ANDAMAN SEA SINCE THE LAST GLACIATION

Candidate: BUNSOMBOONSAKUL Suratta

Affiliations: School of Ocean and Earth Science, Tongji University
Department of Marine Science, Faculty of Science,
Chulalongkorn University

Discipline: Science

Major: Marine Geology

Supervisors: Prof. LIU Zhifei
Assistant Prof. SOMPONGCHAIYAKUL Penjai

July, 2017

同济大学 TONGJI UNIVERSITY

博士学位论文

安达曼海末次冰期以来陆源物质的源区研究

姓 名：潘淑兰 (BUNSOMBOONSAKUL Suratta)

所在院系：同济大学海洋与地球科学学院 Department of Marine Science, Faculty of Science, Chulalongkorn University

学科门类：理学

专 业：海洋科学

指导教师：刘志飞 教授 SOMPONGCHAIYAKUL Penjai 教授

2017 年7月

学位论文版权使用授权书

本人完全了解同济大学关于收集、保存、使用学位论文的规定，同意如下各项内容：按照学校要求提交学位论文的印刷本和电子版本；学校有权保存学位论文的印刷本和电子版，并采用影印、缩印、扫描、数字化或其它手段保存论文；学校有权提供目录检索以及提供本学位论文全文或者部分的阅览服务；学校有权按有关规定向国家有关部门或者机构送交论文的复印件和电子版；在不以赢利为目的的前提下，学校可以适当复制论文的部分或全部内容用于学术活动。

学位论文作者签名：

年　月　日

同济大学学位论文原创性声明

本人郑重声明：所呈交的学位论文，是本人在导师指导下，进行研究工作所取得的成果。除文中已经注明引用的内容外，本学位论文的研究成果不包含任何他人创作的、已公开发表或者没有公开发表的作品的内容。对本论文所涉及的研究工作做出贡献的其他个人和集体，均已在文中以明确方式标明。本学位论文原创性声明的法律责任由本人承担。

学位论文作者签名：

年　月　日

摘 要

安达曼海是一个半封闭的边缘海，是开展沉积物从“源”到“汇”搬运过程研究的良好场所。本项研究包括 4 个主要科学目标，包括：1）揭示安达曼海表层沉积物中的粘土矿物组合，理解可能的现代搬运过程；2）研究末次冰期以来粘土矿物的变化；3）基于多指标的研究来重建印度季风的演化过程；4）探讨末次冰期以来气候变化导致海洋环境变化的可能机制。

本项研究的使用样品材料包括南达曼 61 个表层沉积物样品和 4 个沉积岩芯（ADM 2、ADM、MASS-III-07、以及 MASS-III-10）。其中，通过分析表层样品的粘土矿物组合来描述现代海洋的搬运过程；通过对岩芯进行粘土矿物与元素地球化学分析，来重建末次冰期以来安德曼海的古环境演化。同时，本项研究还通过测试 AMS-^{14}C 年龄和浮游有孔虫氧同位素（$\delta^{18}O$）分析所获的数据，可以用于建立年龄框架。

表层样品的粘土矿物结果显示了 4 个潜在的物源区，包括：缅甸陆架、马来半岛、苏门答腊岛和泰国。缅甸陆架是最主要的物源区，以来自伊洛瓦底和萨尔文河流系统的蒙脱石（约 44%）为主；而马来半岛和苏门答腊以高岭石（分别为 80%和 68%）为主；泰国陆架也以高岭石（47%）为主。根据粘土矿物组合的分析结果，马来半岛、苏门答腊和泰国陆架这三个物源区主要是受到气候条件的控制，而缅甸（主要源区）受到岩性背景的控制。西南季风和东北季风驱动的夏季和冬季分布样式相同的表层环流，影响进入安达曼海沉积物的现代搬运过程。同时，由于强烈的差异沉降作用，导致以粘土矿物组合的蒙脱石为主。

安达曼海南部沉积岩芯中粘土矿物的差异没有发生明显的变化，表明末次冰期以来物源的相对贡献量并没有随时间而变化。记录末次冰期以来两个岩芯 ADM2 和 MASS-III-10 中粘土矿物变化与海平面变化、季风控制因素有关；同时，岩芯 ADM6 受到季风的影响，但岩芯 MASS-III-07 的控制因素尚不明确。

深海岩芯 ADM2 与 ADM6 相比而言，沉积速率较低。岩芯 ADM6 的高沉积速率可能是因为该区域的强动力条件，而且该岩芯的底部发育浊流混合层。浅水岩芯 MASS-III-07 与 MASS-III-10 采于陆坡地区，虽然两者位于同一区域，但其沉降遂率却有所不同，表现为岩芯 MASS-III-07 的沉降速率（12.3 cm/ka）比岩芯 MASS-III-10 更高（2.2-9.9 cm/ka）。岩芯 MASS-III-07 的沉降速率较高，表明该岩芯所处位置可存在过扰动，该区域主要受东北季风驱动的苏门答腊岛物质进入安达曼海的影响。这股洋流可能冲刷掉一些表层沉积物，导致岩芯顶部缺乏保存良好的沉积记录。

关键词：安达曼海，粘土矿物，源区，主量元素地球化学

REFERENCES

Ahmad, S. M., Anil Babu, G., Padmakumari, V. M., Dayal, A. M., Sukhija, B. S., Nagabhushanam, P. (2005). Sr, Nd isotopic evidence of terrigenous flux variations in the Bay of Bengal: Implications of monsoons during the last ~34,000 years. *Geophysical Research Letters, 32*(22), 1-4. doi:10.1029/2005GL024519

Alagarsamy, R., You, C. F., Nath, B. N., Kumar, A. V. S. (2010). Determination of rare earth, major and trace elements in authigenic fraction of Andaman Sea (Northeastern Indian Ocean) sediments by Inductively Coupled Plasma-Mass Spectrometry. *Microchemical Journal, 94*(1), 90-97. doi:http://dx.doi.org/10.1016/j.microc.2009.09.007

Ali, S., Hathorne, E. C., Frank, M., Gebregiorgis, D., Stattegger, K., Stumpf, R., Kutterolf, S., Johnson, J. E., Giosan, L. (2015). South Asian monsoon history over the past 60 kyr recorded by radiogenic isotopes and clay mineral assemblages in the Andaman Sea. *Geochemistry, Geophysics, Geosystems, 16*(2), 505-521. doi:10.1002/2014GC005586

Allen, P. A. (2008). From landscapes into geological history. *Nature, 451*(7176), 274-276.

Allen, P. A., Allen, J. R. (2013). *Basin analysis : principles and application to petroleum play assessment* (3rd ed ed.): Wiley-Blackwell.

Awasthi, N., Ray, J. S., Singh, A. K., Band, S. T., Rai, V. K. (2014). Provenance of the Late Quaternary sediments in the Andaman Sea: Implications for monsoon variability and ocean circulation. *Geochemistry, Geophysics, Geosystems, 15*(10), 3890-3906. doi:10.1002/2014GC005462

Bender, F. (1983). *Geology of Burma*.

Biscaye, P. E. (1965). Mineralogy and sedimentation of recent deep-sea clay in the Atlantic ocean and adjacent seas and oceans. *Bulletin of the Geological Society of America, 76*(7), 803-832. doi:10.1130/0016-7606(1965)76[803:MASORD]2.0.CO;2

Boulay, S., Colin, C., Trentesaux, A., Frank, N., Liu, Z. (2005). Sediment sources and East Asian monsoon intensity over the last 450 ky. Mineralogical and geochemical investigations on South China Sea sediments. *Palaeogeography, Palaeoclimatology, Palaeoecology, 228*(3–4), 260-277. doi:http://dx.doi.org/10.1016/j.palaeo.2005.06.005

Bouquillon, A., Chamley, H., Frohlich, F. (1989). Late Cenozoic clay sedimentation in the northeastern Indian Ocean. *Oceanologica Acta, 12*(3), 133-147.

Bouquillon, A., France-Lanord, C., Michard, A., Tiercelin, J. J. (1990). Sedimentology and isotopic chemistry of the Bengal Fan sediments: the denudation of the Himalaya. *Proc., scientific results, ODP, Leg 116, distal Bengal Fan*, 43-58.

Brown, B. E. (2007) Coral reefs of the Andaman Sea - An integrated perspective. *Vol. 45. Oceanography and Marine Biology* (pp. 173-194).

Cao, P. (2015). The Characteristics of the Sediment in the Southeastern Andaman Sea and Its Response to the India Monsoon Since the Last Glacial Maximum.

Cao, P., Shi, X., Li, W., Liu, S., Yao, Z., Hu, L., Khokiattiwong, S., Kornkanitnan, N. (2015). Sedimentary responses to the Indian Summer Monsoon variations recorded in the southeastern Andaman Sea slope since 26 ka. *Journal of Asian Earth Sciences, 114, Part 3*, 512-525. doi:http://dx.doi.org/10.1016/j.jseaes.2015.06.028

Chakraborty, P. P., Khan, P. K. (2009). Cenozoic geodynamic evolution of the Andaman-Sumatra subduction margin: Current understanding. *Island Arc, 18*(1), 184-200. doi:10.1111/j.1440-1738.2008.00643.x

Chamley, H. (1989). Clay Sedimentology. *Springer*, 623.

Chauhan, O. S., Vogelsang, E. (2006). Climate induced changes in the circulation and dispersal patterns of the fluvial sources during late quaternary in the middle Bengal Fan. *Journal of Earth System Science, 115*(3), 379-386. doi:10.1007/BF02702050

Cheng, H., Fleitmann, D., Edwards, R. L., Wang, X., Cruz, F. W., Auler, A. S., Mangini, A., Wang, Y., Kong, X., Burns, S.J., Matter, A. (2009). Timing and structure of the 8.2. kyr B.P. event inferred from δ 18O records of stalagmites from China, Oman, and Brazil. *Geology, 37*(11), 1007-1010. doi:10.1130/G30126A.1

Colin, C. (1997). Reconstruction du régime de l'érosion des chaînes himalayenne et birmane au cours des deux derniers cycles climatiques (300 derniers ka). Mer d'Adaman et Golfe de Bengale. *Thèse Doctoral*.

Colin, C., Kissel, C., Blamart, D., Turpin, L. (1998). Magnetic properties of sediments in the Bay of Bengal and the Andaman Sea: Impact of rapid North Atlantic Ocean climatic events on the strength of the Indian monsoon. *Earth and Planetary Science Letters, 160*(3-4), 623-635. doi:10.1016/S0012-821X(98)00116-2

Colin, C., Siani, G., Sicre, M. A., Liu, Z. (2010). Impact of the East Asian monsoon rainfall changes on the erosion of the Mekong River basin over the past 25,000 yr. *Marine Geology, 271*(1-2), 84-92. doi:10.1016/j.margeo.2010.01.013

Colin, C., Turpin, L., Bertaux, J., Desprairies, A., Kissel, C. (1999). Erosional history of the Himalayan and Burman ranges during the last two glacial-interglacial cycles. *Earth and Planetary Science Letters, 171*(4), 647-660. doi:10.1016/S0012-821X(99)00184-3

Colin, C., Turpin, L., Blamart, D., Frank, N., Kissel, C., Duchamp, S. (2006). Evolution of weathering patterns in the Indo-Burman Ranges over the last 280 kyr: Effects of sediment provenance on 87 Sr/86 Sr ratios tracer. *Geochemistry, Geophysics, Geosystems, 7*(3). doi:10.1029/2005GC000962

Curray, J. R. (2005). Tectonics and history of the Andaman Sea region. *Journal of Asian Earth Sciences, 25*(1), 187-232. doi:10.1016/j.jseaes.2004.09.001

Doust, H., Noble, R. A. (2008). Petroleum systems of Indonesia. *Marine and Petroleum Geology, 25*(2), 103-129. doi:10.1016/j.marpetgeo.2007.05.007

Doust, H., Sumner, H. S. (2007). Petroleum systems in rift basins - A collective approach in Southeast Asian basins. *Petroleum Geoscience, 13*(2), 127-144. doi:10.1144/1354-079307-746

Dutta, K., Bhushan, R., Somayajulu, B. L. K. (2007). Rapid vertical mixing rates in deep waters of the Andaman Basin. *Science of the Total Environment, 384*(1-3), 401-408. doi:10.1016/j.scitotenv.2007.04.041

Esquevin, J. (1969). Influence de la composition chimique des illites surcristallinite. *Bull. Cent. Rech. Rau-SNPA, 3*(1), 147-153.

Fagel, N., Debrabant, P., André, L. (1994). Clay supplies in the Central Indian Basin since the Late Miocene: climatic or tectonic control? *Marine Geology, 122*(1-2), 151-172. doi:10.1016/0025-3227(94)90209-7

Fontugne, M. R., Duplessy, J. C. (1986). Variations of the monsoon regime during the upper quaternary: Evidence from carbon isotopic record of organic matter in North Indian Ocean sediment cores. *Palaeogeography, Palaeoclimatology, Palaeoecology, 56*(1-2), 69-88. doi:10.1016/0031-0182(86)90108-2

France-Lanord, C., Derry, L., Michard, A. (1993). Evolution of the Himalaya since Miocene time: isotopic and sedimentological evidence from the Bengal Fan. *Himalayan tectonics,* 603-621.

Galy, A., France-Lanord, C. (2001). Higher erosion rates in the Himalaya: Geochemical constraints on riverine fluxes. *Geology, 29*(1), 23-26.

Garzanti, E., Limonta, M., Resentini, A., Bandopadhyay, P. C., Najman, Y., Andò, S., Vezzoli, G. (2013). Sediment recycling at convergent plate margins (indo-burman ranges and andaman-nicobar ridge). *Earth-Science Reviews, 123*, 113-132. doi:10.1016/j.earscirev.2013.04.008

Gebregiorgis, D. (2017). The Late Quaternary History of the South Asian Monsoon. *Dissertation Kiel, Christian-Albrechts-Universität 2016*, 182

Gebregiorgis, D., Hathorne, E. C., Sijinkumar, A. V., Nagender Nath, B., Nürnberg, D., Frank, M. (2016). South Asian summer monsoon variability during the last ~54 kyrs inferred from surface water salinity and river run off proxies. *Quaternary Science Reviews, 138*, 6-15. doi:10.1016/j.quascirev.2016.02.012

Gingele, F. X., De Deckker, P., Hillenbrand, C.-D. (2001). Clay mineral distribution in surface sediments between Indonesia and NW Australia — source and transport by ocean currents. *Marine Geology, 179*(3–4), 135-146. doi:http://dx.doi.org/10.1016/S0025-3227(01)00194-3

Hall, R. (1998). The plate tectonics of Cenozoic SE Asia and the distribution of land and sea. *Biogeography and Geological Evolution of SE Asia*, 99-131.

Hall, R. (2002). Cenozoic geological and plate tectonic evolution of SE Asia and the SW Pacific: Computer-based reconstructions, model and animations. *Journal of Asian Earth Sciences, 20*(4), 353-431. doi:10.1016/S1367-9120(01)00069-4

Hemming, S. R. (2004). Heinrich events: Massive late Pleistocene detritus layers of the North Atlantic and their global climate imprint. *Reviews of Geophysics, 42*(1), RG1005 1001-1043. doi:10.1029/2003RG000128

Herzschuh, U. (2006). Palaeo-moisture evolution in monsoonal Central Asia during the last 50,000 years. *Quaternary Science Reviews, 25*(1-2), 163-178. doi:10.1016/j.quascirev.2005.02.006

Holtzapffel, T. (1985). *Les Minéraux Argileux : Préparation, Analyse Diffractométrique et Détermination, 12*, 136.

Jha, P., Ros, D., Degli Alessandrini, A., Kishore, M. (2010). Speculative petroleum system and play model of East Andaman Basin from regional geology and basin evolution concepts: Addressing the exploration challenges of an extreme frontier area. *8th Biennial International Conference and Exposition on Petroleum Geophysics, Hyderabad, India, P-261*.

Jintasaeranee, P., Weinrebe, W., Klaucke, I., Snidvongs, A., Flueh, E. R. (2012). Morphology of the Andaman outer shelf and upper slope of the Thai exclusive economic zone. *Journal of Asian Earth Sciences, 46*, 78-85. doi:http://dx.doi.org/10.1016/j.jseaes.2011.11.003

Joussain, R. (2016). Erosional history of the Himalayas during the last climatic cycle: sedimentological, mineralogical, and geochemical investigations of sediments from the proximal part of the Bengal deep-sea Fan. *Dissertation, Tongji University and University Paris-Saclay*, 303.

Joussain, R., Colin, C., Liu, Z., Meynadier, L., Fournier, L., Fauquembergue, K., Zaragosi, S., Schmidt, F., Rojas, V., Bassinot, F. (2016). Climatic control of sediment transport from the Himalayas to the proximal NE Bengal Fan during the last glacial-interglacial cycle. *Quaternary Science Reviews, 148*, 1-16. doi:http://dx.doi.org/10.1016/j.quascirev.2016.06.016

Keller, G. H., Richards, A. F. (1967). Sediments of the Malacca Strait, Southeast Asia. *Journal of Sedimentary Petrology, 37*(1), 102-127.

Khan, P. K., Chakraborty, P. P. (2005). Two-phase opening of Andaman Sea: a new seismotectonic insight. *Earth and Planetary Science Letters, 229*(3–4), 259-271. doi:http://dx.doi.org/10.1016/j.epsl.2004.11.010

Kobashi, T., Severinghaus, J. P., Brook, E. J., Barnola, J. M., Grachev, A. M. (2007). Precise timing and characterization of abrupt climate change 8200 years ago from air trapped in polar ice. *Quaternary Science Reviews, 26*(9-10), 1212-1222. doi:10.1016/j.quascirev.2007.01.009

Kurian, S., Nath, B. N., Ramaswamy, V., Naman, D., Gnaneshwar Rao, T., Kamesh Raju, K. A., Chen, C. T. A. (2008). Possible detrital, diagenetic

and hydrothermal sources for Holocene sediments of the Andaman backarc basin. *Marine Geology, 247*(3-4), 178-193. doi:10.1016/j.margeo.2007.09.006

Licht, A., France-Lanord, C., Reisberg, L., Fontaine, C., Soe, A. N., Jaeger, J. J. (2013). A palaeo Tibet-Myanmar connection? Reconstructing the Late Eocene drainage system of central Myanmar using a multi-proxy approach. *J. Geol. Soc. Lond.*

Liu, Z., Colin, C., Huang, W., Phon Le, K., Tong, S., Chen, Z., Trentesaux, A. (2007). Climatic and tectonic controls on weathering in south China and Indochina Peninsula: Clay mineralogical and geochemical investigations from the Pearl, Red, and Mekong drainage basins. *Geochemistry, Geophysics, Geosystems*, *8*(5). doi:10.1029/2006GC001490

Liu, Z., Colin, C., Trentesaux, A., Blamart, D., Bassinot, F., Siani, G., Sicre, M.-A. (2004). Erosional history of the eastern Tibetan Plateau since 190 kyr ago: clay mineralogical and geochemical investigations from the southwestern South China Sea. *Marine Geology, 209*(1–4), 1-18. doi:http://dx.doi.org/10.1016/j.margeo.2004.06.004

Liu, Z., Colin, C., Trentesaux, A., Siani, G., Frank, N., Blamart, D., Farid, S. (2005). Late Quaternary climatic control on erosion and weathering in the eastern Tibetan Plateau and the Mekong Basin. *Quaternary Research, 63*(3), 316-328. doi:10.1016/j.yqres.2005.02.005

Liu, Z., Tuo, S., Colin, C., Liu, J. T., Huang, C.-Y., Selvaraj, K., Chen, Z. (2008). Detrital fine-grained sediment contribution from Taiwan to the northern South China Sea and its relation to regional ocean circulation. *Marine Geology*, *255*(3–4), 149-155. doi:http://dx.doi.org/10.1016/j.margeo.2008.08.003

Liu, Z., Wang, H., Hantoro, W. S., Sathiamurthy, E., Colin, C., Zhao, Y., Li, J. (2012). Climatic and tectonic controls on chemical weathering in tropical Southeast Asia (Malay Peninsula, Borneo, and Sumatra). *Chemical Geology*, *291*, 1-12. doi:http://dx.doi.org/10.1016/j.chemgeo.2011.11.015

Liu, Z., Zhao, Y., Colin, C., Siringan, F. P., Wu, Q. (2009). Chemical weathering in Luzon, Philippines from clay mineralogy and major-element geochemistry of river sediments. *Applied Geochemistry, 24*(11), 2195-2205. doi:http://dx.doi.org/10.1016/j.apgeochem.2009.09.025

Liu, Z., Zhao, Y., Colin, C., Stattegger, K., Wiesner, M. G., Huh, C.-A., Zhang, Y., Li, X., Sompongchaiyakul, P., You, Ch-F., Huang, Ch-Y., Liu, J. T., Siringan, F. P., Le, K. P., Sathiamurthy, E., Hantoro, W. S., Liu, J., Tuo, Sh., Zhao, Sh., Zhou, Sh., He, Z., Wang, Y., Bunsomboonsakul, S., Li, Y. (2016). Source-to-sink transport processes of fluvial sediments in the South China Sea. *Earth-Science Reviews, 153*, 238-273. doi:http://dx.doi.org/10.1016/j.earscirev.2015.08.005

Loschnigg, J., Webster, P. J. (2000). A Coupled Ocean–Atmosphere System of SST Modulation for the Indian Ocean. *Journal of Climate*, *13*(19), 3342-3360. doi:10.1175/1520-0442(2000)013<3342:acoaso>2.0.co;2

Lupker, M., France-Lanord, C., Galy, V., Lavé, J., Gaillardet, J., Gajurel, A. P., Guilmette, C., Rahman, M., Singh, S. K., Sinha, R. (2012). Predominant floodplain over mountain weathering of Himalayan sediments (Ganga basin). *Geochimica et Cosmochimica Acta, 84*, 410-432. doi:http://dx.doi.org/10.1016/j.gca.2012.02.001

Lupker, M., France-Lanord, C., Galy, V., Lavé, J., Kudrass, H. (2013). Increasing chemical weathering in the Himalayan system since the Last Glacial Maximum. *Earth and Planetary Science Letters, 365*, 243-252. doi:10.1016/j.epsl.2013.01.038

Martinson, D. G., Pisias, N. G., Hays, J. D., Imbrie, J., Moore Jr, T. C., Shackleton, N. J. (1987). Age dating and the orbital theory of the ice ages: Development of a high-resolution 0 to 300,000-year chronostratigraphy. *Quaternary Research, 27*(1), 1-29. doi:10.1016/0033-5894(87)90046-9

McLennan, S. M., Hemming, S., McDaniel, D. K., Hanson, G. N. (1993) Geochemical approaches to sedimentation, provenance, and tectonics. *Vol. 284. Special Paper of the Geological Society of America* (pp. 21-40).

Milliman, J. D., Farnsworth, K. L. (2011). *River discharge to the coastal ocean : A global synthesis*. Cambridge: Cambridge University.

Milliman, J. D., Farnsworth, K. L., Albertin, C. S. (1999). Flux and fate of fluvial sediments leaving large islands in the East Indies. *Journal of Sea Research, 41*(1-2), 97-107. doi:10.1016/S1385-1101(98)00040-9

Milliman, J. D., Meade, R. H. (1983). World-wide delivery of sediment to the oceans. *Journal of Geology*, *91*(1), 1-21.

Morrill, C., Overpeck, J. T., Cole, J. E. (2003). A synthesis of abrupt changes in the Asian summer monsoon since the last deglaciation. *Holocene, 13*(4), 465-476. doi:10.1191/0959683603hl639ft

Murgese, D. S., De Deckker, P. (2005). The distribution of deep-sea benthic foraminifera in core tops from the eastern Indian Ocean. *Marine Micropaleontology, 56*(1–2), 25-49. doi:http://dx.doi.org/10.1016/j.marmicro.2005.03.005

Paillard, D., Labeyrie, L., Yiou, P. (1996). Analyseries: macintosh program performs time-series analysis. Eos Tran. *AGU, 77*, 379.

Patchineelam, S. M., de Figueiredo, A. G. (2000). Preferential settling of smectite on the Amazon continental shelf. *Geo-Marine Letters, 20*(1), 37-42. doi:10.1007/s003670000035

Petschick, R. (2000). MacDiff 4.2.3. unpublished computer program, Johann-Wolfgang Goethe Universitat, Frankfurt a. M, Online Available: http://servermac.geologie.un-frankfurt.de/Rainer.html2000.

Petschick, R., Kuhn, G., Gingele, F. (1996). Clay mineral distribution in surface sediments of the South Atlantic: Sources, transport, and relation to oceanography. *Marine Geology, 130*(3-4), 203-229.

Polachan, S., Racey, A. (1993). Lower miocene larger foraminifera and petroleum potential of the Tai Formation, Mergui Group, Andaman Sea. *Journal of Southeast Asian Earth Sciences, 8*(1), 487-496. doi:http://dx.doi.org/10.1016/0743-9547(93)90047-S

Porrenga, D. H. (1967). Glauconite and chamosite as depth indicators in the marine environment. *Marine Geology, 5*(5), 495-501. doi:http://dx.doi.org/10.1016/0025-3227(67)90056-4

Potemra, J. T., Luther, M. E., O'Brien, J. J. (1991). The seasonal circulation of the upper ocean in the Bay of Bengal. *Journal of Geophysical Research: Oceans, 96*(C7), 12667-12683. doi:10.1029/91JC01045

Raju, K. A. K., Ramprasad, T., Rao, P. S., Rao, B. R., Varghese, J. (2004). New insights into the tectonic evolution of the Andaman basin, northeast Indian Ocean. *Earth Planet. Sci. Lett., 7024*, 1-18.

Ramaswamy, V., Gaye, B., Shirodkar, P. V., Rao, P. S., Chivas, A. R., Wheeler, D., Thwin, S. (2008). Distribution and sources of organic carbon, nitrogen and their isotopic signatures in sediments from the Ayeyarwady

(Irrawaddy) continental shelf, northern Andaman Sea. *Marine Chemistry, 111*(3–4), 137-150. doi:http://dx.doi.org/10.1016/j.marchem.2008.04.006

Ramaswamy, V., Rao, P. S., Rao, K. H., Thwin, S., Rao, N. S., Raiker, V. (2004). Tidal influence on suspended sediment distribution and dispersal in the northern Andaman Sea and Gulf of Martaban. *Marine Geology, 208*(1), 33-42. doi:10.1016/j.margeo.2004.04.019

Rao, P. S., Ramaswamy, V., Thwin, S. (2005). Sediment texture, distribution and transport on the Ayeyarwady continental shelf, Andaman Sea. *Marine Geology, 216*(4), 239-247. doi:10.1016/j.margeo.2005.02.016

Rashid, H., Flower, B. P., Poore, R. Z., Quinn, T. M. (2007). A ~25 ka Indian Ocean monsoon variability record from the Andaman Sea. *Quaternary Science Reviews, 26*(19-21), 2586-2597. doi:10.1016/j.quascirev.2007.07.002

Reimer, P. J., Baillie, M. G. L., Bard, E., Bayliss, A., Beck, J. W., Blackwell, P. G., Ramsey, C. B., Buck, C. E., Burr, G. S., Edwards, R. L., Friedrich, M., Grootes, P. M., Guilderson, T. P., Hajdas, I., Heaton, T. J., Hogg, A. G., Hughen, K. A., Kaiser, K. F., Kromer, B., McCormac, F. G., Manning, S. W., Reimer, R. W., Richards, D. A., Southon, J. R., Talamo, S., Turney, C. S. M., van der Plicht, J., Weyhenmeyer, C. E. (2009). IntCal09 and Marine09 radiocarbon age calibration curves, 0-50,000 years CAL BP. Radiocarbon, 51(4), 1111-1150.

Rizal, S., Damm, P., Wahid, M. A., Sündermann, J., Ilhamsyah, Y., Iskandar, T., Muhammad. (2012). General circulation in the Malacca Strait and Andaman Sea: A numerical model study. *American Journal of Environmental Sciences, 8*(5), 479-488. doi:10.3844/ajessp.2012.479.488

Robinson, R. A. J., Bird, M. I., Nay, W. O., Hoey, T. B., Maung, M. A., Higgitt, D. L., Lu, X. X., Aung, S., Tin, T., Swe, L. W. (2007). The irrawaddy river sediment flux to the Indian ocean: The original nineteenth-century data revisited. *Journal of Geology, 115*(6), 629-640. doi:10.1086/521607

Robinson, R. A. J., Brezina, C. A., Parrish, R. R., Horstwood, M. S. A., Nay Win, O., Bird, M. I., Myint, T., Walters, A. S., Oliver, G. J. H., Khin, Z. (2014). Large rivers and orogens: The evolution of the Yarlung Tsangpo–Irrawaddy system and the eastern Himalayan syntaxis. *Gondwana Research, 26*(1), 112-121. doi:http://dx.doi.org/10.1016/j.gr.2013.07.002

Rodolfo, K. S. (1969a). Bathymetry and marine geology of the andaman basin, and tectonic implications for southeast asia. *Bulletin of the Geological Society of America, 80*(7), 1203-1230. doi:10.1130/0016-7606(1969)80 [1203:BAMGOT]2.0.CO;2

Rodolfo, K. S. (1969b). Sediments of the Andaman Basin, northeastern Indian Ocean. *Marine Geology, 7*(5), 371-402.

Rohling, E. J., Cooke, S. (1999). Stable oxygen and carbon isotope ratios in foraminiferal carbonate shells *Modern Foraminifera* (pp. 239-258). Dordrecht: Kluwer Academic Publishers.

Saidova, K. M. (2008). Benthic foraminifera communities of the Andaman Sea (Indian Ocean). *Oceanology*, *48*(4), 517-523. doi:10.1134/ s0001437008040073

Schwab, J. M., Krastel, S., Grün, M., Gross, F., Pananont, P., Jintasaeranee, P., Bunsomboonsakul, S., Weinrebe, W., Winkelmann, D. (2012). Submarine mass wasting and associated tsunami risk offshore western Thailand, Andaman Sea, Indian Ocean. *Natural Hazards and Earth System Sciences, 12*(8), 2609-2630. doi:10.5194/nhess-12-2609-2012

Sijinkumar, A. V., Nath, B. N., Guptha, M. V. S. (2010). Late Quaternary record of pteropod preservation from the Andaman Sea. *Marine Geology, 275*(1-4), 221-229. doi:10.1016/j.margeo.2010.06.003

Sirocko, F., Garbe-Schonberg, D., Devey, C. (2000). Processes controlling trace element geochemistry of Arabian Sea sediments during the last 25,000 years. *Global and Planetary Change*, *26*(1-3), 217-303. doi:10.1016/S0921-8181(00)00046-1

Spencer, T. (2007). Coral reefs and the tsunami of 26 December 2004: Generating processes and ocean-wide patterns of impact. *Atoll Research Bulletin*(544), 1-36.

Stuiver, M., Reimer, P. J., Bard, E., Beck, J. W., Burr, G. S., Hughen, K. A., Kromer, B., McCormac, G., van der Plicht, J., Spurk, M. (1998). INTCAL98 radiocarbon age calibration, 24,000-0 cal BP. Radiocarbon, 40(3), 1041-1083.

Summerfield, M. A., Hulton, N. J. (1994). Natural controls of fluvial denudation rates in major world drainage basins. *Journal of Geophysical Research: Solid Earth, 99*(B7), 13871-13883. doi:10.1029/94JB00715

Szczuciński, W., Jagodziński, R., Hanebuth, T.J.J., Wetzel, A., Mitręga, M., Unverricht, D., Van Phach, P. (2013). Modern sedimentation and sediment dispersal pattern on the continental shelf off the Mekong River delta, South China Sea. *Global and Planetary Change, 110,* 195-213. doi:http://dx.doi.org/10.1016/j.gloplacha.2013.08.019

Thiry, M. (2000). Palaeoclimatic interpretation of clay minerals in marine deposits: An outlook from the continental origin. *Earth Science Reviews, 49*(1-4), 201-221. doi:10.1016/S0012-8252(99)00054-9

Thomas, E. R., Wolff, E. W., Mulvaney, R., Steffensen, J. P., Johnsen, S. J., Arrowsmith, C., Popp, T. (2007). The 8.2 ka event from Greenland ice cores. *Quaternary Science Reviews, 26*(1-2), 70-81. doi:10.1016/ j.quascirev.2006.07.017

Tomczak, M., Godfrey, J. S. (1994). Regional Oceanography: An Introduction (pp. 422). Oxford: Pergamon Press.

Velde, B. (1985). *Clay minerals : a physico-chemical explanation of their occurrence*: Elsevier.

Waelbroeck, C., Labeyrie, L., Michel, E., Duplessy, J. C., McManus, J. F., Lambeck, K., Balbon, E., Labracherie, M. (2002). Sea-level and deep water temperature changes derived from benthic foraminifera isotopic records. *Quaternary Science Reviews, 21*(1), 295-305. doi:http://dx.doi.org/10.1016/S0277-3791(01)00101-9

Wang, H., Liu, Z., Sathiamurthy, E., Colin, C., Li, J., Zhao, Y. (2011). Chemical weathering in Malay Peninsula and North Borneo: Clay mineralogy and element geochemistry of river surface sediments. *Science China Earth Sciences, 54*(2), 272-282. doi:10.1007/s11430-010-4158-x

Wang, P., Li, Q. (2009). In P. Wang & Q. Li (Eds.), *The South China Sea: Paleoceanography and Sedimentology* (pp. 1-23). Dordrecht: Springer Netherlands.

Webster, P. J. (1987). *The Elementary Monsoon*, 3-32.

Webster, P. J. (1994). The role of hydrological processes in ocean-atmosphere interactions. *Reviews of Geophysics, 32*(4), 427-476. doi:10.1029/ 94RG01873

Wefer, G., Berger, W. H., Bijma, J., Fischer, G. (1999). Clues to Ocean History: a Brief Overview of Proxies. In G. Fischer & G. Wefer (Eds.), *Use of*

Proxies in Paleoceanography: Examples from the South Atlantic (pp. 1-68). Berlin, Heidelberg: Springer Berlin Heidelberg.

Wyrtki, K. (1973). Physical oceanography of the Indian Ocean. *The Biology of the Indian Ocean*, 18-36.

Xie, S. P., Xu, H., Saji, N. H., Wang, Y., Liu, W. T. (2006). Role of narrow mountains in large-scale organization of Asian Monsoon convection. *Journal of Climate, 19*(14), 3420-3429. doi:10.1175/JCLI3777.1

Xue, Z., Paul Liu, J., DeMaster, D., Leithold, E.L., Wan, S., Ge, Q., Nguyen, V.L., Ta, T.K.O. (2014). Sedimentary processes on the Mekong subaqueous delta: Clay mineral and geochemical analysis. *Journal of Asian Earth Sciences, 79*, 520-528. doi:http://dx.doi.org/10.1016/j.jseaes.2012.07.012

Zhao, Y., Liu, Z., Colin, C., Paterne, M., Siani, G., Cheng, X., Duchamp-Alphonse, S., Xie, X. (2011). Variations of the Nile suspended discharges during the last 1.75 Myr. *Palaeogeography, Palaeoclimatology, Palaeoecology, 311*(3–4), 230-241. doi:http://dx.doi.org/10.1016/j.palaeo.2011.09.001

VITA

Ms.Suratta BUNSOMBOONSAKUL

PhD candidate

at Chulalongkorn University and Tongji University

Education:

2011 - 2017

Tongji University, Shanghai, China and Chulalongkorn University, Bangkok, Thailand

A Joint Doctoral Program: Marine Geology and Marine Science

Dissertation topic: "Provenance of Detrital Sediments in Southern Andaman Sea during the Last Glaciation"

2004 - 2007

Chulalongkorn University, Bangkok, Thailand

M.Sc., major in Marine Science: Physical Oceanography

Thesis topic: “Linkage of ENSO and coastline change at Phetchaburi and Prachuap khiri khan provinces” (THAI)

1999 - 2003

Chulalongkorn University, Bangkok, Thailand

B.Sc., major in Marine Science: Physical and Chemical Oceanography

Senior Project topic: “Sea surface temperature and atmospheric pressure were connected to El nino – phenomenon” (THAI)